β3 human papillomavirus species share several biological properties with high risk mucosal types

Dissertation

submitted to the Combined Faculties for

the Natural Sciences and for Mathematics of the

Ruperto-Carola University of Heidelberg, Germany

for the degree of

Doctor of Natural Sciences

presented by

Lucia Minoni, M.Sc.
Born in Brescia, Italy

Dissertation

submitted to the Combined Faculties for

the Natural Sciences and for Mathematics of the

Ruperto-Carola University of Heidelberg, Germany

for the degree of

Doctor of Natural Sciences

presented by

Lucia Minoni, M.Sc.
Born in Brescia, Italy

Oral-examination: 8th May 2018

β3 human papillomavirus species share several biological properties with high risk mucosal types

Referees: Prof. Dr. Martin Müller
Prof. Dr. Frank Rösl

TABLE OF CONTENTS

SUMMARY

β human papillomaviruses (HPV) are subdivided into five species and are abundantly detected in the skin, in particular the β and β2 species. Therefore, β HPV types are considered to have a cutaneous tropism. However, several recent studies have described the presence of β HPV also in the mucosal epithelia at different anatomical sites. In particular, β3 HPV types are more prevalent in certain mucosal epithelia rather than in the cutaneous tissues. Studies in different experimental models have also highlighted that β3 HPV49 share functional similarities with the mucosal high-risk (HR) HPV16. However, with the exclusion of HPV49, very little is known about the biology of the other known β3 HPV types (75, 76 and 115).

The aim of this thesis was the characterization of the biological properties of E6 and E7 of all known β3 HPV types, in relation to their interaction with key cellular pathways such as pRb, p53 and hTERT.

Similar to what was previously showed for HPV49 E6/E7, HPV75 and HPV76 E6 and E7, but not HPV115 E6 and E7, efficiently cooperate in the immortalization/extension of lifespan of human foreskin keratinocytes (HFKs). In detail, HPV49, 75 and 76 E6/E7 cause the accumulation of the phosphorylated form of pRb, leading to the release of the E2F factor and unscheduled S-phase entry. As observed for HR HPV16, cell cycle deregulation mediated by β3 HPV onco-proteins leads to $p16^{INK4a}$ accumulation, while no $p16^{INK4a}$ was detected in β2 HPV38 E6/E7 HFKs. Similarly to HPV49 E6, HPV75 and 76 E6s degrade p53 via an E6AP/proteasome-mediated mechanism. Mutation in HPV76 E6 amino-acids that correspond to HPV16 E6 amino-acids involved in the formation of the E6/E6AP/p53 ternary complex results in the failed immortalization of HFKs. All the β3 HPV types, with the exception of HPV115, induce the up-regulation of hTERT expression, another important step in cellular transformation. Comparative analysis of cellular gene expression pattern of HFKs expressing E6 and E7 from HR HPV16, β3 HPV types and β2 HPV38 further highlights the functional similarities of HR HPV16 and β3 HPV49, 75, 76. The expression profiles of these four HPV HFKs show some similarities and diverge substantially from β3 HPV115 E6/E7 and β2 HPV38 E6/E7 HFKs.

In conclusion, the data show that β3 HPV types share some similarities with HR HPV types and pave the way to additional studies aiming to evaluate their tissue tropism and their role in human pathologies.

ZUSAMMENFASSUNG

Die humanen Papillomviren (HPV) des β-Genus sind in fünf Spezies unterteilt, wobei insbesondere die β1- und β2-Spezies häufig in der Haut nachgewiesen werden können. Aus diesem Grund wird davon ausgegangen, dass die β-HPV Typen einen vorwiegend kutanen Tropismus haben. β3 HPV Typen werden dagegen hauptsächlich in bestimmten Schleimhäuten nachgewiesen und nicht wie die anderen β-Typen in kutanem Gewebe. Studien in verschiedenen experimentellen Modellen haben gezeigt, dass der β3 HPV Typ 49 funktionelle Eigenschaften mit dem mukosalen Hochrisikotyp (HR) HPV16 teilt. Mit Ausnahme von HPV49 ist über die Biologie der restlichen, bekannten β3 HPV Typen (HPV75, 76 und 115) bisher nur wenig bekannt.

Das Ziel dieser Arbeit war die Charakterisierung der biologischen Eigenschaften von E6 und E7 aller bekannten β3 HPV-Typen im Hinblick auf ihre Interaktion mit zellulären Schlüssel-Signalwegen wie pRb, p53 und hTERT. Ähnlich wie HPV49 E6/E7 sind auch HPV75 und HPV76 E6/E7 maßgeblich an der Immortalisierung/Verlängerung der Lebensdauer primärer humaner Vorhautkeratinozyten (HFKs) beteiligt, ganz im Gegensatz zu HPV115 E6/E7. Die Expression von HPV49, 75 und 76 E6/E7 resultierte in der Akkumulation der phosphorylierten Form von pRB, welche zur Freisetzung des E2F Transkriptionsfaktors und der außerplanmäßigen S-Phase führte. Wie bereits bei HR HPV16 beobachtet, verursachte auch die Zellzyklusderegulation durch β3 HPV Onkoproteine die Akkumulation von p16INK4a, wohingegen keine p16INK4a Akkumulation bei β2 HPV 38 E6/E7 exprimierenden HFKs festgestellt wurde. Ebenfalls vergleichbar zu HPV49 E6 führte auch die Expression von HPV75 und 76 E6 zur E6AP/Proteasomen-vermittelten Degradation von p53. Basierend auf HPV16 E6 wurde der putative E6AP/p53 Interaktionsbereich im HPV76 Protein durch Mutagenese verändert. Alle vier untersuchten Mutanten von HPV76 E6 verloren die Fähigkeit HFK zu immortalisieren. Alle β3 HPV Typen, mit Ausnahme von HPV115, induzierten die Hochregulation der hTERT Expression, die einen weiteren wichtigen Schritt der zellulären Transformation darstellt. Desweiteren demonstrierten Vergleichsanalysen zellulärer Genexpressionsmuster von HFKs , die E6 und E7 des HR HPV16, der β3 HPV Typen und des β2 HPV38 E6 und E7 exprimierten die Ähnlichkeit der β3 HPV Typen 49, 75 und 76 zum HR Typ HPV16. Das Expressionsprofil dieser vier HPV HFKs wies einige Gemeinsamkeiten auf und unterscheiden sich damit deutlich von den β3 HPV115 und β2 HPV38 E6/E7 HFKs.

Diese Daten zeigen, dass β3 HPV Typen einige Übereinstimmungen in Bezug auf ihre regulierenden Eigenschaften der zellulären Genexpression zu den HR HPV Typen aufweisen und verdeutlichen somit die Notwendigkeit weiterer Studien, zur Erforschung ihres Gewebetropismus und ihrer Rolle in der humanen Pathologie.

1 INTRODUCTION

1.1 HUMAN PAPILLOMAVIRUSES

The human papillomavirus (HPV) belong to the taxonomic family of *Papillomaviridae* and represents a group of non-enveloped double-stranded (ds) DNA viruses. The viruses that make up *Papillomaviridae* are highly diverse, and are present in most mammals and birds.

1.1.1 PHYLOGENETIC CLASSIFICATION

Over 240 papillomaviruses (PV) have been discovered so far, including more than 150 HPVs, and they are grouped by species and classified into 16 genera (indicated with Greek letters), as shown in figure 1. This classification is based on the nucleotide sequence of L1, with a genotype (or type) considered distinct when the sequence is at least 10% divergent from other known PVs [1]. Currently, the alpha, beta and gamma (α, β, γ) genera include the majority of the HPV types.

The phylogeny classification of the PV based on the L1 nucleotide sequence does not necessary correlate with the biological properties of the different HPV types. As an example, the α genus includes HPV types with different tissue tropism and/or oncogenic properties.

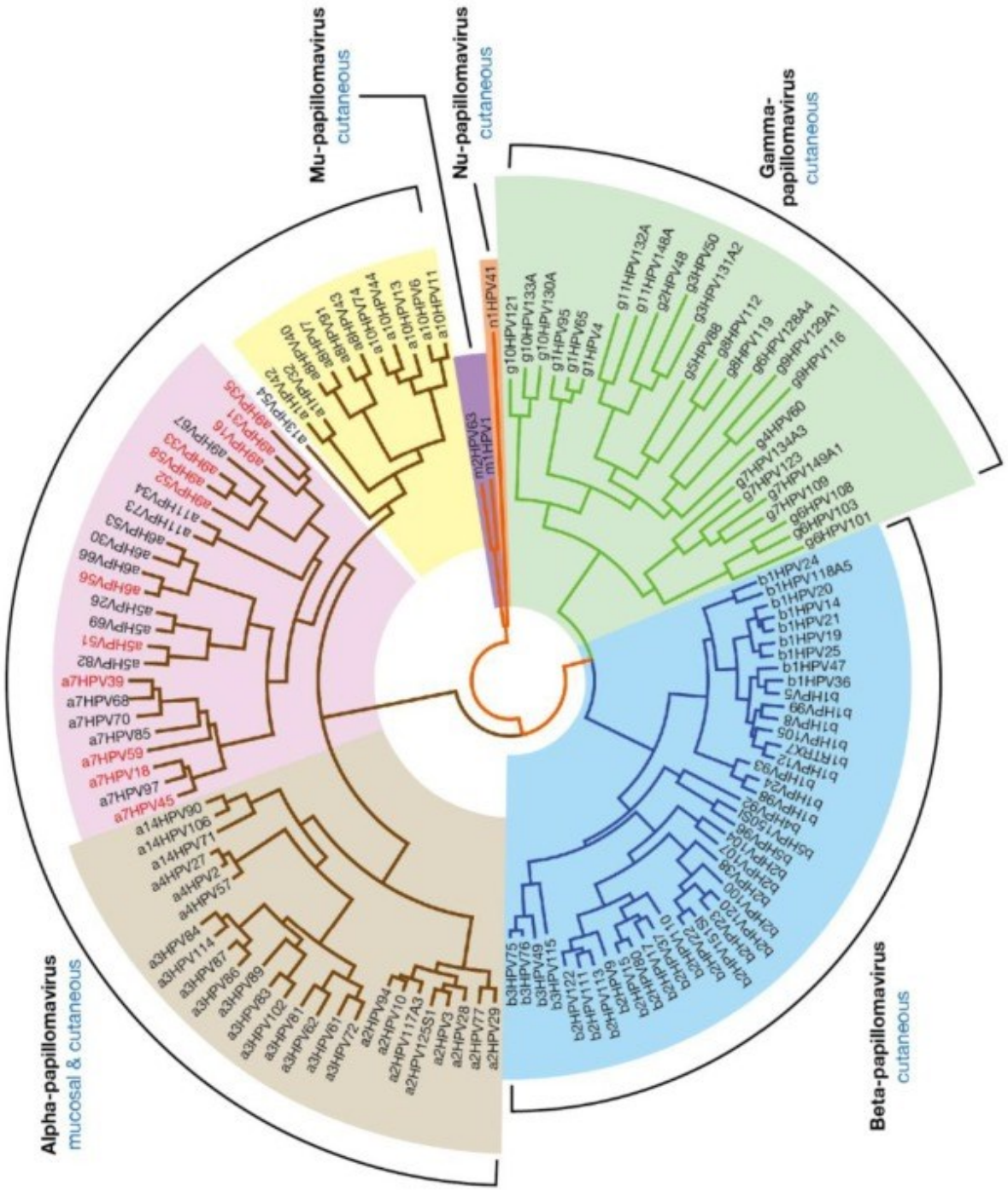

Figure 1: Papillomaviruses phylogenetic tree. Classification of papillomaviruses based on L1 gene sequences alignment. Most of the HPVs belong to the α, β (blue) and γ (green) genera. the α genus HPV types are further sub-divided in low-risk cutaneous (light brown), low-risk mucosal (yellow), or high-risk mucosal (pink) according to their association with the development of cancer. The high-risk types highlighted with red text are confirmed as "human carcinogens" by IARC. Mucosal and cutaneous tropism classification is indicated under each genus. Figure from [2]

1.1.2 HUMAN PAPILLOMAVIRUSES GENOME ORGANIZATION

The HPV double stranded genome is approximately 8000 base pairs in size and, despite the variety of HPVs, its organization is highly conserved. The genome consists of 3 regions: (i) a non-coding long control region (LCR), (ii) an early gene region, and (iii) a late gene region, as shown in Figure 2.

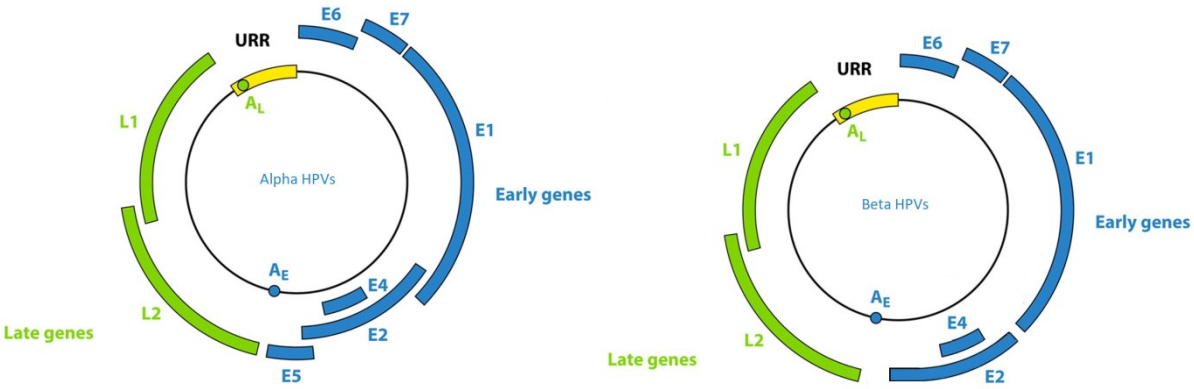

Figure 2: Schematic overview **of the double-stranded DNA genome of α and β human papillomaviruses.** In the left panel the α HPVs genome organization, in the right panel the β HPVs genome organization. The late genes L1 and L2 are depicted in green; the early genes E1, E2, E4, E5, E6 and E7 are depict in blue. Notably, E5 ORF is absent in the β HPV genomes. The URR, also called LCR, is depict in yellow. Figure modified from [3].

The LCR, otherwise known as the upstream regulatory region (URR), is located between the late and early gene regions. It contains many of the responsive elements for transcription factors involved in viral gene expression as well as elements essential for viral DNA replication. Considerable heterogeneity exists among the LCR of the different PVs and, notably, the LCR of the β HPVs is shorter compared to the one of the α HPVs.

The early gene region encodes for genes that are expressed in the early stage of the viral life cycle and are mainly involved in viral replication (E1, E2), cell cycle entry, and immune evasion (E6, E7, E5). This region also contains the E4 gene, which is expressed at the late stage of the viral life cycle and thought to be involved in the virus release. E4 is also thought to be important in the induction of the productive life cycle.

The early protein 1 (E1), with the aid of E2, binds to the viral origin of replication and it assembles into a hexameric helicase. This complex exerts its function to unwind the viral genome, providing the template for the replication of the viral genome [4, 5]. In addition,

the E2 protein also acts as viral transcription regulator by interacting with various host proteins, modifying their function to regulate the viral life cycle. The roles of E4 and E5 are not yet fully understood, however, E4 seems to be involved in the destabilization of the cytokeratin network through the formation of amyloid fibers and in the escape of the virions from the epithelial surface [6, 7]. E5 is a short transmembrane protein that mediates mitogenic signals of growth factors, such as the epidermal growth factor receptor or the plated derived growth factor (PDGF) β receptor [8, 9]. Remarkably, the E5 gene is not present in the β HPV genomes, indicating that the β HPVs have probably evolved to exert the same functions by different mechanisms.

E6 and E7 are the major onco-proteins involved in the HPV-induced carcinogenesis and their biological properties are described in detail in paragraph 1.2. An additional gene, E8, is located within the E1 open reading frame (ORF) and generates a spliced transcript called E8^2C which has been implicated in the regulation of the viral replication [10].The late region comprises the L1 and L2 genes that encode the major and minor capsid proteins, respectively. The viral DNA is encased by a non-enveloped icosahedral capsid of about 50-60 nm, composed of 72 capsomers. Each capsomer is formed by five L1 and one L2 molecule.

1.1.3 HUMAN PAPILLOMAVIRUS TROPISMS

HPVs are also classified as mucosal or cutaneous types according to their ability to infect the mucosal epithelia or the skin, respectively. So far, well-established mucosal HPV types are included in genus α and they can be sub-divided into low-risk (LR) or high-risk (HR), accordingly to their ability to induce benign or malignant lesions respectively. The LR HPV types are normally associated with genital warts while HR HPV types are the etiological cause of cervical cancer as well as a subset of anogenital and head and neck cancers [11]. The classification of α HPVs in HR and LR types parallels their transforming abilities in *in vitro* (cell culture) and *in vivo* model (transgenic mouse).

Many of the cutaneous HPV types belong to the β and γ genera. Several findings have indicated that β HPV types, together with ultra-violet (UV) irradiation, promote the development of Non-Melanoma-Skin Cancer (NMSC) [12].

It is still unclear what biological properties of the different HPV types determine their tissue tropism. Based on available data, one possible hypothesis is that HPV tissue tropism is not controlled at the entry level but it is primarily controlled by the LCR region that controls viral gene expression [13, 14, 15]. Since E5, E6 and E7 present more variability in sequence, it is possible that the tropism depends on the function and regulation of these genes. Another hypothesis suggests that E4, given the considerable heterogeneity among the sequences in the different types, may play a role in the tropism and in the different transmission routes [16].

1.2 HUMAN PAPILLOMAVIRUSES AND CARCINOGENESIS

1.2.1 CANCER AND α HPV TYPES

All HR HPV-associated cancers correspond to approximately 5% of all cancer cases worldwide [17]. Thirteen HPV types (16, 18, 31, 33, 35, 39, 45, 51, 52, 56, 58, 59 and 66) are classified as carcinogenic in humans (Group 1) for their role in the development of cervical cancer [18]. HPV16 and HPV18 are responsible for approximately 50% and 20% of cervical cancer cases respectively [19, 20]

The preferential infection site for the mucosal HPV is the junction between the endocervix columnar cells and the ectocervix stratified squamous epithelial cells, known as the cervical transformation zone. The majority of the HPV infections are cleared by the immune system in a relatively short time, usually between 6 and 12 months, and therefore do not lead to cytological abnormalities. Persistent infections that are not naturally cleared by the immune system are associated with the development of cervical intraepithelial neoplasia (CIN), which may regress or progress to invasive cervical carcinoma after a relatively long period of latency [21]. Figure 3 schematically shows the evolution of an HPV infection from CIN to invasive cancer.

Beside HPV infection, there are various risk factors associated with the development of cervical cancer. These risk factors likely influence the ability of the host immune system to clear the virus, or they may be carcinogenic themselves. Epidemiological studies have

identified certain sexual habits, cigarette smoking, oral contraceptive use and host genetic predisposition as additional risk factors [22, 23, 24, 25, 26].

HR HPV types are also responsible for a set of anogenital cancer (anal, vaginal, vulvar and penile cancers) [27] as well as oropharyngeal cancer (base of the tongue, tonsils, and throat) [28, 29]. However, these cancers are predominately associated with HPV16, while the other HR HPV types appear to play a minor role.

Due to their association with human carcinogenesis, the mucosal HR HPV types have been extensively studied in the last 3 decades. Many studies have demonstrated the transforming properties of the viral onco-proteins in *in vitro* and *in vivo* experimental models.

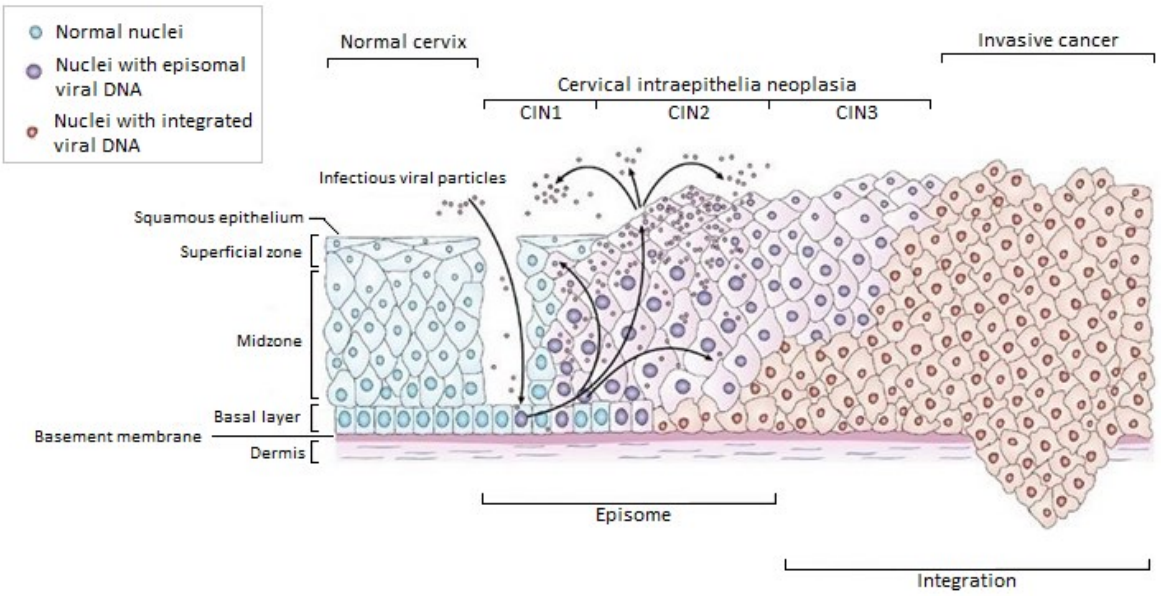

Figure 3: Stage of HPV infection, from CIN to invasive cancer. The basal layer of the cervical epithelium is supported by the basement membrane and by the dermis. Infectious HPV particles can access the basal layer, the primary site of infection, through micro abrasion. Following the infection, the early HPV genes are expressed in the basal layer while the late gene and E4 are expressed in the midzone and in superficial zone. In CIN1 and CIN2 lesions, the viral genome remains episomal. The progression to CIN3 is characterized by viral genome integration with the disruption of E2 gene and therefore up-regulation of E6 and E7. Figure modified from [30].

HR HPV AND CELLULAR TRANSFORMATION

HR HPV genome encodes three transforming proteins: E5, E6, and E7.The E5 onco-protein appears to have a role in the early steps of tumour initiation [31], and its expression is sufficient to promote neoplasia in a transgenic mouse model [32, 33]. Interestingly, the E5 gene is often disrupted in cancer. This is because when the HPV genome integrates into the host cell, the viral genome is subjected to rearrangement. Almost in all the integrations, the E2-region of HPV genome is deleted or separated from the LCR [34, 35, 36]. As consequence, the expression of several viral genes is lost, including E5. The loss of E5 expression during integration provides an explanation why E5 is thought to be an onco-protein in the early stage of carcinogenesis when the genome remains mainly episomal [37]. This is likely an important step in the carcinogenic process as 100% of HPV18-, 80% of HPV16- and 81% of HPV31-driven cancers contain integrated viral genomes [38, 39]

E6 and E7 are essential for the maintenance of the transformed phenotype and are actively transcribed in all HPV-positive cancer cells after integration.

E6 AND E7 TRANSFORMATION IN EXPERIMENTAL MODELS.

The first indication that E6 and E7 are onco-proteins and that they play an important role in the carcinogenesis came from the analysis of cervical cancer-derived cells such as SiHa and CaSki, which express both E6 and E7 [40]. The silencing of E6 and E7 in these cells lines resulted in the rapid cell death, proving the essential role of these proteins for the cell phenotype [41].

Multiple studies have shown that E6 and E7 display transforming abilities both in *in vitro* and *in vivo* experimental models. The expression of E6 and E7 of HPV16 in immortalized fibroblasts (NIH3T3) leads to their full transformation, with the acquisition of anchorage-independent growth ability and ability to form tumours when injected into nude mice [42]. In addition, HR E6 and E7 are able to immortalize human primary keratinocytes, the natural host of the virus [43, 44, 45, 46, 47].

In accordance with the *in vitro* assay described above, transgenic mice expressing both the viral genes under the basal cell keratin 14 (K14) promoter are susceptible to the

development of cancer, promoted by different means such as chemical carcinogens or estrogen treatment [48, 49]. However, the main limitation of the transgenic mouse model is that viral gene expression is regulated by a host promoter and not by the endogenous LCR. The analysis of external factors, such as hormones, on the viral transcription is compromised in this model.

A break-through in the modelling of the HPV life cycle came from the development of organotypic raft culture, in which the HR HPV genome can be episomally maintained in primary keratinocytes. In this system, keratinocytes containing HR HPV genomes are differentiated *in vitro*, leading to recapitulation of the full differentiation program of the host keratinocyte, and allowing for completion of the viral life cycle [50, 51, 52]. The main limitation of this approach is the fact that the viral genome is intact, while in cancer progression, the viral genome is integrated and the expression of E6 and E7 is therefore up-regulated.

MAJOR STEPS INVOLVED IN CELLULAR TRANSFORMATION

During the keratinocyte life cycle, cells exit the basal layer and migrate to the superbasal layer, committing to a program of terminal differentiation. [53].

The papillomaviruses lack most of the proteins necessary for viral DNA synthesis and consequently, they use host DNA synthesis machinery for their own genome amplification, which occurs primarily during the G2-like phase [54, 55]. Therefore, it is vital for the HPV life cycle to uncouple differentiation, essential for the production of viral progeny, from the proliferation, essential for viral DNA synthesis. Thanks to the presence of E7, the infected cells, after they have left the basal layer, are pushed back into the cell cycle, which ensures that these cells maintain their proliferative potential. However, E7 protein is not sufficient to induce cellular immortalization. For example, expression of HPV16 E7 in human keratinocytes triggers an autophagy-like cell death [56]. This cell intrinsic tumour suppressive protection mechanism is often referred to as "trophic sentinel response" and is triggered when there is an oncogenic proliferative signal in conflict with the growth inhibitory signal generated by a lack of mitogenic stimulation. Usually, this results in cell death, differentiation or senescence [57]. To avoid

cell death by the trophic sentinel response, HPV16 E6 targets p53 for degradation via the proteasome pathway [58].

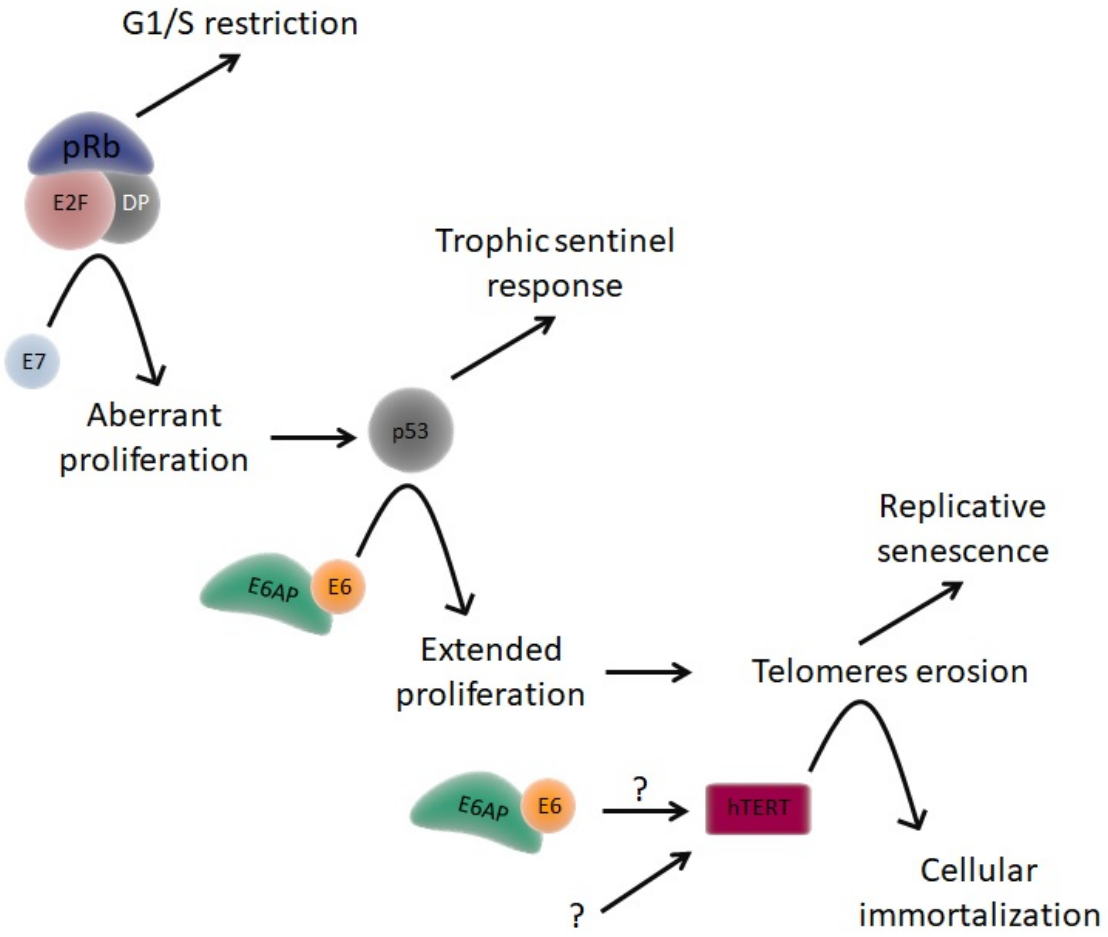

Figure 4: schematic outline of the major steps necessary for cellular transformation induced by HR HPVs. Normal keratinocytes have a limited lifespan and they exit the cell cycle as soon as they leave the basal layer of the epithelium. The expression of HPV16 E7 causes the degradation of pRb and a consequent aberrant proliferation. In normal condition, the aberrant proliferation causes the activation of the trophic sentinel response. The expression of HPV16 E6 cause the degradation of p53, major responsible for the trophic sentinel response, therefore the cells continue to proliferate. As a last mechanism of protection from unlimited proliferation, the telomeres shorten at every DNA replication; the presence of E6 and E7, with still not well characterized mechanisms, cause the re-activation of the human telomerase, resulting in the immortalization of the keratinocytes.

The expression of E6 and E7 causes extended proliferation, but this is not sufficient for cellular immortalization. In fact, the somatic cells have another mechanism of protection to limit the capacity of proliferation: the shortening of telomeres after cell division.

Therefore α HR HPV E6 and E7 evolved to re-activate the human telomerase (hTERT) in somatic cells to subvert this telomerase erosion [59, 60].

The major step involved in the immortalization of human primary keratinocytes are shown in figure 4.

MAJOR CELLULAR TARGETS OF E7 ONCO-PROTEIN

HPV E7 proteins are relatively small polypeptides (approximately 100 amino-acids) and notably, they lack any enzymatic activity. For this reason, E7 needs to hijack cellular protein complexes and modify their functions to promote proliferation. In human cells, E7 proteins are mainly located in the nucleus; interestingly the E7 protein lacks any recognizable nuclear targeting sequence, although it is actively transported in the nucleus through a non-classical Ran-dependent pathway [61, 62].

The main known target of E7 is the retinoblastoma tumour suppressor protein pRb (and the associated pocket proteins p107 and p130 [63]. pRb is a nuclear protein that regulates the activity of the transcription factor family E2F, which is mainly involved in the control of the cell cycle progression. E2F transcription factors (1-3) form a heterodimer complex with DP1. When the E2F1/DP1 complex is associated with pRb, it acts as a transcriptional repressor of genes involved not only in cell cycle progression but also genomic instability and apoptosis [64]. HR HPV E7 proteins can induce the degradation of pRb through the proteasome pathway with a mechanism that involves the reprogramming of the cullin 2 ubiquitin ligase complex. The destabilization of pRb results in the release of E2F1-DP complex, which can act as a transcriptional activator for the genes necessary for the entry and the progression of the S-phase [65, 66]. A schematic representation of the effect of the interaction betweenHPV16 E7 and pRb is shown in figure 5.

As previously mentioned, PV need to uncouple the cellular differentiation program from proliferation. For this purpose, E7 has evolved to interact with $p21^{CIP1}$, an important cyclin-dependent kinase (CDK) inhibitor. $p21^{CIP1}$ steady-state levels increase with the differentiation of the cells where it inactivates cdk2 activity and therefore induces cell cycle arrest. In cells expressing E7 from HR α HPVs, $p21^{CIP1}$ levels are increased via

protein stabilization, however, cdk2 remains highly active, allowing the proliferation of infected cells [67, 68, 69, 70].

E6 of α HPVs subverts p53 functions via the proteasomal degradation. It is therefore interesting that E7 is also able to interfere with the p53 pathway, suggesting a redundancy of mechanisms for the inactivation of p53-mediated apoptosis. In normal cells, p53 half-life is relatively short, due to degradation mediated by the ubiquitin ligase mdm2 [71]. However, in cells expressing E7 of HPV16, p53 is accumulated and its half-life is increased [72, 73]. It has also been observed that mdm2 binds p53 with a lower efficiency when E7 is expressed in the cells compared to normal cells. It is important to note that, despite the increased levels, p53 is transcriptionally inactive [74].

Additional functions of E7 have also been identified such as alteration of cell metabolism and chromosomal instability, both of which are involved in the transformation process [75, 76]. For other E7-interacting partners, such as histone deacetylases and histone acetyl transferase, their relevance for cellular immortalization is still unclear [77].

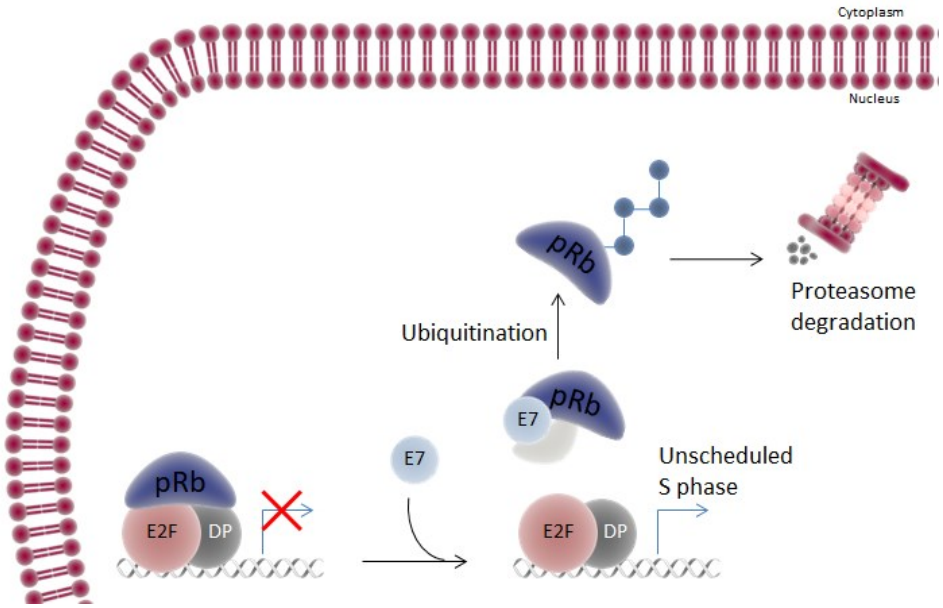

Figure 5: schematic representation of HPV16 E7 effect on pRb pathway. In normal cells, pRb recognizes and binds E2F/DP transcription factors and repress the expression of genes involved cell cycle progression, genomic instability and apoptosis. HPV16 E7 binds to pRb causing its degradation via proteasome pathway. E2/DP complexes are released, and they activate the transcription of genes involved in the cell cycle progression, causing an unscheduled S phase.

E7 AND p16^{INK4a}

The degradation of pRb mediated by E7 is an oncogenic stress event that is sensed by the cells and leads to the up-regulation of the gene that encodes the CDK inhibitor p16 ^{INK4a} [78, 79].

In uninfected cells p16 ^{INK4a} inhibits the activity of CDK4 and CDK6 that phosphorylate pRb, therefore it causes the sequestration of E2F by the un-phosphorylated pRb and the cell cycle arrest [80].

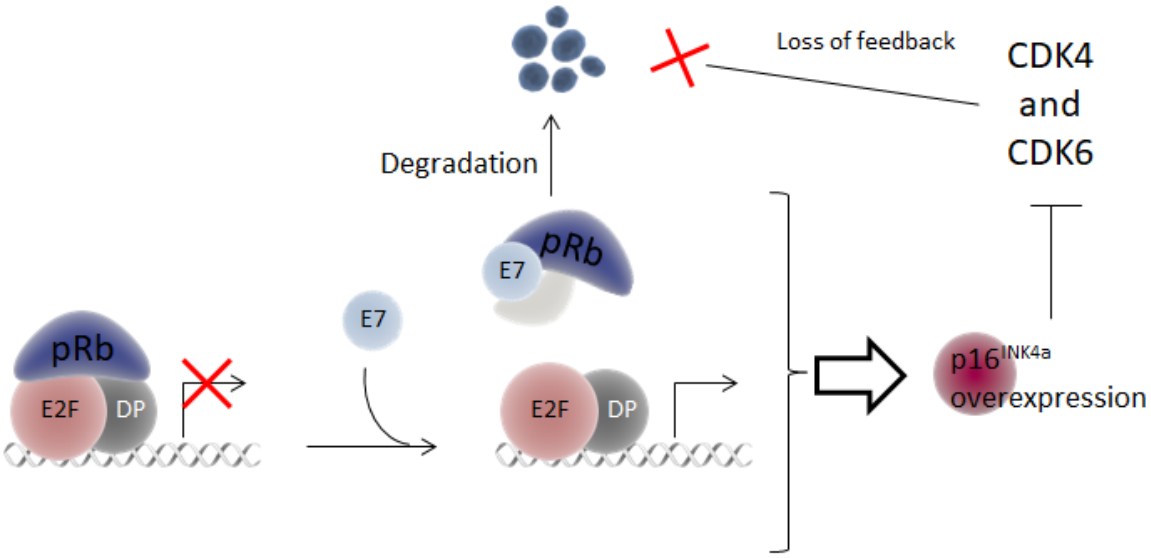

Figure 6: schematic representation of HPV16 E7 effect on p16^{INK4a}. The degradation of pRb is an oncogenic stress that causes an accumulation of p16 ^{INK4a}. In uninfected cells, p16 ^{INK4a} inhibit the phosphorylation of pRb via CDK4 and CDK6. In presence of HPV16 E7, pRb is degraded therefore the negative feedback is lost and p16 ^{INK4a} continues to accumulate.

The accumulation of p16 ^{INK4a} protein, in the absence of pRb (through pRb degradation by HPV16 E7), causes a paradoxical increase in the levels of this protein and a surprising addiction to p16^{INK4a} expression [81, 82]. In fact, p16^{INK4a} inhibits the CDKs, however, the natural target pRb is degraded and p16^{INK4a} continues to accumulate to inhibit uncontrolled cellular replication. A simplified representation of p16^{INK4a} accumulation is shown in figure 6.

MAJOR CELLULAR TARGET OF E6 ONCO-PROTEIN

HPV E6 proteins are relatively small polypeptides (approximately 150 amino-acids) and the main characteristic is the presence of four Cys-X-X-Cys motifs that allow the formation of two zinc fingers [83].

The major effect of the E6 onco-protein is the elimination of the trophic sentinel response caused by the expression of E7 through the inactivation of p53 [84].

It was shown several years ago that p53 is degraded via the proteasome pathway via hijacking of the cellular enzyme E6AP (E6 Associated Protein), as schematically represented in figure 7 [58, 85].

E6AP, also known as UBE3A, is a 100 kDa protein that acts as an E3 ubiquitin-protein ligase and therefore transfers ubiquitin molecules to the target protein. In an uninfected cell, p53 is not a natural target for E6AP, however, in HPV-infected cells, E6 diverts E6AP in order to induce the degradation of p53 [86, 85]. The interaction of E6 with E6AP causes the dimerization and ubiquitination of E6AP and subsequentially a conformation change that allow the binding of the E6-E6AP complex to p53 [87, 88]. Once p53 is ubiquitinated, it becomes available for proteasome degradation where it is a target for cytoplasmic proteasomes.

The consequence of the degradation of p53 mediated by E6/E6AP is the inhibition of the growth arrest and apoptotic function of p53, allowing the cells to aberrantly grow under the stimulus of E7 expression.

Different studies have shown that E6 can interfere with p53 function via mechanisms other than degradation, suggesting that there are redundant mechanisms to target the same pathway. HR E6 proteins can bind the histone acetyl transferase (HAT) p300, inhibiting its enzymatic activity. Besides its chromosomal remodeling function, p300 acetylates p53, causing its activation as a transcription factor [89]. The interaction of E6 with p300 causes the conversion of the p53 complexes from activators to repressors [90].

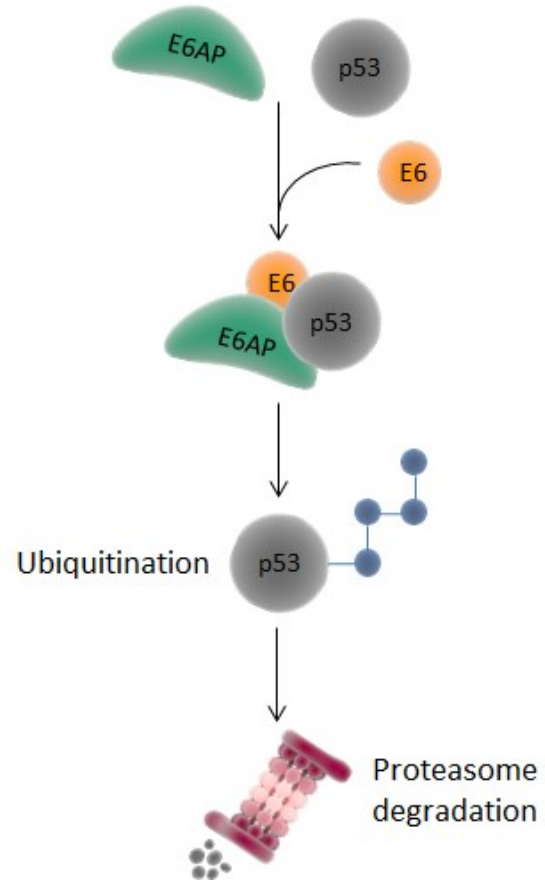

Figure 7: schematic representation of HPV 16 E7 effect on p53 pathway. The interaction between E6 and E6AP causes a conformation change that allows the recruitment of p53 to E6-E6AP complex. E6AP exert its function and ubiquitinates p53, targeting it for proteasome degradation.

Interestingly, E6 can also interfere with the apoptosis with a mechanism that is p53-independent. In fact, E6 binds and causes the degradation of the pro-apoptotic protein Bak [91]. Bak is generally sequestered and released only upon DNA damage, causing the release of cytochrome C and the activation of the apoptotic caspase cascade. In the presence of E6 Bak is degraded, therefore, its pro-apoptotic function is inhibited [92].

A considerable number of other interactors of E6 have been discovered, though the biological significance of many of these is not yet clear. Among them E6 is able to interact with a set of protein containing the PDZ motif; these proteins are important in many cellular signal transduction pathways and the interaction of E6 with these proteins seems to be relevant for the transforming ability of HPV [93, 94].

E6 AND hTERT

The activation of the telomerase enzyme, which adds telomere repeats to the end of chromosomes, is an important step in the immortalization mediated by HR α HPVs [60].

Different studies showed that E6 can activate the telomerase at the transcriptional level, causing an up-regulation of it at the mRNA level [95, 96, 97]. The mechanism by which hTERT is up-regulated has not been elucidated yet, however, there are suggestions that E6AP binding is involved [95, 96]. One model proposes that the E6-E6AP complex binds to the NFX1-91 (a TERT transcription repressor), leads to its ubiquitination and degradation and eventually it causes the E6AP-dependent de-acetylation of histones [98, 99]. A different model indicates c-myc as a target of E6-E6AP complex binding, somehow causing c-myc to be a better transcriptional activator for hTERT [97]. The two proposed model are schematically depicted in figure 8.

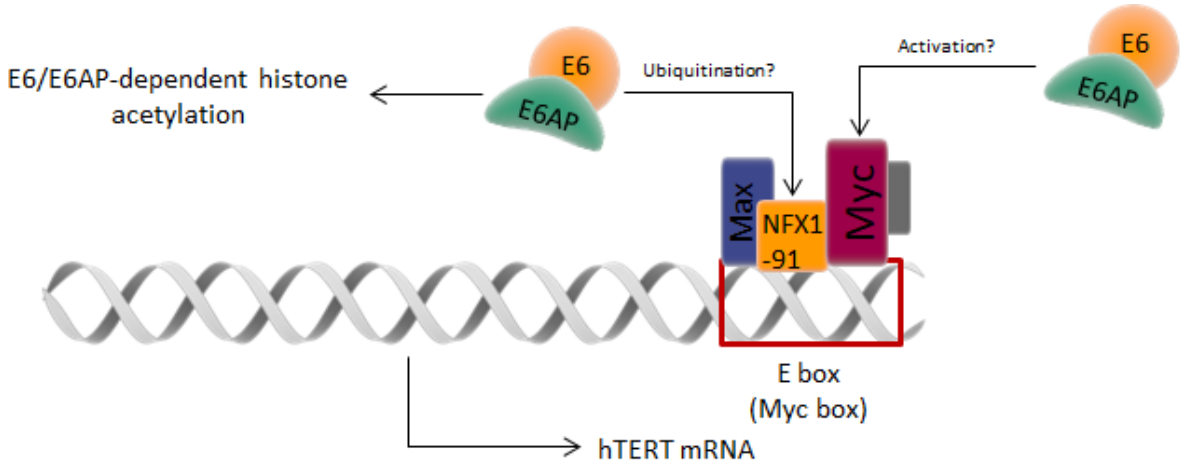

Figure 8: Schematic representation of the proposed model for hTERT up-regulation in presence of HPV16 E6. In the first model, E6-E6AP complex binds NFX1-91 and cause its ubiquitination and degradation. This event cause at the same time an E6AP-dependent de-acetylation of histones. In the second model, c-myc is targeted by E6-E6AP complex leading to a transcriptional activation of hTERT.

Moreover, a study [100] showed that E7 is also partially contributing to hTERT up-regulation. In this study, they showed that in the hTERT promoter there is an E2F site that in normal condition act as an inhibitory element. The binding of E7 to pRb causes an enhancement of hTERT promoter as well as an increase in the telomerase activity. It is important to note that the role of E7 is marginal compared to E6 since E7 alone is

insufficient to initiate the transcription of the endogenous hTERT in primary keratinocytes.

1.2.2 CANCER AND β HPV TYPES

β HPVs AND EPIDERMODYSPLASIA VERRUCIFORMIS

The first β HPV types 5 and 8 have been isolated in the skin of individuals suffering from a genetic disorder, known as epidermodysplasia verruciformis (EV). EV is a rare genetic disorder characterized by the extensive skin warts mainly located in sun-exposed areas, that often evolve into squamous cell carcinoma (SCC) [101, 102]. β HPV 5 and 8 have been detected in 90% of squamous cell carcinomas found in EV affected patients, leading to their classification as "possibly carcinogenic" viruses [103, 104].

Patients with this rare disease are unable to clear β HPV infections, while they are able to clear α HPV infections as well as infections caused by bacteria and other viruses [105, 106].

The genetic background of the disease has been identified for 75% of the cases in mutation in the genes that encode EVER1 or EVER2 [107]. Although the exact role of these two genes in the restriction of HPV infection is not completely understood, it is known that EVER1 and EVER2 are involved in the immune response and skin homeostasis [108, 109].

β HPVs AND NON-MELANOMA SKIN CANCER

IMMUNOSUPPRESSED INDIVIDUALS

Immunosuppressed organ transplant recipients (OTR) are often subject to development of HPV-induced warts as well as actinic keratosis (AK) and cutaneous SCC [110, 111]. Interestingly, HPV-induced warts associate and co-localize with SCC in OTR, suggesting that persistent warts may progress into skin cancer [112]. Moreover, different studies have shown that the prevalence of β HPV DNA in the skin of OTR is higher than in the general population, supporting the hypothesis that β HPVs are the etiologic agent of NMSC in immunosuppressed individuals [113, 114].

IMMUNOCOMPETENT INDIVIDUALS

β HPV genomes are detected in NMSC but they are often also detected in the skin of healthy immunocompetent individuals [115, 116]. However, a meta-analysis of case control studies suggested that β HPV antibody positivity, in particular for the types 5/8/17/20/38, is associated with an increased risk of development of SCC [117].

The prevalence of β HPV genomes is higher in the initial stage of the lesion, the actinic keratosis, compared to the prevalence in the SCC supporting the hypothesis of a role of the β HPVs in the initial stages of the carcinogenesis [118]. HPV may play a role in the initial stage facilitating the accumulation of UV-induced mutation (a well-established risk factor for skin carcinogenesis [119]) in the host genome. After the establishment of the cancer cell phenotype, the presence of the viral genome may not be necessary for the maintenance of the phenotype and therefore it could be lost.

HUMAN PAPILLOMAVIRUS TYPE 38

HPV38 E6 and E7 were the first onco-proteins from β types to show immortalization ability in human foreskin keratinocytes (HFKs) [120]. Different to the HR α HPV types, HPV38 E6/E7 expressing keratinocyte immortalization is preceded by a lag-phase in which the cells remain growth arrested [120].

Reflecting the different tropisms, the mechanisms, shown in Figure 9, by which E6 and E7 of HPV38 interact with p53 and pRb pathway are different from those used by high risk mucosal viruses (described in paragraph 1.2.1). HPV38 E7 induces accumulation of a specific form of p53, that is phosphorylated at serine residues 15 and 392 [121]. This particular form of p53 is efficiently recruited to an internal promoter of p73 causing the expression of the truncated form ΔNp73α, which acts as an antagonist of the p53-regulated pathway [121]. In addition, HPV38 E6 binds p53 with high affinity, however, the consequence of this interaction remains to be fully characterized [122].

Similar to HR α types, HPV38 E7 can associate with pRb, however, its expression in human primary keratinocytes leads to a stabilization of pRb in the hyperphosphorylated form [120]. In this form, pRb loses the ability to bind E2F transcription factors and

therefore E2Fs can induce the expression of the genes involved in the G1/S transition [64].

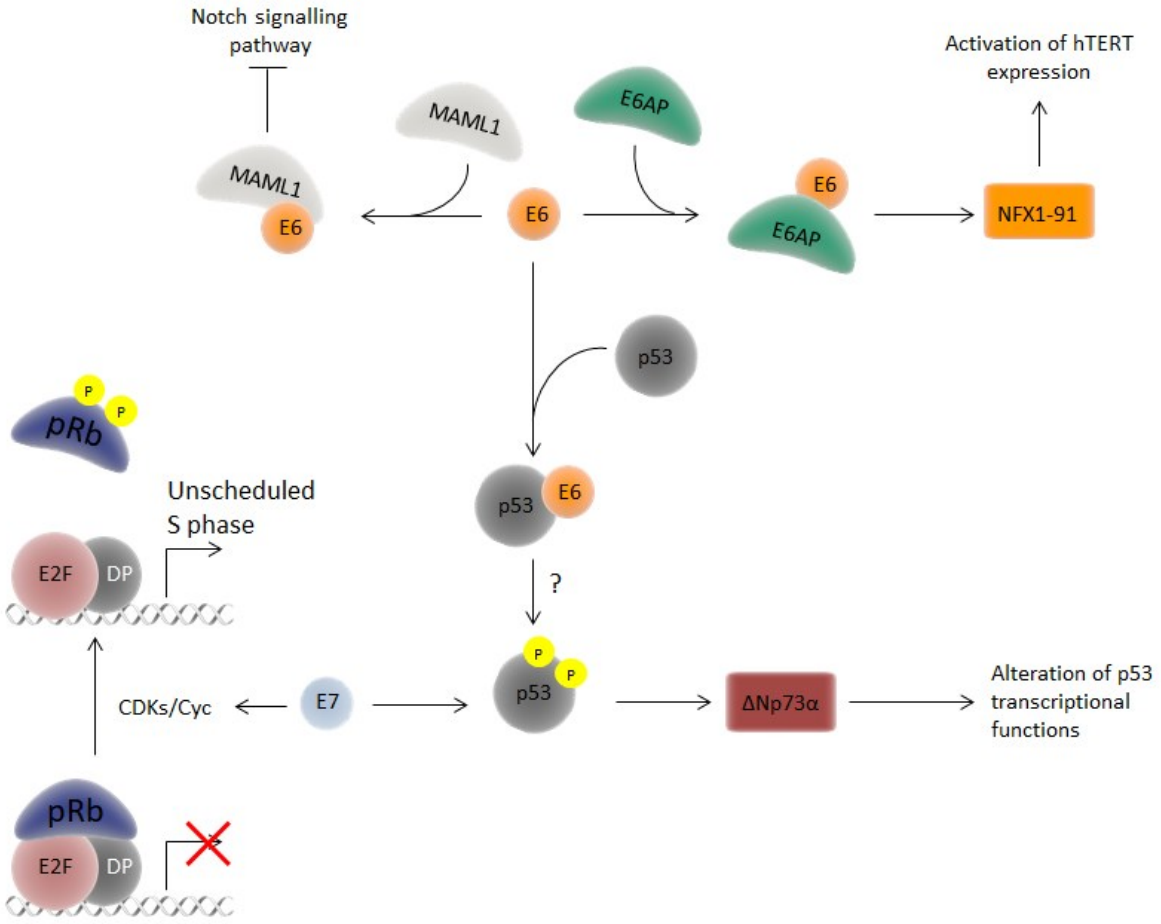

Figure 9: Schematic representation of HPV38 E6/E7 effects on p53 and pRb pathways. HPV38 E7 induces an accumulation of p53 phosphorylated at serines 15 and 392 and consequently a nuclear accumulation of ΔNp73α, that act as an antagonist of the p53-regulated pathway. The consequence of the interaction between HPV38 E6 and p53 remains to be fully characterized. HPV38 E6 bind MAML1 and that causes the repression of Notch transcriptional activation. An additional interaction partner of E6 is E6AP, that target NFX1-91 for degradation, causing the transcriptional activation of hTERT. Finally, HPV38 E7 leads to the stabilization of pRb in the hyperphosphorylated form.

As discussed for HPV16 in paragraph 1.2.1, HPV38 E6 and E7 have additional interaction partners. It is important to note that, similar to all the β HPVs, E6 binds MAML1 (Mastermind-like 1) and in doing so causes the repression of Notch transcriptional activation [123, 124, 125]. The Notch signaling pathway plays an important role in cell-cycle exit and keratinocyte differentiation [126, 127]. Therefore, it is possible

that this interaction would benefit the viral life cycle since HPV needs to uncouple differentiation and proliferation to complete its life cycle.

Moreover, HPV38 can up-regulate the expression of hTERT with two distinct mechanisms. E6 is able to activate the transcription via E6AP and NFX1-91 binding [128] while E7 promotes the accumulation of ΔNp73α which in turn positively regulates hTERT [129].

Transgenic (Tg) mouse models expressing E6 and E7 of HPV38 in the basal layer of the epidermis under the control of the K14 promoter (cytokeratin promoter) have a higher susceptibility to skin cancer compared to wild-type animals only when exposed to UV-radiations [130]. When exposed to UV-irradiation for few weeks, the mice first develop lesions similar to the human AK and later they develop SCC [130]. Interestingly, the Cre-LoxP mediated deletion of E6 and E7 after the development of UV-induced skin lesions did not affect tumour growth [131]. This recent data support the hypothesis that β cutaneous types have a "hit and run" mechanism, accentuating the deleterious effects of the UV radiation.

1.2.3 CANCER AND β3 TYPES

In addition to their ability to target the skin, recent findings have indicated that β HPV types can also infect other anatomical sites such as the oral mucosal epithelium, eyebrow hairs, penile and external genital lesions [132, 133, 134, 135]. Although no findings have supported the direct involvement of HPV types in pathological conditions at any of the anatomical sites described above, a prospective study showed that DNA positivity for some β HPV types in the oral cavity was associated with the risk of head neck and cancer [136].

Of particular interest are the types (HPV49, 75, 76 and 115), that are often found more frequently in mucosal epithelia rather than in the skin [137, 135].

Interestingly biological studies on HPV49 have shown that E6 and E7 of this β3 type share some functional similarities with HR HPV16 onco-proteins [138].

HUMAN PAPILLOMAVIRUS TYPE 49

Like HPV16 and HPV38, expression of HPV49 E6 and E7 leads to the immortalization of human primary keratinocytes. Interestingly, the expression of E6/E7 from HPV49 determines the continuous growth of the cells without the lagging phase that characterizes the other β types, such as HPV38 [138].

Another interesting similarity with HPV16 is the ability of HPV49 E6 to bind the ubiquitin E3 ligase enzyme, E6AP, and to promote p53 degradation via the proteasome pathway [138]. The mechanism of interaction with p53 is clearly different from the one described for other β HPV types, such as HPV38 [120, 121].

By contrast, the mechanism of interaction with pRb pathway is similar to what has been observed for HPV38 with the accumulation of the phosphorylated form of pRb and the subsequent release of E2F [138].

Other additional interaction partners have been identified also for HPV49 E6 and E7; among these MAML1 interacts with E6, similar to what has been shown for many other β HPVs [122]. It is interesting to note that E6 of HPV49 is the only E6 protein of β types proven to be able to interact with both E6AP and MAML1 [122], supporting the hypothesis of intermediate characteristics of this papillomavirus.

Transgenic mouse models, expressing E6 and E7 under the control of K 14 promoter, provide further evidence for the functional similarities between HPV types 16 and 49. K14 β3 HPV type 49 or α HPV type 16 E6/E7-Tg animals were found to be highly susceptible to upper digestive tract carcinogenesis upon initiation with 4-nitroquinoline 1-oxide (4NQO), while K14 β2 HPV type 38 E6/E7-Tg mice were not affected much by 4NQO treatment [139].

2 AIM OF THE THESIS

Although more than 200 human papillomavirus types have been isolated so far, only a small number of these have been extensively studied with respect to their biological properties and association with human diseases. Within the beta genus, species β3 types (HPV49, 75, 76 and 115) are of particular interest for their dual tropism for cutaneous and mucosal epithelia, and for the similarities that E6 and E7 of HPV49 share with the high risk α type 16 [137, 135, 138]. The epidemiological and molecular findings indicate that the β3 species may represent a subgroup of beta types with shared properties with α HR HPV types.

However, with the exclusion of HPV49, very little is known about the biology of the remaining known β3 HPV types (75, 76 and 115).

Therefore, this thesis aimed to compare the immortalization properties of E6 and E7 of all four β3 HPV types and their ability to interfere with major events related to cellular transformation, such as those controlled by pRb and p53.

3 MATERIALS

3.1 BIOLOGICAL MATERIAL

3.1.1 PROCARYOTIC CELLS

SUBCLONING EFFICIENCY™ DH5α™ COMPETENT CELLS (INVITROGEN)

Subcloning Efficiency™ DH5α™ Competent Cells are an E.coli strain used for the cloning of the gene of interest into plasmid vectors. This strain has been designed to have high transformation efficiency: $>1*10^6$ transformed bacteria/μg DNA.

The cells grow at 37 °C.

RESISTANCE: None.

GENOTYPE: F- ϕ80lacZΔM15 Δ(lacZYA-argF)U169 recA1 endA1 hsdR17(rk-,mk-) phoA supE44 thi-1 gyrA96 relA1λ

ROSETTA

The Rosetta™ host strain derives from the BL21 strain and it's designed to enhance the expression of eukaryotic proteins. For this purpose, this strain is engineered to supply tRNAs that are common in the eukaryotic codon usage but rare in *E. coli*. The Rosetta strain carries the pRARE plasmid (with the chloramphenicol resistance gene), suppling tRNAs for the codons AUA, AGG, AGA, CUA, CCC, and GGA. Moreover, this strain carries a chromosomal copy of the T7 RNA polymerase under the control of the lacUV5 promoter. Therefore, the Rosetta strain can be used to produce recombinant protein from genes cloned in pET system, after the induction with IPTG.

RESISTANCE: Chloramphenicol.

GENOTYPE: F- ompT hsdSB(rB- mB-) gal dcm (DE3) pRARE (CamR)

3.1.2 EUKARYOTIC CELLS

NIH/3T3

NIH 3T3 mouse embryonic fibroblast cells come from a cell line isolated and initiated at the New York University School of Medicine, Department of Pathology. The line has been obtained from desegregated NIH Swiss mouse embryo fibroblasts and now is recognized as the standard fibroblast cell line.

MEDIUM: DMEM +++

PHOENIX

The Phoenix cell line has been developed by the Nolan lab in Stanford University from the 293T cell line (a human embryonic kidney line transformed with adenovirus E1a and carrying a temperature sensitive T antigen co-selected with neomycin). The Phoenix cells can be used as a packaging line since they carry a construct capable of producing gag, pol and env for ecotropic and amphotropic viruses. The unique feature of this cell line is that it is highly transfectable with either calcium phosphate mediated transfection or lipid-based transfection protocols-- up to 50% or higher of cells can be transiently transfected.

MEDIUM: DMEM +++

PRIMARY KERATINOCYTES

Human primary keratinocytes cells are found in the basal layer of the stratified epithelium and they have different roles. The structural role is to form tight junctions with the nerves of the skin and keep Langerhans cells and lymphocytes of the dermis, in place. Since the skin is the first line of defence, keratinocytes play also a role in immune system. The keratinocytes, in fact, serve as a barrier between the organism and its environment. They prevent the entering of pathogens and toxin into the body, but they also prevent the loss of moisture and heat. These cells are also immune-modulators: they secrete inhibitory cytokines in the absence of injury meanwhile they stimulate inflammation in response to injury.

The HPK used for this project were isolated from the foreskin of 3 different donors and donate to the group by the following groups:

- Donor 1: cells donated by Dr. Hans-Jürgen Stark - Genetics of Skin Carcinogenesis (DKFZ, Heidelberg)
- Donor 2 and 3: cells donated by the Laboratoire des substituts cutanes, Hopital E. Herriot (Lyon, France).

MEDIUM: FAD

NATURALLY IMMORTALIZED KERATINOCYTES (NIKS)

The NIKs cell line was isolated and characterized by *Allen-Hoffmann et al.* in 2000. This cell lined arose from the BC-1-Ep strain of normal foreskin keratinocytes and maintained steady-state levels of transforming growth factor (TGF-α), transforming growth factor-β1, epidermal growth factor receptor, c-myc, and keratin 14 mRNAs, similarly to the parental cell line. NIKs are non-tumourigenic and produces a fully stratified squamous epithelium in organotypic culture [140].

MEDIUM: DMEM +++

HNC136

HNC136 cell line is derived from head and neck tumour patient.

MEDIUM: DMEM +++

3.2 MEDIA AND SUPPLEMENTS

3.2.1 PROCARYOTIC CELLS

LB MEDIUM

	Concentration
Tryptone	1% (w/v)
Yeast Extract	0.5% (w/v)
NaCl	0.5% (w/v)
Deionized H_2O	To volume

Adjust the pH to 7,5. Autoclave it.

LB AGAR MEDIUM

	Concentration
Tryptone	1% (w/v)
Yeast Extract	0.5% (w/v)
NaCl	0.5% (w/v)
Agar	1.5% (w/v)
Deionized H_2O	To volume

Autoclave it. Add antibiotics when the temperature is lower than 40 ^{o0} C.

ANTIBIOTICS

	Working concentration
Ampicillin (Amp)	100 μg/ml
Kanamycin (Kan)	50 μg/ml
Chloramphenicol (Chl)	25 μg/ml

3.2.2 EUKARYOTIC CELLS

FAD

	Working concentration	Company
Ham's F-12, with L-Glutamine	73 % (v/v)	GIBCO, Invitrogen
DMEM high glucose with glutamine (= Dulbecco's Modified Eagle Medium)	23% (v/v)	GIBCO, Invitrogen
Fetal Bovine Serum (FBS)	4 % (v/v)	GIBCO, Invitrogen
Pen Strep (Penicillin/Streptomycin)	100 U/ml	GIBCO, Invitrogen
Adenine, (6-aminopurine)	24 μg/ml	SIGMA
Recombinant Human EGF (= Epidermal Growth Factor)	10 ng/ml	R&D company
Insulin solution human	10 μg/ml	Sigma Aldrich
Hydrocortisone	400 ng/ml	Sigma Aldrich
Ciprofloxacin hydrochloride	10 μg/ml	EUROMEDEX
Cholera Toxin	8,3 ng/ml	List Biological laboratories, INC

DMEM + + +

	Working concentration	Company
DMEM high glucose with glutamine	90% (v/v)	GIBCO, Invitrogen
Fetal Bovine Serum (FBS)	10 % (v/v)	GIBCO, Invitrogen
Pen Strep (Penicillin/Streptomycin)	100 U/ml	GIBCO, Invitrogen
Ciprofloxacin hydrochloride	10 μg/ml	EUROMEDEX

OPTI-MEM

Opti-MEM™ Reduced Serum Medium, GIBCO, Invitrogen

DPBS

"Dulbecco's phosphate-buffered saline" by Gibco.

TRYPSIN

Trypsin-EDTA (0,25%), phenol red, Life Technologies

MITOMYCIN C

Mitomycin C from *Streptomyces caes* 2mg, Sigma Aldrich

CRYOMEDIUM

90% FBS + 10% DMSO

3.3 HUMAN CELLS TREATMENTS AND MANIPULATION

Designation	Company
MG132	Sigma Aldrich #C2211
Cycloheximide	Ozyme #2112S
Doxorubicin	Sigma Aldrich #D1515
Lipofectamine 2000	Invitrogen #11668027
PolyFect	Qiagen #301105
Effectene	Qiagen #301425

3.4 RETROVIRAL INFECTION

Designation	Company
CalPhos Mammalian transfection kit	BD-Biosciences
Chloroquine 25 mM	Sigma Aldrich
Polybrene 5mg/ml	Sigma Aldrich
G418 100 mg/ml	Sigma Aldrich

3.5 MOLECULAR CLONING

3.5.1 PLASMIDS

pLXSN

pLXSN is a retroviral vector composed of elements from Moloney murine leukemia virus (MoMuLV) and Moloney murine sarcoma virus (MoMuSV). The 5' LTR comprises promoter/enhancer sequences that control the transcription of ψ^+ extended viral packaging signal and of the gene of interest, which is cloned into the multiple cloning site (MCS). The MCS has four unique cloning sites that are EcoRI, HpaI, XhoI, and BamHI. The SV40 early promoter P_{SV40e} regulates transcription of the neomycin resistance gene for eukaryotic selection. The ColE1 origin of replication serves for replication of pLXSN in bacteria as well as the ampicillin resistance gene allows selection of pLXSN-transformed bacteria. After transfection of pLXSN into a packaging cell line, pLXSN expresses the ψ^+ packaging signal generating infectious but replication-incompetent retroviral particles. The pLXSN features are shown in the schematic representation of figure 10.

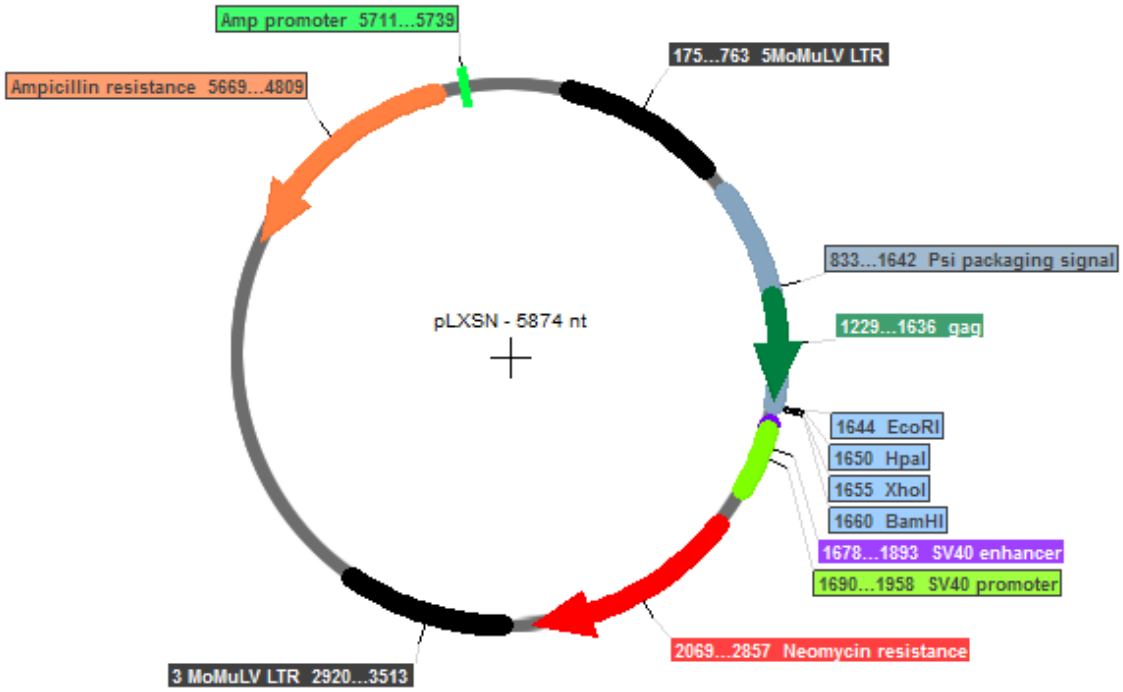

Figure 10: pLXSN vector features. pLXSN is a 5874 bp retro-viral vector containing the MoMuLV 5' LTR that control the transcription of Psi packaging signal and of the gene of interest. The neomycin resistance (in red), allow the selection of successfully infected cells. The ampicillin resistance gene (in orange) with its promoter allows for selection in bacteria.

Description	Reference
pLXSN(E6/E7)HPV16	M. Tommasino
pLXSN(E6/E7)HPV49	M. Tommasino
pLXSN(E6/E7)HPV75	This thesis
pLXSN(E6/E7)HPV76	This thesis
pLXSN(E6/E7)HPV115	This thesis
pLXSN(E6/E7)HPV76 mut E39R	This thesis
pLXSN(E6/E7)HPV76 mut Y42R	This thesis
pLXSN(E6/E7)HPV76 mut D44A	This thesis
pLXSN(E6/E7)HPV76 mut F45E	This thesis

pET MBP 1C

The pET system is used for the expression of recombinant proteins in *E. coli*, under the control of a strong bacteriophage T7 transcription. The expression of the recombinant protein can be induced only when the system is provided with a source of T7 DNA polymerase, usually using engineered *E. coli* strain (such as the *Rosetta* strain). The use of the T7 induction system ensures the target gene expression is silent in the un-induced state as well as the high quantity of the protein of interest after the induction. Target genes are firstly cloned using non-expressing hosts (such as DH5α strain) and afterword transferred to expression host, where the T7 DNA polymerase gene is under the control of the *lac* promoter and therefore can be induced by the addition of IPTG.

The pET-MBP_1c plasmid is a pET vector modified by Gunter Stier (Universität Heidelberg, Heidelberg, Center for Biochemistry) to carry the ORF of the Maltose Binding Protein (MBP). This modified version of the pET vector maintains all the characteristics of the pET system and, in addition, the recombinant protein is expressed as a fusion protein with the maltose binding protein. The MBP is a part of the maltose/maltodextrin system of *Escherichia coli* and can be used to increase the solubility of recombinant proteins. The mechanism underlying the increased solubility of the fusion proteins is still not fully understood but the MBP is able to prevent the aggregation of the protein of interest. Moreover, the MBP can be used as an affinity tag for the purification of the recombinant proteins using amylose coupled-beads.

The pET MBP 1c features are shown in the schematic representation of figure 11.

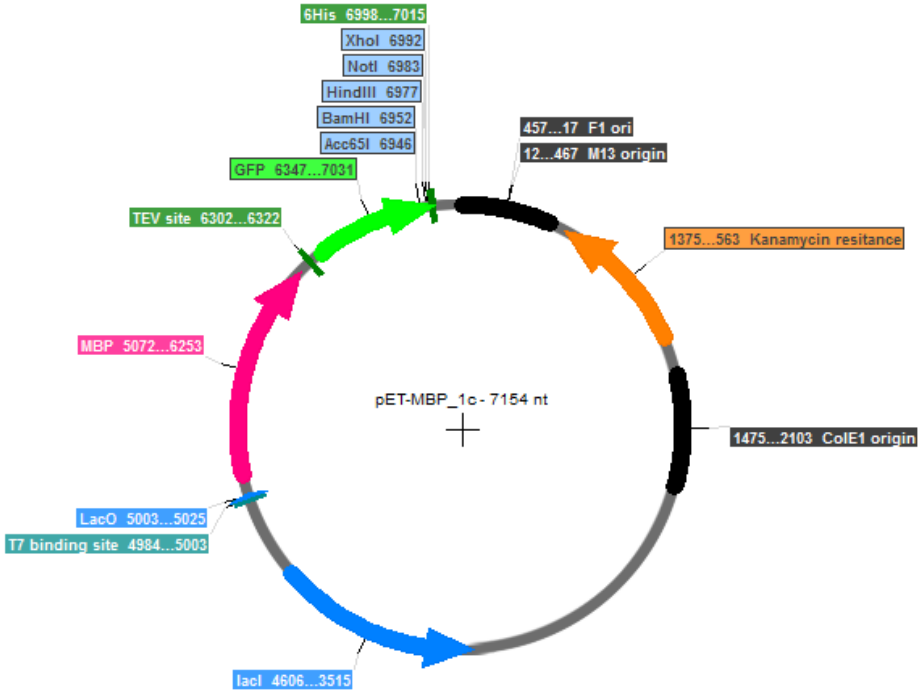

Figure 11: pET MBP 1c vector features. The main feature of this plasmid is the maltose binding protein gene (in pink). This gene can be expressed only in presence of T7 DNA polymerase that recognizes the T7 binding site. The kanamycin resistance gene (in orange) allows the selection of successfully transformed bacteria.

Description	Reference
pET MBP 1c (E6) HPV16	This thesis
pET MBP 1c (E6) HPV49	This thesis
pET MBP 1c (E6) HPV75	This thesis
pET MBP 1c (E6) HPV76	This thesis
pET MBP 1c (E6) HPV115	This thesis
pET MBP 1c (E6) HPV76 mut E39R	This thesis
pET MBP 1c (E6) HPV76 mut Y42R	This thesis
pET MBP 1c (E6) HPV76 mut D44A	This thesis
pET MBP 1c (E6) HPV76 mut F45E	This thesis

3.5.2 ENZYMES

Designation	Company
Restriction enzymes	New England Biolabs
HotStarTaq DNA Polymerase	Qiagen
T4 DNA ligase	Roche
Mesa Green qPCR Master Mix Plus for SYBR Assay (Eurogentec)	Eurogentec

3.5.3 OLIGONUCLEOTIDES FOR siRNA KNOCKDOWN

Designation	Sequence	Company
ON-TARGETplus Human UBE3A siRNA (E6AP)	Not provided	Dharmacon (L005137000005)
ON-TARGETplus Human CDKN2A siRNA (p16)	Not provided	Dharmacon (L-011007-00-0005)
Scramble	Not provided	Eurofins

3.5.4 OLIGONUCLEOTIDES FOR CLONING

All the listed nucleotides have been designed to have four adenines (AAAA) at the 5', in order to improve the cutting of the PCR product by the restriction enzymes.

All oligonucleotides listed were ordered and produced at MWG Eurofins in Ebersberg, Germany.

Vector	#	Gene	Restriction enzyme	Sequence 5'-3'
pLXSN	1	(E6)HPV76 fw	EcoRI	AAAAGAATTCATGGCTAGACCTGCTAAGGT
	2	(E7)HPV76 rev	BamHI	AAAAGGATCCTTATCGTCCGCCATTGCGAAT
pET MBP 1c	3	(E6)HPV16 fw	NcoI	AAAACCATGG*gt*ATGCACCAAAAGAGAACTGCA
	4	(E6)HPV49 fw	NcoI	AAAACCATGG*gt*ATGGCTAGACCTGTTAAGGTA
	5	(E6)HPV75/6 fw	NcoI	AAAACCATGG*gt*ATGGCTAGACCTGCTAAGGTA
	6	(E6)HPV115 fw	NcoI	AAAACCATGG*gt*ATGGCTAGGCCAGGCAGGG
	16	(E6)HPV16 rev	BamHI	AAAAGGATCCTTACAGCTGGGTTTCTCTACG
	17	(E6)HPV49 rev	BamHI	AAAAGGATCCTCATTCTATAACTCTGCAATG
	18	(E6)HPV75 rev	BamHI	AAAAGGATCCTCATTCTATCACTCTGCAATG
	19	(E6)HPV76 rev	BamHI	AAAAGGATCCTCATTCTATTACTCTGCAATG
	20	(E6)HPV115 rev	BamHI	AAAAGGATCCTCATTCTATTGTTCTACAATG

n= nucleotide introduced to restore the frame in the fusion protein

Highlighted in blue EcoRI restriction site

Highlighted in red BamHI restriction site

Highlighted in green NcoI restriction site

3.5.5 OLIGONUCLEOTIDES FOR REAL TIME PCR (RT-PCR)

All oligonucleotides listed were ordered and produced at MWG Eurofins in Ebersberg, Germany.

Gene	Sequence 5'-3'
Cdc2	fw: AATCTATGATCCAGCCAAACGAA
	rev: TTCTTAATCTGATTGTCCAAATCATTAAA
Cdk2	fw: GGCTGCATCTTTGCTGAAAT
	rev: CCCAGAGTCCGAAAGATCCG
p21	fw: GACACCACTGGAGGGTGACT
	rev: CCACATGGTCTTCCTCTGCT
PUMA	fw: GGATGAAATTTGGCATGGGGTCT
	rev: GGACAAGTCAGGACTTGCAG
hTERT	fw: TTC AAG GCT GGG AGG AAC AT
	rev: ACA TGC GTG AAA CCT GTA CG
SERPINE	fw: ATCGAGGTGAACGAGAGTGG
	rev:ACTGTTCCTGTGGGGTTGTG
MT1X	fw: AACTCCTGCTTCTCCTTGCC
	rev: GCTCTATTTACATCTGAGAGCACAG
GADD45a	fw: TGCGAGAACGACATCAACAT
	rev: GCAGGATCCTTCCATTGAGA
GAPDH	fw: AAGGTGGTGAAGCAGGCGT
	rev: GAGGAGTGGGTGTCGCTGTT

3.5.6 OLIGONUCLEOTIDES FOR SITE-DIRECTED MUTAGENESIS

All oligonucleotides listed were ordered and produced at MWG Eurofins in Ebersberg, Germany.

HPV76 mutant	Sequence 5'-3'	Mutagenized codon
E39R	fw: CTGACCTATTGGGAACTCTTACGGTTTGATTATAAGGACTTCC	GAG → CGG
	rev: GAAGTCCTTATAATCAAACCGTAAGAGTTCCCAATAGGTCAG	
Y42R	fw: GGGAACTCTTAGAGTTTGATCGGAAGGACTTCCATTTAGTGTGG	TAT → CGG
	rev: CCACACTAAATGGAAGTCCTTCCGATCAAACTCTAAGAGTTCCC	
D44A	fw: CTTAGAGTTTGATTATAAGGCCTTCCATTTAGTGTGGAAGGACG	GAC → GCC
	rev: CGTCCTTCCACACTAAATGGAAGGCCTTATAATCAAACTCTAAG	
F45E	fw: CTTAGAGTTTGATTATAAGGACGAGCATTTAGTGTGGAAGGACGG	TTC → GAG
	rev: CCGTCCTTCCACACTAAATGCTCGTCCTTATAATCAAACTCTAAG	

Highlighted in red the mutagenized codon

3.5.7 BUFFERS AND SOLUTIONS

AGAROSE GEL ELECTROPHORESIS

Designation	Composition / Company
50X TAE buffer	ABCYS Eurobio
Massruler Loading Dye	Life Technologies
MassRuler DNA Ladder, Mix, ready-to-use	Life Technologies
GelRed staining	Biotium
1% agarose gel	1% agarose (w/v) 1X TAE buffer 0.004 % GelRed (v/v)

3.6 REAGENTS FOR PROTEIN ANALYSIS

3.6.1 ENZYMES

Lambda Protein Phosphatase, New England Biolabs.

3.6.2 IP BUFFER

Ingredient	Working concentration
Tris HCl pH 7.5	20 mM
NaCl	200 mM
EDTA	1 mM
NP40	0.5%
H_2O	Up to 10 ml
cOmplete™, Mini, EDTA-free Protease Inhibitor Cocktail (Roche)	1 tablet

3.6.3 PROTEIN BUFFER 10X

Ingredient	
Glycin	144.1g
TRIS	30.3 g
H_2O	To volume of 1 l

3.6.4 SDS-POLYACRYLAMIDE ELECTROPHORESIS

The following recipes are intended for one gel (1.5 mm) using the "Mini-PROTEAN" cast system from Biorad.

RUNNING GEL

Ingredient	Volume	
	Gel 10%	**Gel 12%**
Acrylamide 30%	3.3 ml	4.0 ml
Tris 1 M pH 8.8	2.5 ml	2.5 ml
SDS 10%	0.1 ml	0.1 ml
APS 10%	0.1 ml	0.1 ml
TEMED	0.004 ml	0.004 ml
H_2O	4.0 ml	3.3 ml

STACKING GEL

Ingredient	Volume
Acrylamide 30%	0,33 ml
Tris 0,5 M pH 6.8	0,25 ml
SDS 10%	0,02 ml
APS 10%	0,02 ml
TEMED	0,002 ml
H_2O	1,4 ml

RUNNING BUFFER

Ingredient	Volume
Protein buffer 10x	100 ml
SDS	10 ml
H_2O	890 ml

PROTEIN MARKER

PageRuler™ Prestained Protein Ladder, 10 to 180 kDa; Thermo Fisher (Germany)

LAEMMLI BUFFER 6X

Ingredient	
SDS	1.2 g
Bromophenol blue	6 mg
Glycerol	4.7 ml
Tris HCl 0.5 M pH 6.8	1.2 ml
Beta-mercaptoethanol	0.5 ml
H_2O	2.1 ml

3.6.5 WESTERN BLOT ANALYSIS

TRANSFER BUFFER

Ingredient	Volume
Protein buffer 10x	100 ml
Methanol	200 ml
H_2O	700 ml

OTHER SOLUTIONS

Designation	Composition/Company
Blocking solution	10 % (w/v) skim milk PBS Tween
Antibody buffer	5 % (w/v) skim milk PBS Tween
PBS Tween	1X PBS 0.064 % (v/v)
Stripping solution	15 g Glycine 10 ml Tween 20 1 g SDS 1 l H_2O, pH 2.2
Clarity™ Western ECL Blotting Substrates	BioRad, Munich, Germany

3.7 IMMUNOLOGICAL ASSAYS

3.7.1 ANTIBODIES

All the following antibodies have been used with a 1:1000 dilution if not differently stated.

Designation	Description	Reference
β-actin (C4)	Mouse monoclonal antibody detecting human actin.	MP Biomedicals, #0869100
Phospho pRb (Ser795)	Polyclonal rabbit antibody that detects endogenous levels of Rb only when phosphorylated at serine 795.	Cell signaling, #9301
Total pRb	Mouse monoclonal antibody that recognizes an epitope between amino acids 332-344 of the human retinoblastoma protein.	BD Pharma, #554136
Cdc2 (ab-2)	Mouse monoclonal antibody detecting Cdc2/Cdk1	Calbiochem, #CC01
Cyclin A (H-432)	Rabbit polyclonal antibody raised against full length cyclin A of human origin.	Santa Cruz, #sc751
$p16^{INK4a}$	Mouse monoclonal to CDKN2A/p16INK4a	NovoCastra, DCS-50
p53 DO1	Mouse monoclonal antibody raised against amino acids 11-25 of p53 of human origin.	Santa Cruz, #sc126
E6AP-330	Mouse monoclonal Anti-E6AP antibody purified from hybridoma cell culture.	Sigma Aldrich, #E8655
GAPDH (6C5)	Mouse monoclonal antibody raised against GAPDH.	Santa Cruz, #sc-32233
Secondary mouse (dil 1:2000)	Anti-Mouse IgG (H+L), HRP Conjugate	Promega, W4021
Secondary Rabbit (dil 1:2000)	Anti-Rabbit IgG (H+L), HRP Conjugate	Promega, W4011

3.8 MALTOSE BINDING PROTEIN PULLDOWN

BUFFER AND SOLUTIONS

Designation	Composition
IPTG 100 mM	0,238 g IPTG 10 ml H_2O
IP buffer	See 6.6.2
MBP-buffer	10 mM Hepes pH 7.4 100 mM NaCl 1 mM EDTA 10% Glycerol 0,1% triton X-100

BEADS

Anti-MBP Magnetic Beads. E8037S, New England Biolabs.

3.9 ILLUMINA ARRAY

3.9.1 INSTRUMENTS AND CONSUMABLE

Designation	Company
Nanodrop®	Thermo Scientific
2100 bioanalyzer	Agilent
RNA 6000 Nano kit	Agilent
HumanHT-12 v4 Expression BeadChips	Illumina
TotalPrep RNA Amplification Kit (Ambion®)	Illumina
BeadArray Reader	Illumina

3.9.2 SOFTWARE

Designation	Company
Genome Studio V2010.2	Illumina
BRB-ArrayTools software v4.2	https://brb.nci.nih.gov/BRB-ArrayTools/
R software	https://www.r-project.org/
Venny	http://bioinfogp.cnb.csic.es/tools/venny/

3.10 LIQUID CHROMATOGRAPHY AND MASS SPECTROMETRY

3.10.1 INSTRUMENTS AND CONSUMABLES

Designation	Company
0.2 μm Captiva ND plates	Agilent Technologies
a Rapid EPS well plate sealing tape	BioChromato
6550 quadrupole time-of-flight mass spectrometer coupled to 1290 Infinity UHPLC system	Agilent Technologies
Acquity UPLC HSS T3 column (1.8 μm, 2.1 × 100 mm)	Waters

3.10.2 SOFTWARE

Designation	Company
MassHunter Acquisition B.05.01	Agilent Technologies
MassHunter Qualitative Analysis B.06.00	Agilent Technologies
DA Reprocessor, Mass Profiler Professional 12.1	Agilent Technologies
Profinder B 06.00 software	Agilent Technologies

3.11 CHEMICALS

All chemicals were of analytical grade or better and purchased from one of the following companies:

Company	Location
Gibco	Eggenstein, Germany
Life Technologies	Karlsruhe, Germany
Fisher-Scientific	Schwerte, Germany
Merck	Darmstadt, Germany
Roth	Karlsruhe, Germany
Sigma-Aldrich	Munich, Germany

3.12 KITS

Designation	Company
QIAquick PCR Purification Kit	Qiagen
QIAquick Gel Extraction Kit	Qiagen
QuikChange Lightning Site-Directed Mutagenesis Kit	Agilent technologies
NucleoSpin® RNA extraction kit	MACHEREY-NAGEL GmbH
RevertAid First Strand cDNA Synthesis Kit	Thermo Fisher
NucleoSpin® Plasmid mini prep kit	MACHEREY-NAGEL GmbH
PureLink™ HiPure Plasmid Filter Maxiprep Kit	Invitrogen
Senescence β-**Galactosidase S**taining Kit	Cell Signalling

3.13 LABORATORY EQUIPMENT

3.13.1 ELECTRICAL EQUIPMENT

Designation	Company
800 W microwave	Bosch, Gerlingen-Schillerhohe, Germany
Bacterial culture shaker	Informs AG, Bottmingen, Switzerland
Microbio Safe 12 hood	Thermo Fisher, Germany
Incubateur CO_2 jaquette eau series 3	Thermo Fisher, Germany
Developing Machine AgfaCurix60	Agfa, Munich, Germany
Computers and monitors	Dell, Round Rock, United States
ChemiDoc™ XRS+ System	BioRad, Munich, Germany
Mini-PROTEAN® Tetra Handcast Systems	BioRad, Munich, Germany
Sub-Cell® GT Cell	BioRad, Munich, Germany
Mini Trans-Blot® Cell	BioRad, Munich, Germany
PowerPac™ Basic Power Supply	BioRad, Munich, Germany
GFC water bath	Grant Instruments, Cambridge, UK
Ice maker	Hoshizaki, Willich-Munchheide, Germany
Impulse Sealer	RNS Corp, Taipei, Taiwan
Integra pipetboy	Integra Bioscience GmbH, Fernwald, Germany
Cell counter	Biorad TC20 ™
microscope Statif inverse TS100	NIKON
MilliQ ultra-pure water unit	Millipore Merck, Darmstadt, Germany
Nanodrop spectrophotometer	PegLab, Erlangen, Germany

Designation	Company
Nitrogen tank Chrono	Messer, Krefeld, Germany
pH meter	Sartorius, Göttingen, Germany
Refrigerators and freezers	Liebherr, Ochsenhausen, Germany
Sartorius Scale	Sartorius, Göttingen, Germany
Thermomixer 5436	Eppendorf, Hamburg, Germany
Ultra-low freezer	Eppendorf Inc., Enfield, USA
Vortex Genie 2™	Bender and Hobein, Ismaning, Germany
Western Blot Exposition Cassette	Kodak, Stuttgart, Germany
Centrifuge 5810	Eppendorf, Germany
Centrifuge 5430	Eppendorf, Germany
Centrifuge 5424R (cold)	Eppendorf, Germany
Centrifuge 5415D	Eppendorf, Germany
Centrifuge 5417C	Eppendorf, Germany
Centrifuge 5415R	Eppendorf, Germany

3.13.2 COMMON USE EQUIPMENT

Designation	Company
1,5 ml and 2 ml reaction tubes	Eppendorf, Hamburg, Germany
0,2 ml reaction tubes	Eppendorf, Hamburg, Germany
15 ml reaction tubes	Fisher Scientific, Waltham, United States
50 ml reaction tubes	Fisher Scientific, Waltham, United States
25 cm^2, 75 cm^2 and 150 cm^2 tissue culture flasks	Fisher Scientific, Waltham, United States
6, 10 and 15 cm cell culture plates	Corning, New York, United States
6-, 12-, 24-, 48 and 96-well tissue culture plates	Corning, New York, United States
Cryotubes, 2 ml	Carl Roth GmbH, Karlsruhe, Germany
Examination gloves XCEEDTM Nitril	Starlab, Ahrensburg, Germany
One-time use filter, 0.2/0.4 µm	Renner, Dannstadt, Germany
Parafilm "M"	American National Can, Chicago, USA
qPCR 96 well plate non skirted white	Eurogentec, France
Petri dishes	Greiner, Frickenhausen, Germany
Pipettes (1000, 200, 20, 10 and 2µl)	Gilson Middleton, USA
Pipette Tipps (1000, 200µl, 20µl, 10µl)	STARLAB, Hamburg, Germany
Syringes and needles	BD Franklin Lakes, USA
Whatman filter paper 3MM	Schleicher & Schuell, Dassel, Germany
Magnetic rack DynaMag™-2 Magnet	Fisher Scientific, Waltham, United States
PVDF membrane	EMD Millipore, Burlington, United States

3.13.3 SOFTWARE AND WEBSITES

Designation	Company
Adobe CS4/CS6	Adobe, San Jose, USA
Microsoft Office 2003, 2010	Microsoft, Redmond, USA
Image Lab™ Software	BioRad, Munich, Germany
Webcutter	http://rna.lundberg.gu.se/cutter2
PaVE	https://pave.niaid.nih.gov/
BRB-ArrayTools software v4.2	NIH
Serial Cloner	http://serialbasics.free.fr/Serial_Cloner.html
Human Metabolome Database	http://www.hmdb.ca/
METLIN database	https://metlin.scripps.edu

4 METHODS

4.1 CULTIVATION AND MANIPULATION OF PROKARYOTIC CELLS

4.1.1 TRANSFORMATION OF BACTERIA BY HEAT SHOCK

- Put 1 ng of pure DNA or 5 μl of ligation product in 50 μl of bacteria (DH5α)DH5α) or 80 μl (Rosetta)
- Put the solution for 30 minutes on ice
- Then 30 seconds at 42°C
- And again in ice for 2 min
- Put the bacteria in 300 μl of LB without antibiotics and incubate with agitation for 1 h and 30 min at 37°C
- Take a rate of 50 μl and put in a Petri dish with LB + antibiotic; incubate at 37°C overnight
- Centrifuge the rest of the bacteria, re-suspend in 100 μl of LB and put in a Petri dish with LB + antibiotic; incubate at 37°C overnight

Each colony formed originates from a single transformed bacterial cell. Therefore, each cell within each colony contains identical plasmid DNA.

4.1.2 CULTIVATION AND STORAGE OF BACTERIA

BACTERIAL CULTURE

- Take a colony with a sterile tip and dissolve it in 6 ml of LB medium with antibiotic.
- Incubate in agitation at 37°C overnight
- Process the bacteria to purify the plasmid DNA (mini-prep) or
- Take the pre-inoculum and put it in 200 ml of LB with antibiotic (maxi-prep)
- Put the culture at 37°C in agitation overnight.

LONG TERM BACTERIAL STORAGE

For long-term storage of verified (sequenced) bacterial clones, 500 µl of a liquid culture was transferred to a 2ml cryotube and 500 µl of glycerol (100%) were added. The glycerol stocks were stored at -80^{0}C.

4.2 CULTIVATION AND MANIPULATION OF EUKARYOTIC CELL

All cell lines were cultivated in an incubator at 37^{0}C, 5% CO2 and 90% humidity. Passaging of the cells was performed when cells reached around 80% confluency.

4.2.1 CULTIVATION OF NIH/3T3 FIBROBLASTS

The fibroblast cells are fast growing cells and every 3/4 days is necessary to split them because they became confluent.

The NIH/3T3 are kept in culture in T75 flasks.

SPLIT OF NIH/3T3

- Remove the medium
- Add 8 ml of DPBS and wash the cells
- Add 1 ml of trypsin and incubate 1 minute at 37°C
- Add 9 ml of DMEM +++ to inactivate the trypsin
- Centrifuge for 3 minutes at 900 rpm
- Discard the supernatant
- Re-suspend the pellet into 10 ml of DMEM +++
- Put an amount of the re-suspended cells in the flask (the amount depends on the dilution).

4.2.2 CULTIVATION OF PHOENIX

The Phoenix cells are adherent cells but, unlike the NIH/3T3, they attach to the surface poorly. It' necessary to pay attention while washing the cells and changing the media to

avoid the detachment of the cells from the surface of the dish. The protocol of the split of the cells is the same used for the NIH/3T3.

The Phoenix are kept in culture in 10 cm dishes.

4.2.3 CULTIVATION OF HUMAN KERATINOCYTES (PRIMARY AND EXPRESSING E6/E7)

The human keratinocytes were cultivated with the support of feeder layer (NIH/3T3 fibroblasts) with a protocol modified from Rheinwald and Green [141]. The cells of the feeder layer not only secrete soluble factors into the culture medium but deposit ECM molecules on the culturing surface that facilitate attachment and growth of co-cultured cells [142].

The NIH/3T3 cells added to the human primary keratinocyte are treated with the mitomycin to block their proliferation. The feeder layers need to be changed every time the keratinocytes are split or every 2/3 days since the NIH/3T3 cells treated with the mitomycin die.

The keratinocytes are kept in culture in T25 flasks.

PREPARATION OF THE FEEDER (NIH/3T3)

- Take a flask of NIH/3T3 (around the 80% of confluence), add 250 µl mitomycin C and incubate at 37°C for 2 hours
- Remove the medium
- Add 3 ml of DPBS and wash the cells
- Add 1 ml of trypsin and incubate at 37°C for 1 minutes
- Add 9 ml of DMEM +++ to inactivate the trypsin
- Centrifuge for 3 minutes at 900 rpm
- Remove the solution
- Add 10 ml of FAD
- Counts the cells

CHANGE OF FEEDER LAYER

- Remove the medium
- Add 3 ml of DPBS to wash the cells
- Add 3 ml of DPBS + EDTA and let it acts for 3 minutes. Only the fibroblasts tear away from the flask meanwhile the keratinocyte remain adherent to the flask.
- Remove the solution
- Add 3 ml of DPBS to wash the cells
- Remove the solution
- Add 5 ml of FAD into the flask
- Add "x" µl of counted NIH/3T3 (for the amount of the NIH/3T3 see the table 1)
- Mix with a cross movement

SPLIT OF KERATINOCYTES

- Remove the medium
- Add 3 ml of DPBS to wash the cells
- Add 3 ml of DPBS + EDTA and let it acts for 3 minutes.
- Remove the solution
- Add 3 ml of DPBS to wash the cells
- Remove the solution
- Add 1 ml of trypsin and incubate at 37°C for 5-7 minutes
- Add 9 ml of DMEM +++ to inactivate the trypsin
- Centrifuge for 3 minutes at 900 rpm
- Remove the supernatant
- Re-suspend the pellet into the appropriate amount of FAD
- Add "x" µl of counted NIH/3T3 (for the amount of the NIH/3T3 see the table 1)
- Mix with a cross movement

For the maintenance of the culture always split the keratinocytes 1:2.

Table 1: Amount of feeder for each type of support.

Type of support	Number of NIH/3T3 cells
Small flask	2.5 x 10^5 cells
Big flask	7 x 10^5 cells
6 cm^2 dish	1.5 x 10^5 cells
10 cm^2 dish	5 x 10^5 cells
6 wells dish	1 x 10^5 cells

4.2.4 CULTIVATION OF HNC136

The protocol of the split of the cells is the same used for the NIH/3T3 except for the incubation time at 37 ^{0}C with trypsin, which varies accordingly to the cell type.

This cells line can be maintained in culture in T75 or T150 flasks.

HNC136 are usually split 1:2 for maintenance.

4.2.5 CELLS COUNTING

- Put 10 μl of re-suspended cells in an Eppendorf
- Add 10 μl of trypan blue (allows to distinguish the vital from the not vital cells) and mix
- Take 10 μl of the mix and add them to the counting plate
- Read the concentration of cells in the counting machine (Biorad TC20 ™).

4.2.6 CRYOPRESERVATION AND THAWING OF MAMMALIAN CELLS

CRYOPRESERVATION

For cryopreservation, the cells were harvested by trypsinization and centrifuged. After centrifugation, the cell pellet was resuspended in 1ml cryomedium and the cell solution stored in cryotubes. Freezing of the cells was performed in a slow freeze chamber with

isopropanol at -80°C for at least 24h before the cells were transferred to liquid nitrogen. Using a container filled with isopropanol allows freezing the cells slowly by reducing the temperature at approximately 1°C per minute. When the cells are re-suspended in cryomedium put them immediately in the freezer to avoid the death of the cells (DMSO is toxic).

THAWING

- Take the cryotubes out of liquid nitrogen and thaw the cell solution by keeping in the hands (attention: once the cells are thaw, do the next steps immediately)
- Transfer 1 ml of cells in a falcon and add 10 ml of DMEM +++
- Centrifuge at 900 rpm for 3 minutes
- Discard the supernatant
- Gently resuspend the pellet in the appropriate medium.

When thawing the human keratinocytes, prepare in advance the inactivated feeder cells as described in paragraph 4.2.3.

4.2.7 CELL TREATMENTS

DOXORUBICIN

- Plate $3.5x10^5$ HFKs cells or HFKs cells expressing E6/E7 of the different HPVs in a well of a 6 well plate. Add the appropriate amount of feeder cells.
- After 24 hours remove the feeder as described in paragraph 4.2.3 and
- treat the cells with doxorubicin or DMSO
- collect the cells after 8 hours of treatment; preserve the 2/3 of the pellet in one 1.5 ml tube for future protein extraction and the remaining 1/3 of the pellet in another 1.5 ml tube for future RNA extraction.

MG132

- Plate 3.5x10^5 HFKs cells or HFKs cells expressing E6/E7 of the different HPVs in a well of a 6 well plate. Add the appropriate amount of feeder cells.
- After 24 hours remove the feeder as described in paragraph 4.2.3 and
- treat the cells with MG132 or DMSO
- collect the cells after 4 hours of treatment; preserve the 2/3 of the pellet in one 1.5 ml tube for future protein extraction and the remaining 1/3 of the pellet in another 1.5 ml tube for future RNA extraction.

CYCLOHEXIMIDE

- Plate 3.5x10^5 NIKs pLXSNØ cells or NIKs cells expressing E6/E7 of the different HPVs in a well of a 6 well plate.
- After 24 hours, treat the cells with cycloheximide or DMSO
- collect the cells after 1, 2, 4 and 6 hours of treatment.

4.2.8 siRNA KNOCK-DOWN

- Seed 4x10^5 HFKs or HFKs expressing E6/E7 in a well of a 6 wells-plate; add the appropriate amount of feeder cells.
- After 24 hours from the seeding, transfect the cells with the same 10 nM of scramble or siRNA using Lipo2000.
- After 6 hours replace the medium with fresh FAD without cholera toxin, Penicillin/streptomycin and Ciprofloxacin.
- After 24 hours replace the medium with complete FAD.
- After 48 hours from the transfection remove the feeder and collect the cells.

4.3 RETROVIRUS INFECTION

The retrovirus infection donor 1 has been performed in Heidelberg in a P2 plus laboratory by myself while the retrovirus infection donor 2 and 3 has been performed in Lyon in a P3 laboratory by Cecilia Sirand and Gessica Tore.

4.3.1 TRANSFECTION

Two days before transfection seed the Phoenix cells in 10 cm dishes, in this way they will be 50/70% confluent the day of the transfection.

Infect the Phoenix cells with the construct, following the protocol:

PREPARE THE DNA SOLUTION

- in a 15 ml Falcon mix the DNA (10 μg) with H_2O (to a volume of 440 μl) and 62 μl of $CaCl_2$ (2M)
- mix gently
- add 500 μl of HBS (2X) drop by drop
- shake with energy the solution

PREPARE THE PHOENIX CELLS

- remove the old medium from the Phoenix cell cultures
- add 5 ml of fresh medium
- add 5 μl of Chloroquine and gently mix

ADD THE DNA SOLUTION

- add the DNA solution drop by drop evenly distributing the solution in the dish
- transport the cells into the P3 laboratory

CHANGE MEDIUM

- after 6/8 hours wash twice the phoenix cells with DPBS
- add 5 ml of fresh medium.

CHANGE MEDIUM

- after 24 hours change the medium without the wash with DPBS

4.3.2 INFECTION

PREPARE RETROVIRAL SUSPENSION

- Collect medium of the transfected Phoenix cells and pass twice the medium through the 0.22 μm filter.
- Add 5 μl of Polybrene into each retroviral suspension

INFECT THE PRIMARY KERATINOCYTE

- Add the retrovirus suspension to the keratinocytes
- After 3 hours remove the retrovirus suspension
- Add fresh FAD medium

4.3.3 SELECTION

- Split the cells 1:1 and start the selection 24 hours after the infection using the neomycin.

Split 1:1 a flask of HPK not infected and add neomycin; when these cells die, the selection is over.

4.3.4 TEST FOR THE EXIT OF THE CELLS FROM THE P3

To exit the cells from the P3 it is necessary to prove that the transformed HPK cells do not produce viruses and so they are not dangerous anymore.

- Plate $0.5*10^5$ NIH/3T3 cells in a 6 wells plate for each transformed HFK line
- add the medium from the transformed HFK on the NIH/3T3 cells
- start the selection with neomycin
- When all the NIH cells die the transformed cells can go out of P3.

4.4 MOLECULAR METHODS

4.4.1 PURIFICATION OF PLASMID DNA

MINI-PREP

Isolation of plasmid DNA with the NucleoSpin® Plasmid mini prep kit was performed from a single bacterial colony previously cultured in 6 ml liquid LB medium containing the corresponding antibiotics. The preparation of plasmid DNA was performed according to manufacturer´s instructions.

MAXI-PREP

Isolation of plasmid DNA with the PureLink™ HiPure Plasmid Filter Maxiprep Kit was performed using 200ml LB medium with corresponding antibiotics which were inoculated with either 1 ml from a liquid bacterial culture or from a bacterial glycerol stock. The preparation of the plasmid DNA was performed according to manufacturer´s instructions

4.4.2 DNA VISUALIZATION

AGAROSE GEL ELECTROPHORESIS

To visualize the DNA or to purify the DNA after digestion, prepare the gel as follow. The percentage of agarose depends on the size of the DNA to visualize.

- In a jar prepare 0.5 g (for a 1% gel) or 0.4 g (for a 0.8% gel) of agarose and add 50 ml of TAE 1X.
- Cover the jar with his cap without closing it and put it in the microwave to the maximum heating until the agarose is completely melted.
- Under chemical hood add 1 µl of red gel and mix gently.
- Assembly the tray with the combs for the wanted number of wells.
- Pour the prepared solution into the tray and wait until the complete solidification.
- Remove the combs and put the tray into the electrophoretic system. The TAE 1X buffer must submerge completely the agarose gel.
- Load the samples in the wells.
- Close the electrophoretic system and set the voltage (85V for 40 minutes).

Before application of the DNA samples to the gel, the samples were mixed with 6x DNA loading dye in a ratio 1:6. To determine the size of the corresponding DNA fragments, a marker was loaded on the gel.

The DNA fragments were visualized with the ChemiDoc machine.

4.4.3 MOLECULAR CLONING

POLYMERASE CHAIN REACTION (PCR)

The Polymerase Chain Reaction (PCR) was performed to amplify the DNA sequences of interest for cloning into selected destination vectors. The DNA sequences were amplified using corresponding template DNAs encoding for the sequence of interest. Primers needed for the amplification process were generated as described in paragraph 3.5.3 and ordered as well as produced at MWG Eurofins, Ebersberg, Germany. Each Primer was generated for a specific cloning process, containing different restriction sites. The sites to be included in the primer sequence were selected depending on the specific destination vector used for later cloning steps.

All PCRs were performed using the HotStarTaq DNA Polymerase from Qiagen, according to the manufacturer´s instructions (table 2 and table 3). The annealing temperature (T_m) strongly depends on the primers used for the PCR reaction.

Table 2: reaction mix

	C_i	C_f	V
Buffer	10X	1X	2.5 µl
dNTP	10 µM	200 µM	1 µl
Primer forward	10 µM	0,3 µM	1.5 µl
Primer reverse	10 µM	0,3 µM	1.5 µl
HotStartTaq pol	5 U/µl	2,5 U/reaction	1 µl
DNA	//	//	1 µl
H_2O	//	//	To volume
			25 µl

Table 3: Standard PCR program

Temperature	Time	
95 °C	15 min	
94 °C	1 min	35 cycles
T_m	1 min	
72 °C	1 min/kb of DNA to extend	
72 °C	10 min	
4 °C	∞	

PCR PURIFICATION

For the purification of the fragment of DNA obtained from PCR, the QIAquick PCR Purification Kit from Qiagen was used. The purification procedure was carried out according to the manufacturer´s instructions. The DNA was eluted in 10 µl.

ENZYMATIC RESTRICTION OF PCR PRODUCTS

To prepare the PCR product for ligation into the target vector, the PCR products were doubled digested with the appropriate restriction enzymes. NEB restriction enzymes were used with CutSmart buffer after the compatibility for double digestion was checked on the NEB website. A mix was prepared as in table 4 and the samples were incubated at 37°C for 1 hour.

Table 4: standard PCR product digestion mix

	C_i	C_f	V_i
PCR amplified fragments	//	//	10 µl
Cut Smart Buffer	10X	1X	2 µl
Restriction enzyme 1	10 U/µl	0.27 U/µl	0.8 µl
Restriction enzyme 2	10 U/µl	0.27 U/µl	0.8 µl
H_2O	//	//	To volume
			20 µl

ENZYMATIC RESTRICTION OF VECTOR

To prepare the vector for ligation with the insert, the vector was doubled digested with the appropriate restriction enzymes. NEB restriction enzymes were used with CutSmart buffer after the compatibility for double digestion was checked on the NEB website. A mix was prepared as in table 5 and the samples were incubated at 37°C for 1 hour.

Table 5: standard vector digestion mix

	C_i	C_f	Volume per reaction
Vector	//	0,1 µg/µl	//
Cut Smart Buffer	10X	1X	3 µl
Restriction enzyme 1	10 U/µl	0.4 U/µl	0.8 µl
Restriction enzyme 2	10 U/µl	0.4 U/µl	0.8 µl
H_2O	//	//	To volume
			20 µl

GEL EXTRACTION

For purification of specific DNA fragments after enzymatic restriction, the QIAquick Gel Extraction Kit from Qiagen was used. After the DNA fragments were separated by agarose gel electrophoresis (paragraph 4.4.2), DNA was visualized with the help of a 254nm UV-light to excise the corresponding part of the gel for purification. The following purification procedure was carried out according to the manufacturer´s instructions.

LIGATION

The ligation mix was according to manufacturer´s instruction from Roche (see table 6). Vector DNA and insert were used in a molar ratio of 1:3. The ligation mix was either incubated at 16°C overnight.

Table 6: ligation standard mix.

	Volume per reaction
Vector DNA	X µl
Insert DNA	Y µl
T4 DNA ligase	1 µl
Buffer 10X	2 µl
H_2O	To volume
	20 µl

BACTERIAL TRANSFORMATION AND PLASMID DNA EXTRACTION

After the ligation, 5 µl of the ligation mix was used to transform *E.coli* bacteria as described in paragraph 4.1.1. The following day 5 colony of each transformation were incubated in 6 ml of LB with the appropriate antibiotics. The plasmid DNA was extracted using a NucleoSpin® Plasmid mini prep kit to be analyzed via analytic digestion.

ANALYTIC DIGESTION

To test isolated plasmid DNA for the absence or presence of a specific insert, 5µl of the DNA sample were used. For enzymatic restriction a master mix was prepared as in table 7 and the samples were incubated at 37°C for 1 hour. To analyze the restricted plasmid DNA, the digestion products were loaded on a agarose gel and visualized with the ChemiDoc machine.

Table 7: analytic digestion mix.

	C_i	C_f	V
PCR amplified fragments	//	//	5 µl
Cut Smart Buffer	10X	1X	2 µl
Restriction enzyme 1	10 U/µl	0.1 U/µl	0.2 µl
Restriction enzyme 2	10 U/µl	0.1 U/µl	0.2 µl
H_2O	//	//	To volume
			20 µl

SEQUENCING

Among the clones analyzed through mini prep and sub-sequential analytical digestion, only the ones with the insert were sent to sequencing to confirm the identity of the insert and the correctness of the sequence. All the sequences have been sent to and analyzed by GATC Biotech AG.

SITE DIRECTED MUTAGENESIS

For the site directed mutagenesis the "QuikChange Lightning Site-Directed Mutagenesis Kit" by Agilent Technologies was used. The manufacturer protocol was followed and for each mutant 100 ng of dsDNA template was used.

4.4.4 RNA MANIPULATION

RNA EXTRACTION

For the RNA extraction, the kit "NucleoSpin® RNA" by Macherey-Nagel has been used, following the manufacturer's instruction. To avoid degradation of RNA, keep the samples in ice until retro-transcription. The RNA concentration has been measured using the Nano-Drop machine.

RETRO-TRANSCRIPTION

For the retro-transcription, the kit "RevertAid H Minus Reverse Transcriptase" by Thermo Scientific has been used. After the extraction of the RNA the following protocol has been followed:

- Prepare the mix as table 8:
- Mix gently and centrifuge briefly
- Incubate at 70 °C for 5 minutes, then put in ice and centrifuge briefly
- With the samples in ice add the reagents as table 9:
- Mix gently and centrifuge briefly
- Incubates 5 minutes at room temperature
- Add the 1 μl of retro-transcriptase enzyme
- Incubate 10 minutes at 25°C, 1 hour at 42°C and 10 minutes at 70°C.

Table 8: RNA-primer mix.

RNA (800 ng)	X μl
Primer random	1 μl
H_2O	To volume
	12 μl

Table 8: dNTPs mix.

Buffer 5X	4 μl
Riboblock inhibitor	1 μl
dNTP	2 μl

REAL TIME RETRO-TRANSCRIPTASE PCR (REAL TIME RT- PCR)

- Prepare the mesa green mix as in table 9 (for each sample of each couple of primers):
- Vortex the mix and briefly centrifuge it

- Prepare the cDNA mix as in table 10 (for each sample of each different DNA sample):
- Vortex the mix and briefly centrifuge it
- Add the mesa green mix to the plate wells
- Add 9.2 of the cDNA mix to each well
- Close with the proper plastic foil
- Briefly centrifuge the plate
- Put the plate in the qPCR machine and set the program as in table 11:

Table 9: Mesa green mix.

Mesa green	10 µl
primer forward (10 µM)	0.4 µl
primer reverse (10 µM)	0.4 µl

Table 10: cDNA mix.

H_2O	6.7 µl
cDNA	2.5 µl

Table 11: Standard Real time RT-PCR program.

Temperature	**Time**	
95 °C	10 min	
95 °C	15 s	45 cycles
60 °C	45 s	
72 °C	45 s	
95 °C	1 min	
55 °C	30 s	
95 °C	30 s	

4.5 PROTEIN ANALYSIS

4.5.1 PROTEIN EXTRACTION

During the protein extraction the pellet, the IP solution and the proteins were always kept on ice to avoid degradation. An adequate amount of IP buffer (paragraph 3.6.2) was used to re-suspend the pellet. After incubation on ice for 30 minutes, the lysate has been centrifuged at 13000 rpm and the supernatant collected and used for further analysis or stored at -20 °C.

4.5.2 DETERMINATION OF PROTEIN CONCENTRATION BY BRADFORD ASSAY

To determine the concentration of protein of a specific sample, a BSA calibration curve was generated by titration. Therefore a 10 μg/μl BSA stock solution was diluted in H2O to get a final concentration of 2 μg/μl BSA. From this BSA dilution a 1:2 dilution series was prepared up to 0.125 μg/μl . The BSA dilutions were analyzed with the Bradford Assay and a curve of concentrations and absorbance values was generated.

Following the preparation of the calibration curve, the samples were analyzed:

- For each sample prepare 2 ml of reagent A + 40 μl of reagent B
- Prepare also a "blank" sample without protein
- Mix and add 1 ml in a cuvette for protein
- Add 5 μl of protein extract
- Add another 1 ml of reagents mix to the cuvette
- Incubate at 37 °C for 30 minutes
- Read the OD at the spectrophotometer at 562 nm wavelength

4.5.3 LAMBDA PROTEIN PHOSPHATASE (PP) TREATMENT.

The lambda protein phosphatase enzyme detaches the phosphoryl group from the phosphorylated serine, threonine and tyrosine residues of a protein. To 20 μg of protein

extract, 1 µl of NEB "Lambda Protein Phosphatase (Lambda PP)" and the appropriate amount of buffer were added. The reaction mix was incubated for 30 minutes at 30°C.

4.5.4 ACRYLAMIDE GEL

SDS-polyacrylamide gels were prepared by combining two kinds of gels with different pore size and pH, the stacking gel (3% polyacrylamide, pH 6.8) and the running gel (percentage of polyacrylamide depending on the experiment, pH 8.8). After the polymerization of the SDS polyacrylamide, the ready-to-use gel was placed into the destined running system and the 1X running buffer was added.

Twenty µg of protein samples were prepared by adding 6X loading buffer (containing SDS and β-mercaptoethanol) and water to a final volume of 20 µl. The samples were denaturized at 95°C for 10min.

The samples were loaded into the wells of the SDS polyacrylamide gel and 5 µl of a protein ladder was loaded into a well for use as size standard. Until the proteins reached the interface of stacking gel to separation gel the power was set to 80V and increased afterwards to 120V for separation of the proteins according to their molecular weight.

4.5.5 WESTERN BLOT ANALYSIS

TRANSFER

For western blot analysis, the proteins had to be transferred from the SDS-polyacrylamide gel to the PVDF (Polyvinylidene fluoride) membrane, where the proteins could be analyzed by specific antibody detection. The hydrophobicity of PVDF makes it an ideal support for binding proteins in electrophoretic blotting applications. Because of the hydrophobic nature of PVDF, it does require a pre-wetting step in methanol of 15 seconds. PVDF is resistant to solvents and, therefore, these membranes can be easily stripped and reused to look at other proteins.

After the activation of the PVDF membrane in methanol, the transfer "sandwich" has been prepared as in figure 12 The transfer method is "wet", therefore the preparation of the "sandwich" has been performed in a tray with 1X transfer buffer.

To increase the efficiency of the transfer, the transfer buffer was maintained cold with a cooling unit and through continuous stir. The transfer was then performed at 120mA/per gel for 90 min to ensure an adequate transfer of all proteins to the membrane.

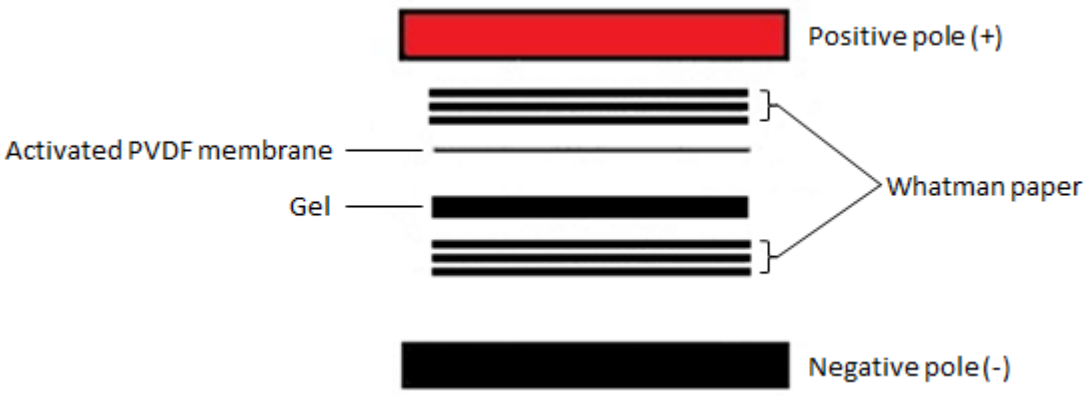

Figure 12: Layers of the transfer sandwich. The proteins in the SDS-page are negatively charged and transfer from the negative to the positive pole. The gel is position close to the negative pole and the activated PVDF membrane is laid above the gel, close to the positive pole. Three layers of Whatman paper are positioned at the extremities of the sandwich to protect the PVDF membrane and the gel.

MEMBRANE BLOCKING

After the transfer of the protein from the gel to the membrane, to block remaining protein binding sites on the PVDF membrane, the membrane was incubated in 10% skim milk dissolved in PBS-tween at room temperature for 1h incubate.

PRIMARY ANTIBODY

The primary antibody solution, directed against the protein of interest, was prepared with 5% skim milk in PBS-tween. The antibody dilution was decided following the manufacturer's instruction (usually 1:1000 dilutions).

After a brief wash of the membrane with PBS-tween, the primary antibody solution has been incubated overnight at 4 °C on the rocking platform shaker.

SECONDARY ANTIBODY

After incubation with the primary antibody, excess antibody was removed by washing the membrane three times with PBS-tween for 10min. The corresponding secondary antibody conjugated with horse reddish peroxidase (HRP) was diluted 1:2000 in 5% skim milk in

PBS-tween and added to the membrane at room temperature for 1h. The previously described washing steps were repeated after incubation of the secondary antibody to remove unbound antibody from the membrane.

DEVELOP

For detection of the proteins solution A, containing luminol plus enhancer and solution B, a peroxide solution of the chemiluminescence kit (paragraph 3.6.5) were mixed in a 1:1 ratio and the membrane was incubated in the substrate solution for 1min. The position of the bound secondary antibody and therefore indirectly the protein of interest were visualized using a Chemidoc machine.

STRIPPING

The removal of primary and secondary antibodies from a western blot membrane is useful when one wants to investigate more than one protein on the same blot. After the wash of the membrane at room temperature for 15 minutes in PBS-tween, the membrane was incubated with the stripping solution (Paragraph 3.6.5) at room temperature for 15 minutes. The membrane was then washed with PBS-tween and re-activated with a brief passage in methanol. After a wash with PBS-tween, the membrane was blocked with milk 10% for 1h at room temperature.

4.6 MALTOSE BINDING PROTEIN (MBP) PULLDOWN

4.6.1 PREPARATION OF BEADS

PRODUCTION OF FUSION PROTEINS

The fusion proteins have been produced in *E. coli* Rosetta, a strain engineered to produce recombinant proteins. The following protocol has been used:

- Transform E.coli Rosetta cells and plate on agarose LB+ kan dishes
- Grow the bacteria in LB+KAN till the OD600 of 0.6
- Collect 1 ml of "Not Induced" bacteria
- Add 0.5 mM of IPTG and grow the cells for 2 hours at 37°C
- Collect 1 ml of "Induced" bacteria

- Harvest the cells by centrifugation
- Centrifuge the "induced" and "not induced" bacteria, remove the supernatant and resuspend in 100 µl of Laemmli loading buffer. Load on a SDS-page to see the production of the fusion proteins

PRODUCTION OF MAGNETIC BEADS WITH FUSION PROTEINS

To obtain magnetic beads with the fusion proteins that can be used later for the pulldown, the lysate from the induced bacteria was incubated with amylose magnetic beads. The following protocol has been used:

- Re-suspend the pellet in 1 ml MBP buffer
- Disrupt the cells by sonication (in ice)
- Centrifuge for 30 min at 4°C at 5000 rpm
- incubate the supernatants with 50 µl of amylose magnetic beads for 1 h at 4°C
- wash 8 times with MBP buffer
- store the beads in 10 µl aliquots

4.6.2 CELL EXTRACT PREPARATION

The cells of interest were harvest and lysate with an appropriate amount of IP lysis buffer and the protein concentration was measured with the Bradford Assay.

4.6.3 PULLDOWN

PRE-CLEARING

A pre-clearing step was performed to decrease the non-specific binding of the cell proteins to the maltose binding protein. The cell protein extract was incubated at 4°C for 1 hour on a rotating wheel with 10 µl of MBP-GFP beads.

INCUBATION

10 µl immobilized maltose binding protein (MBP) fusion proteins were incubated with 600 µg of pre-cleared protein for 2h at 4 °C. After the incubation 8 washes with MBP buffer were performed to remove all the not-bound proteins.

4.6.4 WESTERN BLOT

After the washes, the beads were re-suspended in 15 µl of Laemmli buffer and denatured for 10 min at 95°C. The beads, as well as 5 µl of input cell lysate, have been loaded on SDS-polyacrylamide gel and a western blot has been performed as described in paragraph 4.5.5. In addition, the membrane has been stained with Red Ponceau for the identification of the fusion proteins.

4.7 MICROARRAY-BASED WHOLE GENOME EXPRESSION PROFILING AND DATA ANALYSIS

The micro array experiment was performed by Genetic Cancer Susceptibility Group at IARC (Lyon, FR). The analysis of the micro array data was performed in collaboration with the bio-informatician of Infection and Cancer Biology group (Lyon, FR).

4.7.1 RNA QUALITY CONTROL

RNA concentration and purity were evaluated with the Nanodrop® (Thermo Scientific). RNA integrity and quantification were characterized by measuring the 28s/18s rRNA ratio and RIN (RNA Integrity Number) using the Agilent 2100 bioanalyzer instrument and the RNA 6000 Nano kit. The RIN software classifies the integrity of eukaryotic total RNAs on a scale of 1 to 10, from most to least degraded.

4.7.2 MICRO ARRAY

Genome-wide gene expression profiling analysis was performed on Illumina HumanHT-12 v4 Expression BeadChips (24,000 annotated genes covered). Candidate probe sequences included on the HumanHT-12 v4 Expression BeadChip derived from the NCBI RefSeq (Build 36.2, Rel22) and the UniGene (Build 199) databases. Using the Illumina TotalPrep RNA Amplification Kit (Ambion®), 500 ng of extracted RNAs were converted to cDNAs and subsequent biotin labelled single-stranded cRNAs. The distribution of homogeneous in vitro transcription products (cRNAs) was checked with the Agilent 2100 bioanalyzer instrument and the RNA 6000 Nano kit. 750 ng of biotin labelled cRNAs of the 7 samples (including 2 controls) were hybridized overnight to 4

HumanHT-12 Expression BeadChips. Subsequent steps included washing, streptavadin-Cy3 staining and scanning of the arrays on an Illumina BeadArray Reader. The Illumina Genome Studio V2010.2 was used to obtain the signal values (AVG-Signal), with no normalization and no background subtraction. Data quality controls were performed using internal controls present on the HumanHT-12 beadchip and were visualized as a control summary plot and for each sample as noise-to-signal ratios calculated by P95/P05 signal intensities. All samples had P95/P05 >10, defined as sample quality threshold

The microarray experiments are MIAME compliant and have been deposited at the NCBI Gene Expression Omnibus (GEO) database (http://www.ncbi.nlm.nih.gov/geo) under accession GSE100681.

4.7.3 DIFFERENTIAL EXPRESSION ANALYSIS

Differential expression analysis was performed using BRB-ArrayTools software v4.2. The raw signal intensities of all samples were log-transformed and quantile normalized without background subtraction with the exclusion of any probe showing excess dispersion (defined by more than 85% of individual probe values differing from the median by more than 1.5-fold). Class comparison for Microarray Analysis using the t-test method was performed for identification of differentially expressed probes. Probes with a p-value of < 0.001, with a minimum of 1.5-fold change and a False Discovery rate (FDR) of <0.01 were considered significantly differentially expressed. The different condition was then hierarchically clustered (complete-linkage clustering) based on the Pearson distance of the log2 fold change value for each gene

4.7.4 HEATMAP

The heatmap was generated with the use of "heatmap.2" function available under "gplots" package version 3.0.1 with R version 3.4.3.

The different conditions were hierarchically clustered (complete-linkage clustering) based on the Pearson distance of the log2 fold change value for each gene.

4.7.5 PATHWAY ANALYSIS

The genes de-regulated in each condition were analyzed for pathway enrichment using the Erinchr software and the KEGG database (2016 version) was used as annotated gene set. The results were ranked based on the combined score and represented in histograms.

4.7.6 COMPARATIVE ANALYSIS

The genes de-regulated in each β3 expressing HFKs were compared to the genes de-regulated in HPV16 and HPV38 expressing HFKs using Venny software (http://bioinfogp.cnb.csic.es/tools/venny/). From the number of genes shared between each β3 type and HPV16 or HPV38 a percentage of shared genes was calculated.

4.8 LC/MS SUPERNATANT ANALYSIS

4.8.1 SAMPLE PREPARATIONS

The samples were filtering the precipitate with 0.2 μm Captiva ND plates (Agilent Technologies) into a polypropylene well plate. The plate was then sealed with a Rapid EPS well plate sealing tape (BioChromato) and kept at 4°C until analysis. Quality control (QC) samples were prepared from a pool created from small aliquots of all study samples.

4.8.2 ANALYTICAL METHODS AND INSTRUMENTATION

All of the samples were analyzed by mass spectrometry (MS) by using a 6550 quadrupole time-of-flight mass spectrometer coupled to a 1290 Infinity UHPLC system (Agilent Technologies).

Analysis of the sample batch was initiated with 10 priming injections of the QC sample to achieve a stable instrument response. Study samples were injected in a randomized order, and the same QC sample was injected every 10 samples to monitor instrument performance and sample stability over the course of the entire data acquisition. The same batch of samples was successively analyzed by reversed-phase (RP) chromatography. The RP analysis was performed on a Waters Acquity UPLC HSS T3 column (1.8 μm, 2.1 ×

100 mm) at 45°C. A flow rate of 0.4 mL/min was used with a linear gradient of 0.05% formic acid in water (eluent A) and 0.05% formic acid in methanol (eluent B). The gradient profile was as follows: 5–100% eluent B from 0 to 6 min and 100% eluent B from 6 to 10.5 min, followed by a 2-min equilibration with 5% eluent B.

The mass spectrometer was operated in positive electrospray ionization (Pos) mode with the use of the following conditions: drying gas (nitrogen) temperature, 175°C; drying gas flow rate, 12 L/min; sheath gas temperature, 350°C; sheath gas flow rate, 11 L/min; nebulizer pressure, 45 pounds/square inch; capillary voltage, 3500 V; nozzle voltage, 300 V; and fragmentor voltage, 175 V. Data acquisition was performed by using a 2-GHz extended dynamic range mode across a mass range of 50–1050 m/z. The scan rate was 1.67 Hz, and data acquisition was in centroid mode. Continuous mass axis calibration was performed by monitoring 2 reference ions from an infusion solution throughout the runs (m/z 121.050873 and m/z 922.009798). Data were acquired by using MassHunter Acquisition B.05.01 (Agilent Technologies).

4.8.3 RAW DATA PREPROCESSING AND FILTRATION

Preprocessing of the acquired data was performed by using MassHunter Qualitative Analysis B.06.00, DA Reprocessor, Mass Profiler Professional 12.1 and Profinder B 06.00 software (Agilent Technologies). Recursive feature extraction was used to find compounds as singly charged proton adducts [M+H]+. Initial data processing was performed by using MassHunter Qualitative Analysis with a Molecular Feature Extraction algorithm set to small molecules. Threshold values for mass and chromatographic peak heights were set to 1500 and 10,000 counts, respectively. Two mass peaks were required for a molecular feature, and the peak spacing tolerance for grouping of isotope peaks was 0.0025 m/z + 7 parts per million (ppm), with the isotope model set to common organic molecules. Data were filtered to keep MS features, which were matched to metabolites in either the Human Metabolome Database or the METLIN database on the basis of their accurate mass (±10 ppm mass error), and only retain features that may be more easily identified in subsequent analyses.

5 RESULTS

5.1 *IN VITRO* TRANSFORMING ABILITIES OF β3 HPV E6 AND E7 PROTEINS

As a first step of the experimental activities, the transforming abilities of E6 and E7 derived from the four β3 HPV types (HPV49, 75, 76 and 115) were evaluated in HFK cells.

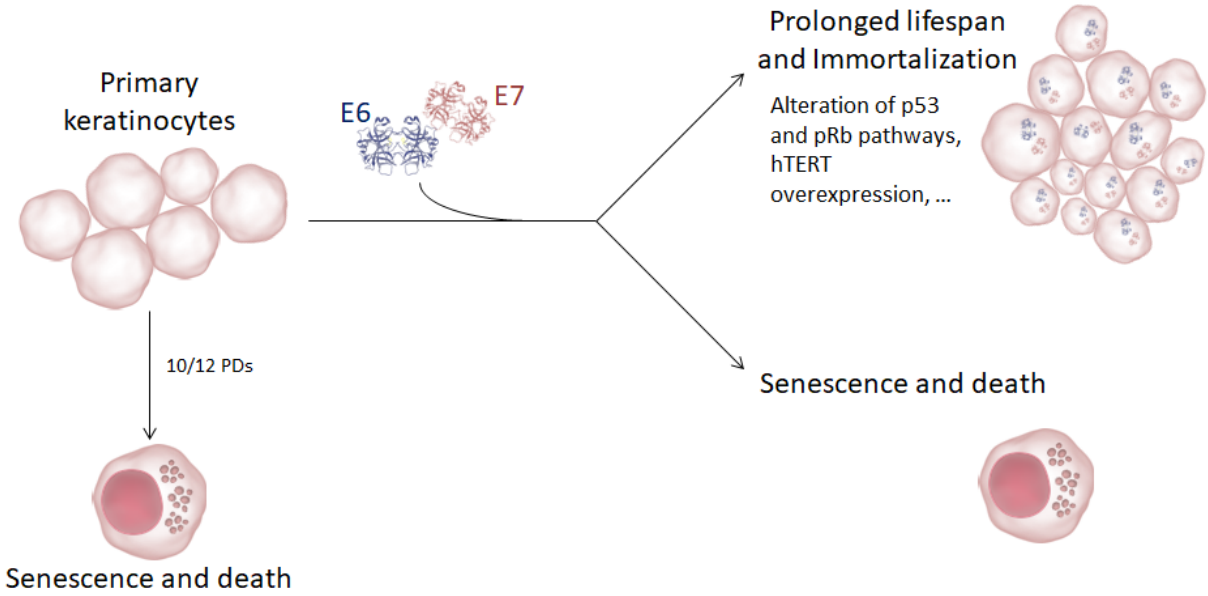

Figure 13: Schematic representation of HFKs cellular fate in the absence or presence of E6 and E7. In monolayer culture, the HFKs enter senescence and eventually die after approximately 10-12 PDs. In the presence of E6/E7 from different HPV types, cells either enter into senescence and die or have a prolonged lifespan that can ultimately lead to the immortalization of the keratinocytes. The prolongation of the lifespan requires alteration of different cellular pathways such as p53, pRb and hTERT.

In vivo, keratinocytes located at the basal layer are able to maintain a stem cell-like property while the keratinocytes located in the parabasal layers commit to a differentiation program and gradually exit from the cell cycle. In an *ex-vivo* setting, such as monolayer culture, the lifespan of HFKs is limited to around 10-12 Population Doubling (PDs). After this brief period of time, the cells enter into senescence and eventually die by autophagic programmed cell death [143]. The senescent cells can be recognized under the

microscope by their characteristic appearance: 5- to 100-fold larger size than young cells, numerous dense particles that are probably protein aggregates and several vacuole-like structures of various sizes [143, 144].

Many studies have shown that stable expression of E6 and E7 from certain HPV types such as HPV16 leads to an extension of HFK lifespan and immortalization. This behavior is schematically shown in Figure 13.

In the context of a natural infection, the E6 and E7 ORFs are transcribed as a single polycistronic mRNA. To accurately mimic this in the tissue culture setting, the β3 genome fragment covering the two entire ORFs was cloned into the retroviral vector pLXSN. In addition to the four β3 HPV types, the E6 and E7 proteins from HPV16, which are known to immortalize cells *in vitro,* were included as a positive control. The retroviral expression system was chosen to minimize possible artifacts due to ectopic expression of viral proteins. Indeed, in the retroviral vector pLXSN, the two potential onco-proteins are expressed under the control of a weak promoter. In addition, retroviral transduction results in a single-copy integrant into the host cell, avoiding high expression of E6 and E7. To produce recombinant retroviruses, the different pLXSN constructs were transfected into the packaging cell line Phoenix, as described in the chapter "Methods". The pLXSN vector expresses a neomycin-resistance marker under the control of an independent promoter. Therefore, the retro-transduced HFKs were selected using media supplemented with neomycin. The expression of the E6/E7 polycistronic transcript was determined by RT-PCR. As shown in Fig. 14, the HPV76 E7 PCR primers also amplify HPV49 and 75 mRNA, possibly due to genome similarities within the β3 species. On the contrary, primers for HPV49, 75 and HPV115 showed high specificity and only amplified the intended target sequence (Fig. 14). To confirm that the immortalized HFKs expressed the specific β3 HPV genes and no cross-contamination of the different HFK lines occurred during long term culture, additional analysis was performed at various stages during the long term experiment. DNA from the different cell lines was extracted and the E6/E7 region amplified using universal primers (designed on the plasmid). The resulting PCR product was then sent for sequencing. The results

obtained from the sequencing showed that all the cell lines contained the correct plasmid at all the time points (data not shown).

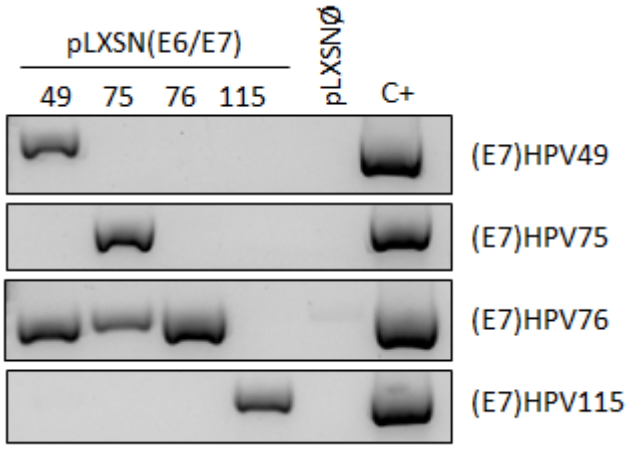

Figure 14: Transduced HFKs express the correct polycistronic E6/E7 mRNA. Total RNA was extracted from HFKs transduced with the indicated retroviruses and subject to retro-transcription to form cDNA. PCR was performed using the indicated cDNA template with HPV-specific primers or the corresponding vector preparation as a positive control (C+).

The immortalization assay was performed on HFKs from three different donors, in order to assess the eventual effect of the genetic background of the donor on the immortalization abilities and the biological properties of E6 and E7.

In the first and second donor, expression of HPV49 and 76 E6/E7 proteins induced the continuous growth of the HFKs, which have now reached more than 100 PDs, as shown in figure 15A and Table 12. By contrast, HPV115 E6/E7-transduced HFKs were only able to proliferate for a few PDs and died approximately at the same time of the HFKs transduced with empty pLXSN (donor 1), or at the end of the drug selection process (donors 2 and 3) (Fig. 15A and Table 12). Interestingly, HPV75 E6/E7 HFKs from donor one appeared to proliferate less than HPV49 and 76 E6/E7 HFKs derived from the same donor background and only reached approximately 60 PDs, despite being in culture for the same amount of time (Fig. 15A and Table 12). However, no difference was observed in the proliferation rate of HPV49, 75 and 76 E6/E7 HFKs from donor 2 (Table 12), suggesting that, at least for HPV75 E6/E7, the efficiency in promoting cellular proliferation may be influenced by the genetic background of the donor. HFKs from the third donor was cultured for a number of days not sufficient to draw a conclusion about

the immortalization abilities. Moreover, HFKs from a fourth donor expressing E6 and E7 from HPV76 was generated and kept in culture for 60 PDs (data not shown). As shown in figure 15A, HFKs expressing HPV16 E6/E7 grow continuously and reach immortalization with a higher proliferation rate compared to HPV49 or HPV76 E6/E7 expressing keratinocytes.

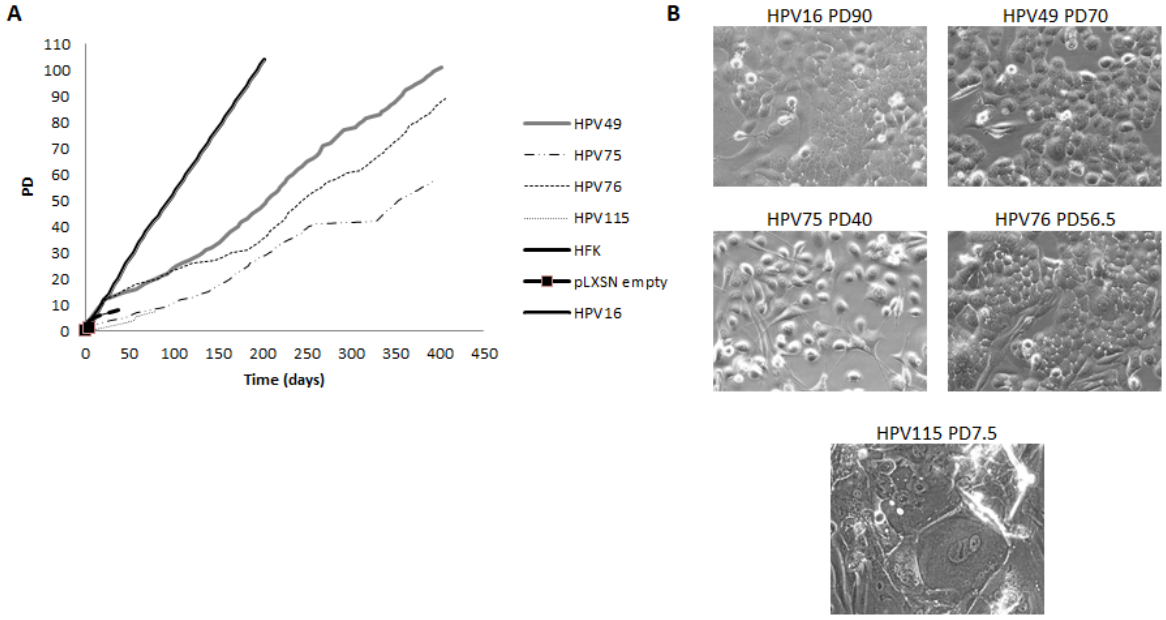

Figure 15: Stable expression of β3 E6/E7 proteins have different outcomes on the lifespan of primary keratinocytes. (A) Growth curve of human foreskin keratinocytes (donor 1) expressing E6/E7 from the indicated HPVs. (B) Morphology of human foreskin keratinocytes transduced with the indicated recombinant retroviruses at the indicated PDs. The elongated cells visible in the microphotographs are NIH/3T3 fibroblasts. The same magnification was used for all the microphotographs (20X).

In line with the low proliferative rate, the microphotographs in figure 15B show that HPV115 E6/E7 HFKs displayed features of arrested and senescent cells, such as irregular shape, intercellular bridges and large and multi-nucleated cells. By contrast, HFKs expressing the E6/E7 proteins of the other β3 HPV types, as well as of HPV16, showed the typical morphology of highly proliferative cells characterized by small size, high brightness and regular shape (Fig. 15B).

As HFKs expressing HPV115 E6/E7 had a reduced lifespan in all donor backgrounds, it was not possible to include them in the downstream analysis, shown in the following paragraphs.

Table 12: **Immortalization abilities of β3 types E6/E7 in three different donors.** E6 and E7 from β3 HPV differentially affect the cell growth ability when retro-transduced in primary keratinocytes. Population doublings (PD) reached to date by the indicated keratinocytes (from 3 different donors) stably expressing E6 and E7 of β3 HPVs or carrying the empty retroviral vector (pLXSNØ). (*Not Done)

Retrovirus	Donor 1	Donor 2	Donor 3
pLXSNØ	Dead at 1 PD	Dead at 1 PD	Dead at 1 PD
pLXSN(E6/E7)HPV49	108 PD (immortalized)	102 PD (immortalized)	5 PD
pLXSN(E6/E7)HPV75	63.5 PD	101 PD (immortalized)	ND*
pLXSN(E6/E7)HPV76	101 PD (immortalized)	101 PD (immortalized)	6 PD
pLXSN(E6/E7)HPV115	Dead at 7.5 PD	Dead at 1 PD	Dead at 1 PD

5.2 β3 TYPES 49, 75 AND 76 E6/E7 EFFICIENTLY ALTER CELL CYCLE-RELATED PATHWAYS

5.2.1 pRb PATHWAY IS ALTERED IN β3 HPV E6/E7 HFKs

The extension of lifespan and immortalization of primary cells are intimately linked to the deregulation of the cell cycle. Many previous studies showed that E7 from different α and β types are able to inhibit the pRb pathway, promoting unscheduled S-phase entry (see chapter 1).

A previous study focusing on β3 type 49 showed that this E7 can inactivate pRb via hyper-phosphorylation (see paragraph 1.2.3) [138]. This mechanism is different from the one used by HPV16 E7, which binds pRb and leads to its degradation by proteasome pathway (see paragraph 1.2.1).

As there appears to be a difference in the mechanism used by HPVs to inactivate the pRb pathway, the status of pRb in HFKs expressing E6/E7 from β3 HPV types 49, 75 and 76 was determined. As shown in figure 16A, HPV49, 75 and 76 E6/E7 HFKs have high levels of total pRb compared to both control cells (HFKs) and HPV16 E6/E7 HFKs. Immunoblotting using a specific antibody against pRb phosphorylated at Serine795 (pRb Ser795) showed a band in all the analyzed β3 types but not in control HFKs or HPV16 E6/E7 expressing HFKs (fig. 16A). To further prove the phosphorylation status of pRb, protein, extracts of control HFKs or E6/E7 expressing HFKs were treated with lambda protein phosphatase (λ-PP) for 30 minutes. λ-PP is a Mn^{2+}-dependent protein phosphatase that releases the phosphate group from phosphorylated serine, threonine and tyrosine residues. After λ-PP treatment, the band corresponding to the phosphorylated-pRb was no longer visible for all the β3 types (fig. 16A). Thus, all these three β3 HPV types are able to promote pRb phosphorylation, while in HPV16 E6/E7 HFKs, as expected, pRb was not detectable in both the total or phosphorylated (Ser795) forms. The experiment was repeated three times in cells derived from two different donors (data not shown), and slight differences in the efficiency in promoting pRb phosphorylation were detected; these differences are most likely due to the different proliferative status of the cell cultures. However, in all experiments, the band detected with the antibody against

phosphorylated pRb (Ser795) was considerably higher in abundance than the one detected in the control HFKs.

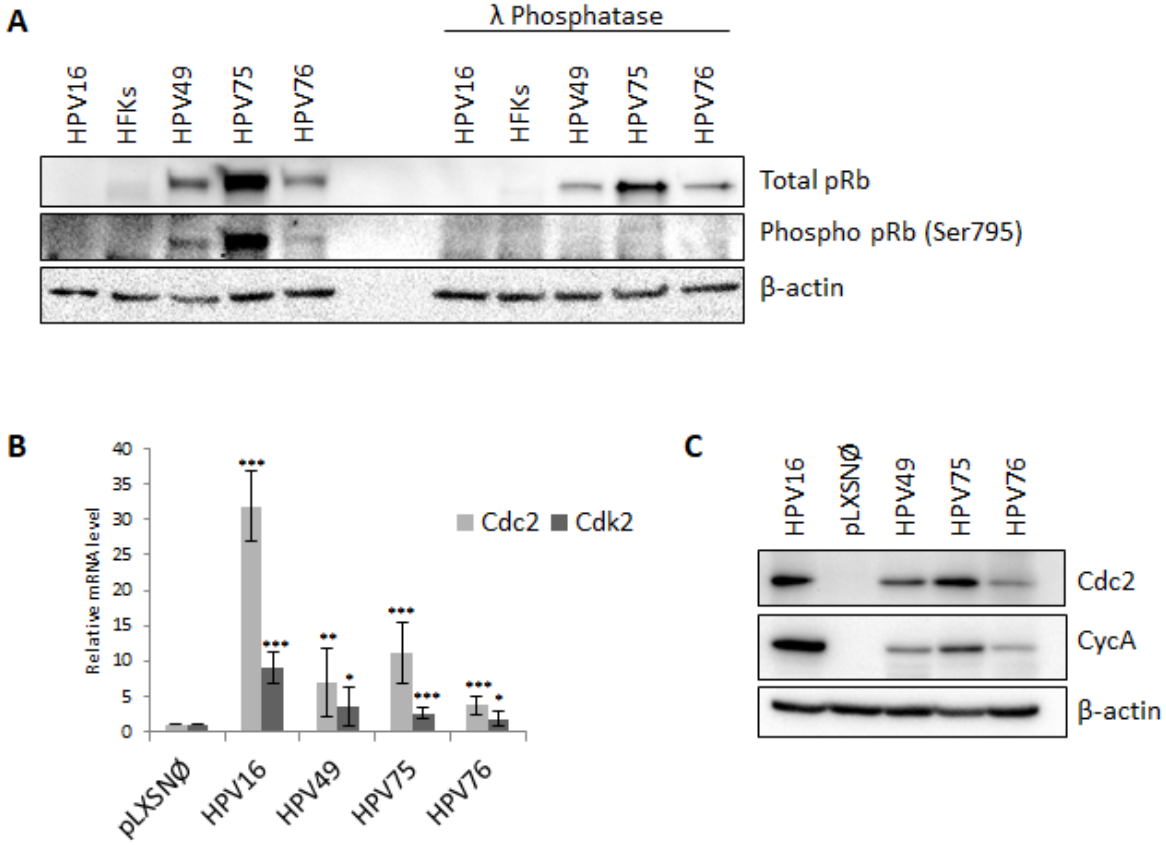

Figure 16: β3 E6/E7 proteins alter pRb function in cell cycle control. (A) Protein extracts from HFKs or from those expressing E6/E7 of the indicated HPV types were incubated for 30 minutes at 30°C in presence or absence of lambda phosphatase (λ-pp). Samples were analyzed by immunoblotting using total pRb, phosphorylated pRb (Ser795), and β-actin antibodies. (B) Retro-transcribed total RNA was used as a template for real-time PCR with primers specific for cdc2, cdk2 gene or GAPDH. Cdc2 and cdk2 expression levels were normalized to GAPDH levels. The result shown in the histogram is the mean of a total of six independent experiments performed in keratinocytes from two independent donors. (C) Protein extract from HFKs or transduced HFKs expressing E6/E7 of the different β3 types were analyzed by immunoblotting using cdc2, cyclin A and β-actin antibodies.

As mentioned in chapter 1, the destabilization of pRb, either through degradation or phosphorylation, results in the release of E2F1-DP complex, which in turn induces the expression of genes encoding positive regulators of cell cycle, such as cdc2 and cyclin A [65, 66]. Accordingly, an increase in the mRNA levels of cdc2 and cdk2 was observed in HFKs expressing E6/E7 from β3 types as well as HPV16, compared to control HFKs

(pLXSNØ) (fig. 16B). Reflecting the higher rate of growth of HFKs expressing E6/E7 from HPV16 (fig. 15A) compared to β3 E6/E7 HFKs, higher level of cdc2 and cdk2 mRNA levels were observed in HPV16 E6/E7 HFKs in comparison to the β3 HFKs (fig. 16B). Moreover, the protein levels of the two cell cycle effector proteins cdc2 and cyclin A (CycA) were assessed by immunoblotting (fig. 16C). In line with the mRNA level shown in figure 16B, the protein level of cdc2 was detectable at higher level with a specific antibody in the cells expressing E6/E7 from HPV16 and all the β3 types when compared to the HKFs expressing the empty vector (pLXSNØ) (fig. 16C). Another gene regulated predominantly by the E2F complex is cyclin A, a cyclin associated with the passage of the transition point between G_1 and S phase. As seen in figure 4C, CycA protein levels were higher in HKFs expressing E6/E7 when compared to control HFKs. This data indicates that the cells are indeed in active proliferation.

5.2.2 $p16^{INK4a}$ PATHWAY IS ALTERED IN β3 HPV E6/E7 HFKs

Previous studies showed that the cell cycle deregulation mediated by HR HPV16 onco-proteins is associated with an accumulation of the cell cycle inhibitor $p16^{INK4a}$ [81]. This event appears to be specific for the alpha HR HPV types since HFKs immortalized by β2 HPV38 E6 and E7 do not express $p16^{INK4a}$ (unpublished data).

Therefore, the levels of $p16^{INK4a}$ were determined in HFKs expressing E6/E7 from HPV16 as a positive control, HPV38 as a negative control alongside the β3 HFKs (fig. 17A and 17B). As shown in the immunoblot in figure 17A, accumulation of $p16^{INK4a}$ was detected in HFKs expressing HPV49, 75 or 76 E6/E7 (fig. 17A) compared to control HFKs. However, $p16^{INK4a}$ accumulation was much higher in HPV16 E6/E7 expressing HFKs than in those expressing the β3 E6/E7 proteins (fig. 17A and 17B). The differences between HPV16 and the β3 types in $p16^{INK4a}$ accumulation reflect the differences in efficiency in altering the expression of cell cycle regulators (such as cycA and cdc2), shown in figure 16B and 16C. In addition, $p16^{INK4a}$ signal was not detected in the HPV38 E6/E7 expressing cells, confirming the previous observation and indicating that β2 and β3 HPV types interfere with the cell cycle by distinct mechanisms.

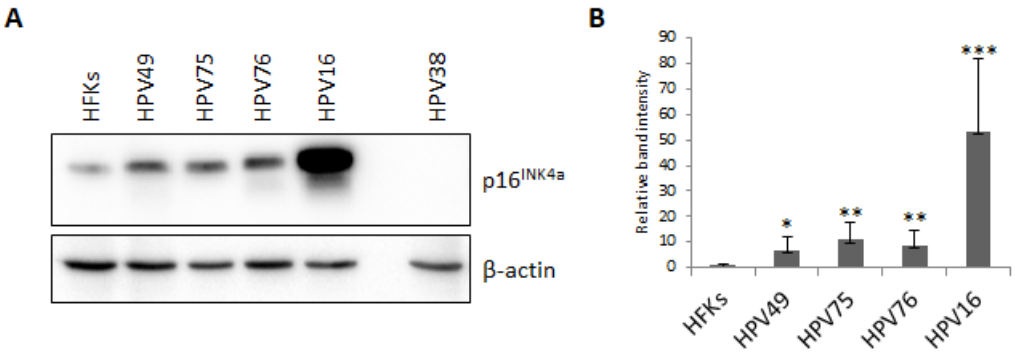

Figure 17: β3 E6/E7 proteins promotes p16^{INK4a} accumulation in primary keratinocytes. (A) Protein extracts from HFKs or transduced HFKs expressing E6/E7 of the different β3 types were analyzed by immunoblotting using p16^{INK4a} and β-actin antibodies. (B) Band intensities were quantified, normalized to β-actin levels, and then displayed relative to the control HFK cells. Data shown represented five independent experiments performed in two independent keratinocytes donor. (*P<0.05, ** P<0.01, ***P<0.005).

5.3 p53 IS DEGRADED VIA PROTEASOME PATHWAY IN β3 HPV E6/E7 HFKs

As described in paragraph 1.21, the second key step towards the immortalization of the keratinocytes is the alteration of p53 functions, with a bearing on cell cycle arrest and apoptosis.

Several studies have shown that different HPV types use distinct mechanisms to alter the function of the tumour suppressor p53 [12]. To date, HPV49 E6 is the only known β HPV onco-protein that shares the same mechanism of HR HPV16 E6 in promoting p53 degradation, via the interaction with E6AP and the proteasome pathway [138]. Therefore, the ability of the other β3 types to degrade p53 was tested.

Immunoblotting analysis using a p53 specific antibody showed that p53 basal levels (-Doxo) were lower in β3 E6/E7 expressing HFKs when compared to control HFKs (fig. 18A). In the same condition, p53 was not detectable in HFKs expressing HPV16 E6/E7.

In uninfected cells, p53 levels accumulate following cellular stress whereby p53 exerts its function as a cell cycle arrest effector, eventually promoting apoptosis. By contrast in HPV16 infected cells, p53 is not only degraded in normal conditions but also in the condition of cellular stress, allowing continuous proliferation [58]. To establish whether the β3 E6/E7 proteins could counteract p53 function in both stressed and non-stressed conditions, HFKs expressing E6/E7 were treated with doxorubicin (fig. 18A); doxorubicin is an intercalating agent that causes apoptosis of the cells via p53-dependent mechanisms. [145]

As expected, high accumulation of p53 was detected after the treatment with doxorubicin in control HFKs, but no band was seen either before or after doxorubicin treatment in cells expressing E6/E7 from HR types 16 (fig. 18A). In β3 HPV E6/E7 HFKs, p53 accumulation is attenuated compared to mock HFKs but still detectable by immunoblotting (fig. 18A).

The accumulation and activation of p53 after cellular stress causes the up-regulation of a number of genes involved in the cell cycle and apoptosis, such as p53 up-regulated modulator of apoptosis (PUMA), as well as the primary mediator of p53-dependent cell

cycle arrest in response to DNA damage $p21^{Waf1}$, a CDK inhibitor associated with the inhibition of Cdk2 [146, 147]. In keeping with previous work that showed p53 mediates cell cycle arrest and apoptosis, an increase in both PUMA and $p21^{Waf1}$ mRNA levels was observed after doxorubicin treatment in mock HFKs (fig. 18B). On the contrary, despite the slight accumulation of p53 after doxo treatment (fig. 18A), no transcriptional activation of either $p21^{Waf1}$ or PUMA was observed in HPV49 and HPV76 E6/E7 HFKs (fig. 18B). Instead, doxorubicin treatment of HPV75 E6/E7 keratinocytes resulted in a considerable increase of both $p21^{Waf1}$ and PUMA mRNA levels (fig. 18B), suggesting that this β HPV type is less efficient than HPV49 and HPV76 in targeting p53. HPV75 cells appear to retain part of this function. As expected, $p21^{Waf1}$ and PUMA mRNA levels were not increased after doxorubicin treatment in cells expressing E6/E7 from HPV16 (fig. 18B).

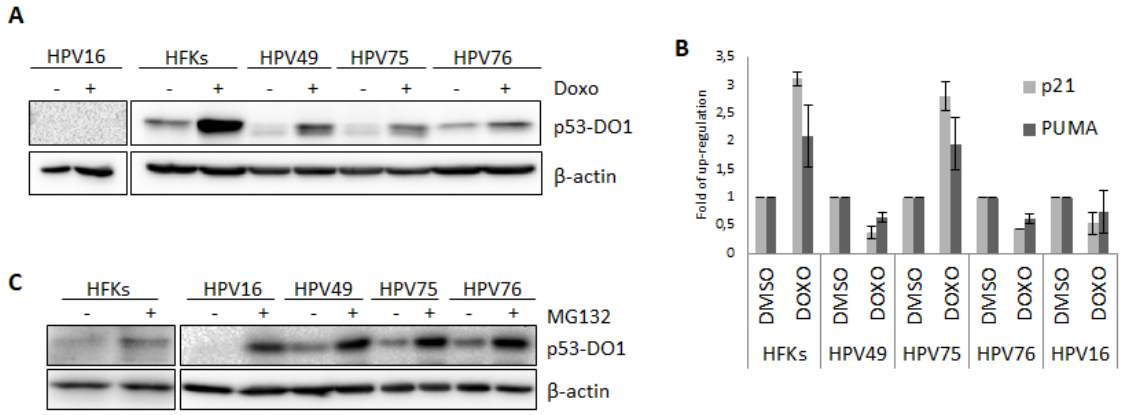

Figure 18: p53 is degraded in HFKs expressing E6/E7 from β3 types. (A) HFKs cells as indicated were treated for 8 hours with a DNA damaging agent doxorubicin (Doxo) used at the final concentration of 2 μg/ml or with DMSO as a control. Protein levels of p53 and β-actin were determined by immunoblotting using specific antibodies. (B) Total RNA extracted from cells treated as in figure 3A was retro-transcribed and used as a template for RT-Real-Time PCR analysis of PUMA and p21 gene expression, normalized to GAPDH. The result shown in the histogram is the mean of three independent experiments performed in one donor. (C) The indicated HFKs were treated for 4 hours with the proteasome inhibitor (MG132, final concentration 10μM), and protein levels of p53 and β-actin determined by immunoblotting using specific antibodies.

The low levels of p53 observed before and after doxorubicin treatment (fig. 18A) in HFKs expressing E6 and E7 from the β3 types indicate that p53 is targeted by degradation through the mediation of the viral onco-proteins, as previously demonstrated for HPV16 (see paragraph 1.2.1). Cells were therefore treated with proteasome inhibitor MG132. MG132 treatment caused an increase in p53 protein levels in HPV16 E6/E7 HFKs, detectable with immunoblotting (fig. 18C). Similarly, there was the rescue of p53 protein levels in HFKs expressing E6/E7 from HPV49, 75 and 76 (fig. 18C). On the contrary, no difference in p53 protein level was observed when MG132 treatment was applied on mock HFKs (fig. 18C). These results show that p53 is targeted for degradation by proteasome pathway also in cells expressing E6 and E7 from the β3 types.

As described in paragraph 1.2.1, the ubiquitin ligase E6AP is involved in the HPV16 E6-mediated degradation of p53. To examine its involvement in p53 degradation in β3 E6/E7 HFKs, E6AP expression was silenced by small interfering RNA (siRNA) and p53 protein levels were evaluated by immunoblotting (fig. 19A and 19B). In β3 E6/E7 HFKs the silencing of E6AP expression led to an increase of p53 protein levels (fig. 19A), similar to HPV16. The quantification of the immunoblots (fig. 19B) showed that the rescue of p53 was significantly higher in HPV16 E6/E7 HFKs when compared to β3 HFKs, suggesting that a ubiquitin ligase different from E6AP might be also involved in the degradation of p53.

In addition, maltose-binding protein (MBP) pull-down were performed with MBP-GFP or MBP-E6 fusion proteins and the interaction with p53 and E6AP proteins was analyzed with immunoblotting (fig. 19C and 19D). As shown in figure 19C, a light band corresponding to p53 was detected when cell lysate was incubated with HPV16 and β3 E6-MBP fusion proteins but not when the cell lysate was incubated with the MBP-GFP fusion protein. Similarly, a band corresponding to E6AP was detected in all the E6-MBP fusion proteins, but a slight signal was detected using the control MBP-GFP fusion protein (fig. 19C). For this reason, quantification of the bands from different pull-downs was performed and the background signal from MBP-GFP fusion protein subtracted from the signal obtained with the E6-MBP fusion protein (fig. 19D). The pull-down experiments showed that E6 from β3 types form a complex with p53 and E6AP, even

though the binding detect via immunoblotting is lower when compared to the binding detected for HPV16 E6.

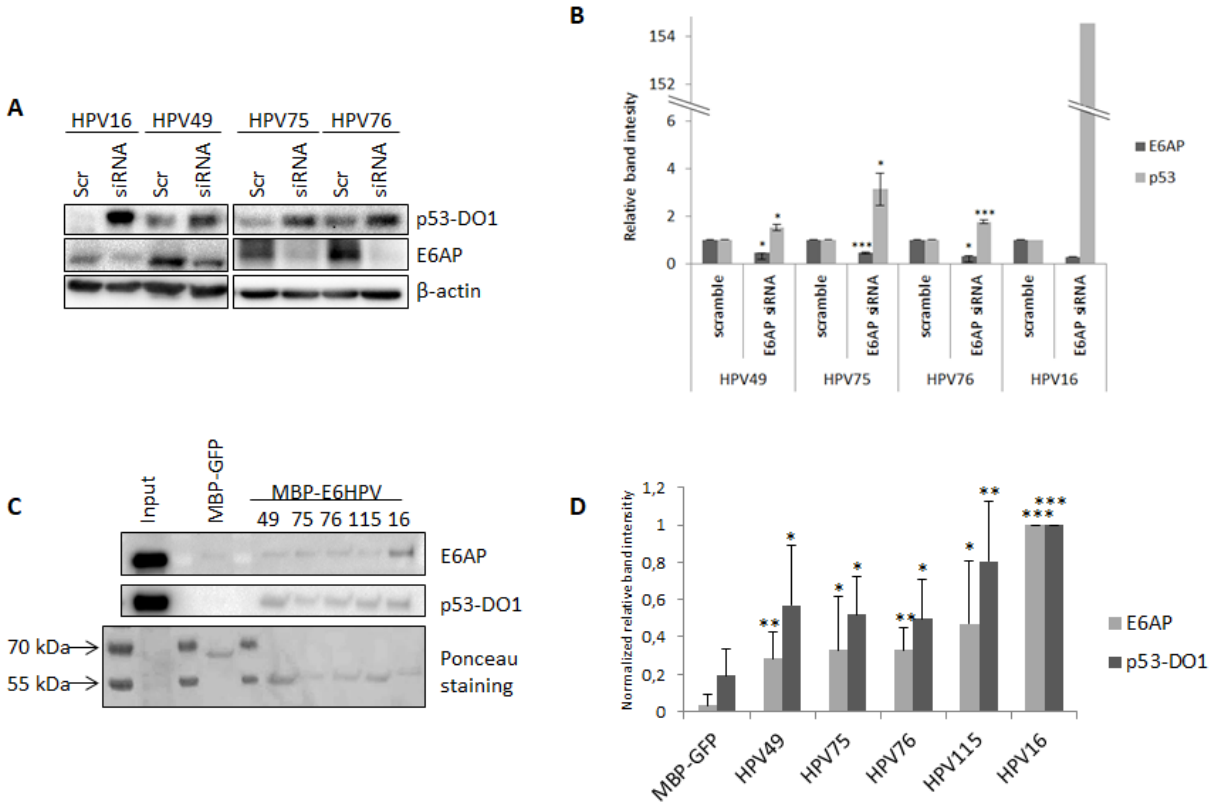

Figure 19: p53 is degraded in HFKs expressing E6/E7 from β3 types with a mechanism similar to HR HPV16. (A) HPV16, 49, 75 and 76 E6/E7 transduced HFKs were transiently transfected with siRNA directed against E6AP (siRNA) or a scramble control (Scr). Levels of p53, E6AP and β-actin were determined by immunoblotting using specific antibodies. (B) Band intensities were quantified, normalized to β-actin levels, and then expressed relative to those treated with the scramble siRNA. Data are the means of three independent experiments performed in primary keratinocytes from two donors. (C) The indicated E6-MBP or MBP-GFP fusion proteins were incubated with 600 µg HNC136 total protein extract. Levels of p53 and E6AP were determined by immunoblotting using specific antibodies. Fusion protein levels were determined with Ponceau staining. (D) Band intensities were quantified and normalized to the fusion protein levels and expressed as a percentage of the input. The histogram on the right panel shows the relative amounts of binding of p53 and E6AP to the different E6, compared to HPV16 E6, set as calibrator. The results are the mean of 5 independent experiments. (*P<0.05, ** P<0.01, ***P<0.005).

5.4 β3 TYPES 49, 75 AND 76 E6/E7 EFFICIENTLY UP-REGULATE hTERT EXPRESSION

A major step in the immortalization of HFKs by HPV16 E6 and E7 is the up-regulation of human telomerase (hTERT) transcription (see paragraph 1.2.1). Therefore, the mRNA levels of hTERT were assessed in control HFKs, HFKs carrying the empty plasmid and HFKs expressing E6/E7 from HPV16 and the β3 types.

As shown in figure 20A, hTERT mRNA levels were significantly higher in HPV49, 75 and 76 E6/E7 HFKs, when compared to both control HFKs and HFKs carrying the empty vector (pLXSNØ). On the contrary, the cells expressing E6 and E7 from HPV115 show low levels of hTERT, comparable to HFKs and pLXSNØ HFKs (fig. 20A). As expected, hTERT transcription is highly up regulated in HPV16 E6/E7 expressing keratinocytes (fig. 20A).

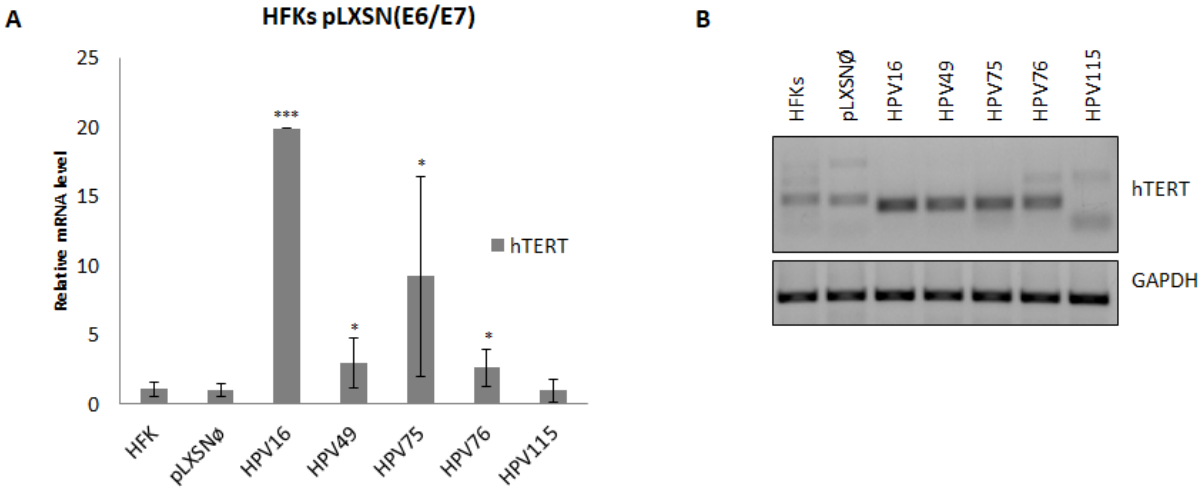

Figure 20: β3 E6/E7 HFKs with prolonged lifespan efficiently up-regulate hTERT expression. (A) total RNA extracted from cells at the same passage was retro-transcribed and used as a template for RT-Real-Time PCR analysis of hTERT gene expression, normalized to GAPDH. The result shown in the histogram is the mean of three independent experiments performed in two donors. (B) RT RT-PCR products of figure 20A (hTERT and GAPDH) were run on a 1.5% agarose gel.

Given the very low level of hTERT mRNA in HFKs and pLXSNØ HFKs, this data set was then confirmed by loading the PCR product on an agarose gel (fig. 20B). The gel confirmed low levels of hTERT in HFKs and pLXSNØ HFKs. The presence of multiple

bands indicates the existence of different mRNA species derived from alternative splicing or non-specific amplification (fig. 20B). On the contrary, a very clear band of amplification was obtained for HFKs expressing E6 and E7 from HPV16 and β3 types.

5.5 HPV76 E6 TRANSFORMING PROPERTIES ARE AFFECTED BY MUTATIONS IN THE CORRESPONDING REGIONS OF HPV16 E6 INVOLVED IN p53 AND E6AP BINDING

Given the ability of β3 E6s to target p53 for degradation (fig. 18), the link between the interaction of E6 with p53 and the immortalization activity was evaluated. For this additional experiment, HPV76 has been selected as an example of the β3 immortalizing type.

5.5.1 MUTANTS DESIGN

Recent studies of the Zanier group in Strasbourg on the structure of E6-E6AP-p53 complex have shown that four amino-acids of E6 are essential for the formation of the complex and for the subsequent degradation of p53 [88, 148]. The two aspartic acids in position 44 and 49 (D44, D49) are involved in the formation of a polar bridge with p53 and mutations in these positions (D44R, D49R) result in the impaired formation of the complex and p53 degradation. The phenylalanine in position 47 is part of a hydrophobic core crucial for the interaction with p53 and its mutation (F47R) results in an impaired ability to degrade p53. Instead, the leucine in position 50 mediates the interaction between E6 and the LxxLL motif of E6AP and other cellular proteins and mutation in this position (L50E) results in a loss of E6AP binding and p53 degradation [88, 148].

Considering that E6 of β3 types 49, 75 and 76 have similar abilities to HPV16 in the degradation of p53, their sequences were aligned and compared to alpha HPV types (HR and LR) (fig. 21). The alignment showed that despite the E6s of β3 are shorter both at the N- and C-terminal, the overall sequence is conserved when compared to the alpha types (fig. 21). In particular, the region of interaction with p53 and E6AP described above is highly conserved, with the exception of the amino-acid of HPV115 corresponding to D49 of HPV16 (fig. 21, close up).

Based on these information, a set of four mutants was created via site direct mutagenesis on the sequence of E6 of HPV76. The four mutagenized amino-acids are E39, Y42, D44

and F45 and they correspond, respectively, to D44, F47, D49 and L50 of HPV16 E6 (fig. 21).

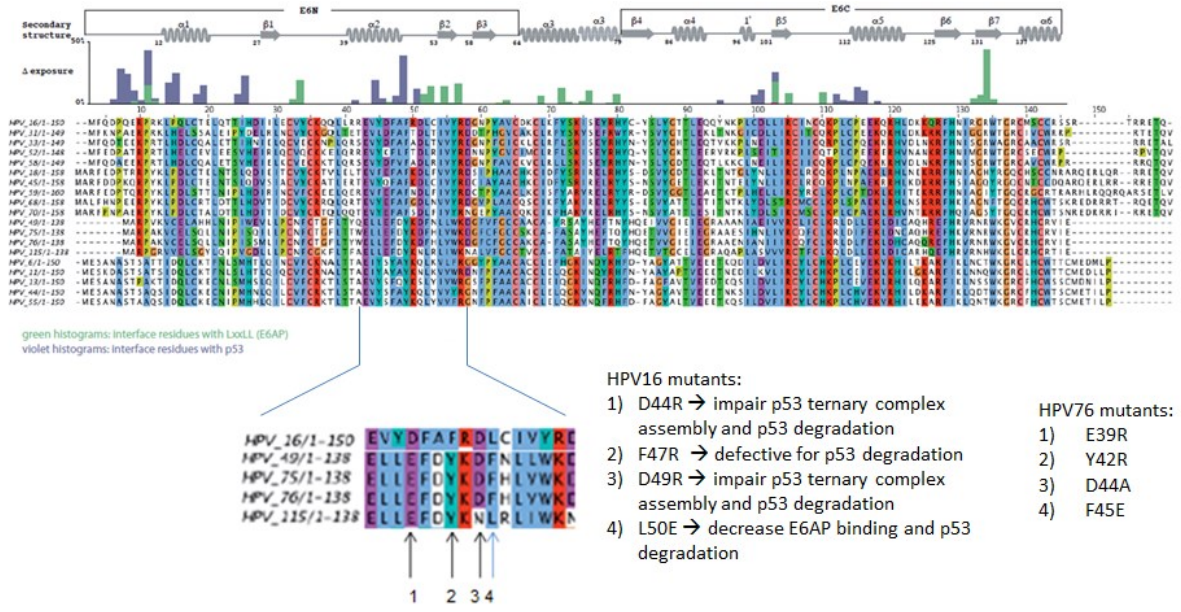

Figure 21: Alignment of the E6 protein sequences from different α and β HPV types. Dark arrows indicate HPV16 E6 amino-acids directly involved in p53 binding, while light blue arrow indicates the amino-acid involved in binding the LxxLL motif of E6AP. Indicated in the figure the mutations of HPV16 E6 and their phenotype and the corresponding mutations designed for HPV76 E6.

5.5.2 HPV76 E6 MUTANTS FAIL IN THE IMMORTALIZATION OF PRIMARY KERATINOCYTES

To assess the ability of E6 mutants to immortalize HFKs, HFKs were transduced with HPV76 E6/E7 constructs carrying the wild type E7 and the wild type or the mutated E6s. As expected, and as previously shown, HFKs expressing WT E6/E7 showed an increased lifespan (fig. 22A) and the typical morphology of highly proliferative cells (fig. 22B). On the contrary, the mutant F45E rapidly died after the end of the selection (fig. 22A). HPV76 E6 E39R, Y42R and D44A were also unable to cooperate with wild type E7 in increasing the lifespan of the keratinocytes and subvert the senescence program even though, different to the F45E mutant, the cells remained in a senescent state for approximately 80-100 days before death (fig. 22A). The morphology of the cells reflected their inability to subvert the senescence, as shown in figure 22B.

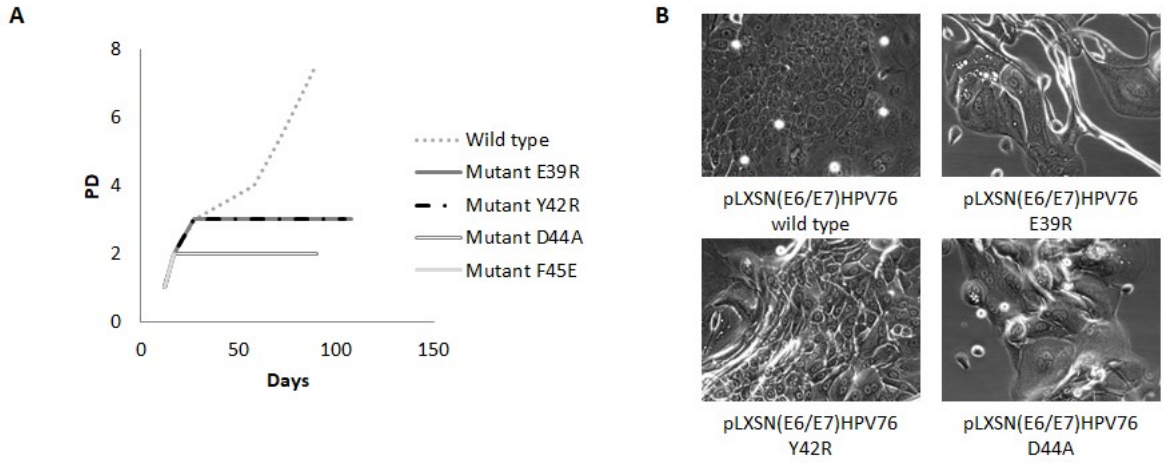

Figure 22: HFKs expressing mutated E6 and wild type E7 do not become immortalized. (A) Growth curve of human primary keratinocytes expressing E6/E7 with wild type E6 or mutated E6, as indicated. Population doublings (PD) are shown on the y axis. (B) Morphology of HFKs transduced with the indicated recombinant retroviruses at PD2. The same magnification was used for all the microphotographs (20X).

5.5.3 HPV76 E6 E38R, Y42R, F45E MUTANTS FAIL TO DEGRADE p53

Given the short lifespan of the primary keratinocytes carrying the different mutant E6, naturally immortalized keratinocytes (NIKs) stably expressing WT E7 and WT or mutated E6 were generated. With this new experimental model, the ability of HPV76 E6 mutants to target p53 for degradation was analysed in comparison to the WT E6.

The cells were treated with doxorubicin for 8 hours and then analysed via immunoblotting for p53 protein levels. As expected, p53 protein levels increased upon doxorubicin treatment while NIKs carrying HPV76 WT E6 and WT E7 showed low levels of p53 both in basal condition and after treatment (fig. 23A). These results also indicated that the doxorubicin challenge results obtained in HFKs are reproducible in NIKs and therefore that the new model is suitable for the study of the functionality of the E6 mutants. The immunoblotting shown in figure 11A shows that p53 levels were accumulated after doxorubicin treatment in NIKs expressing HPV76 E6 E39R, Y42R and F45E mutants when compared to their untreated counterparts (fig. 23A). Interestingly, among these mutants, only F45E shows increased level of p53 compared to control NIKs (pLXSNØ) in the untreated condition (fig. 23A). By contrast, p53 protein levels in the mutant D44A did not change with treatment (fig. 23A). The D44A mutant,

therefore, retained the ability of wild type E6 to prevent p53 accumulation induced by cellular stress.

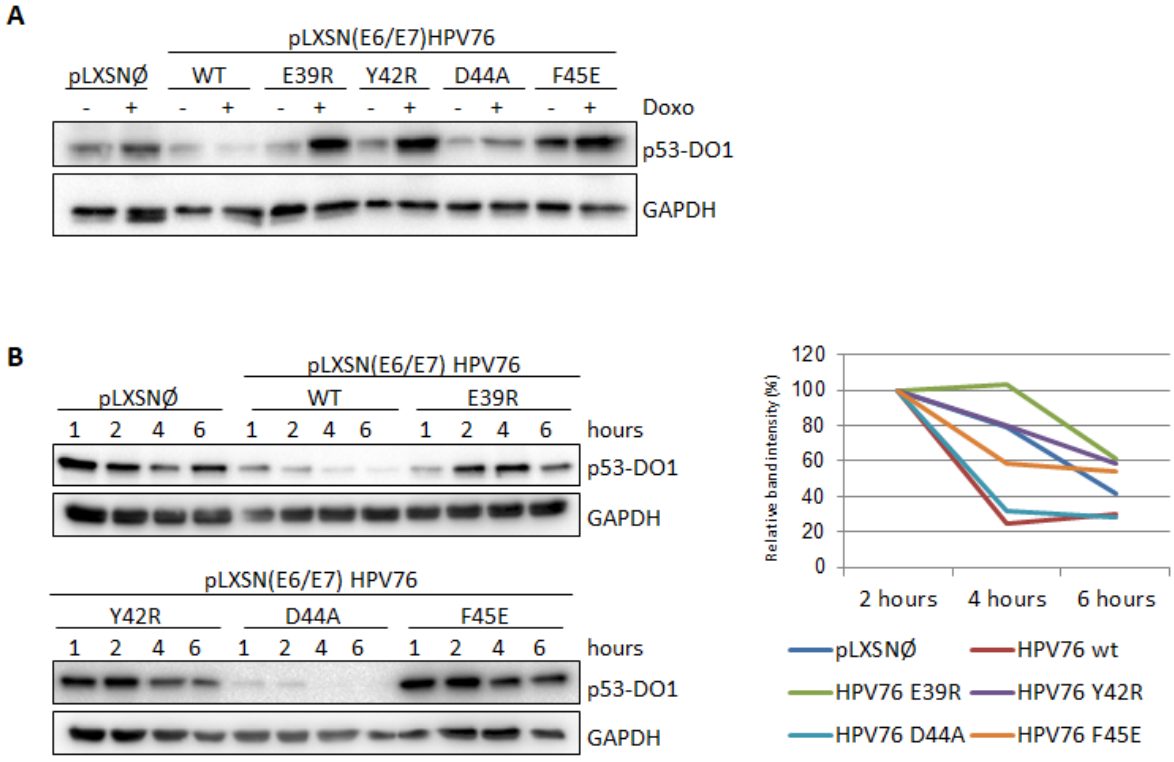

Figure 23: Mutation of HPV76 E6 in amino-acidic residues corresponding to p53 and E6AP binding sites in HPV16 E6, alter its biological activities. (A) NIKs transduced with E7 and with the indicated E6 or empty vector (pLXSNØ) as control, were treated with the DNA damaging agent doxorubicin (Doxo) used for 8 h (final concentration 10 mg/ml). Levels of p53 and GAPDH were determined by immunoblotting using specific antibodies. (B) NIKs transduced as described in Fig 8A were treated with the protein synthesis inhibitor (Cycloheximide, final concentration 10 µg/ml) and collected at the indicated time points. Twenty micrograms of total protein extract from NIKs-pLXSNØ, WT and E39R E6 mutant were run on a separate immunoblotting than NIKs expressing Y42R, D44A and F44E E6 mutants (upper and lower panel respectively). Levels of p53 and GAPDH were determined by immunoblotting using specific antibodies. The histogram on the right side shows the quantification of the p53 signal, normalized to GAPDH levels and calibrated against the levels of p53 at 2 hours of treatment (set as 100%). Data are the means of three independent experiments.

To further corroborate the data obtained on the efficiency of the different HPV76 E6 mutants to target p53 for degradation, p53 half-life was determined. The cells were treated for 1, 2, 4 and 6 hours with cycloheximide (CHX), a chemical agent that blocks the *de novo* protein synthesis and therefore allows to calculate the stability of the protein of

interest. The protein extracts were analysed via immunoblotting using a p53 specific antibody. As shown in figure 23B, in pLXSNØ NIKs p53 levels decrease with time and after 6 hours approximately 60% of p53 protein is degraded (fig. 23B, right panel). Similarly to the pLXSNØ NIKs, p53 has a half-life of approximately 6 hours in NIKs expressing HPV76 E6 E39R, Y42R and F45E mutants (fig. 23B). Corresponding to results obtained with the doxorubicin challenge, HPV76 E6 WT and D44A mutant showed a decreased p53 half-life, with approximately only 20% of the protein remaining in the cells after 6 hours of cycloheximide treatment (fig. 23B).

5.5.4 E39R E6 MUTANT FAIL TO UP-REGULATE hTERT EXPRESSION

As described in paragraph 5.4, HPV76 E6 can up-regulate the transcription of hTERT, in a manner similar to HPV16. In HPV 16, an important role in the up-regulation of hTERT is played by E6 and some studies have shown that the interaction between E6 and E6AP might be involved [95, 96]. One of the mutations carried out in HPV76 E6 (F45E) is an amino-acid suspected to play a role in the binding with E6AP, possibly with a bearing on hTERT up-regulation.

Therefore, the mRNA levels of hTERT were assessed in NIKs carrying the empty plasmid and NIKs expressing HPV76 wild type E7 and wild type or mutant E6. As shown in figure 24, NIKs carrying the wild type HPV76 E6/E7 have a higher level of hTERT mRNA when compared to control NIKs, a result that is mirrored in the primary keratinocytes (fig. 20A). Interestingly, the F45E E6 mutant induces high hTERT expression levels, similarly to the levels observed for the HPV76 E6 wild type (fig. 24). The levels of hTERT mRNA were also significantly higher in the Y42R and D44A mutants compared to mock NIKs (fig. 24). hTERT mRNA is considerably lower in the E39R mutant compared to the other E6 containing NIKS and resembles the NIKs cells expressing the empty vector (fig. 24).

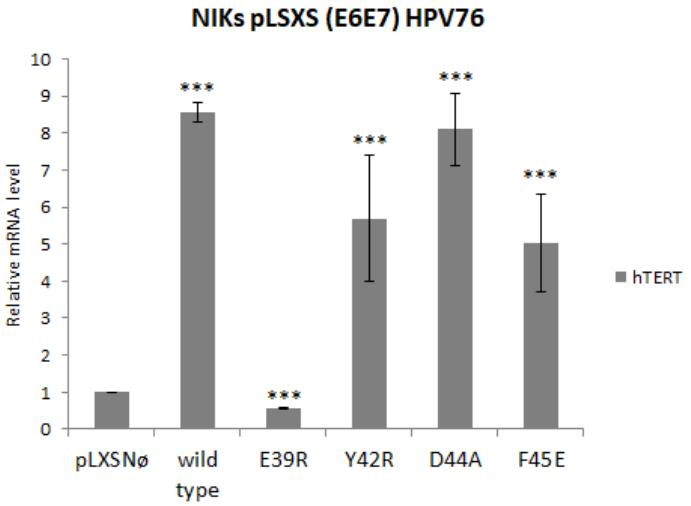

Figure 24: HPV76 E6 mutants retain hTERT up-regulation ability with the exception of E39R mutant. Total RNA extracted from NIKs carrying the indicated constructs was retro-transcribed and used as a template for were RT-Real-Time PCR analysis of hTERT gene expression, normalized to GAPDH. The result shown in the histogram is the mean of three independent experiments.

The summary of the data obtained on the E6 mutants is shown in Table 13. The mutagenesis in all the amino-acids corresponding to the regions of HPV16 E6 involved in p53 and E6AP interactions results in an impaired ability to immortalize human primary keratinocytes. Interestingly, the D44A mutant retained the ability to degrade p53 and up-regulate hTERT, indicating that a mutation of this particular amino-acid affects other E6 properties that are essential for the extension of the life-span. Moreover, mutation of amino-acid 39 (E39R) led to an impairment in both the degradation of p53 and hTERT up-regulation, indicating that this amino-acid plays and important role in both pathways. On the contrary, the mutation of amino-acids 42 and 45 led only to the loss of p53 degradation, confirming the role of these two amino-acids of HPV76 E6 dependent degradation of p53, as shown for the corresponding amino-acids in HPV16 E6.

Table 13: summary of the E6 wild type and E6 mutants properties. The immortalization ability has been tested in primary keratinocytes, while p53 degradation and hTERT up-regulation abilities have been tested in NIKs. The symbol ✓ indicates a retained ability while the symbol × indicates an abolished ability. The phenotype of HPV16 E6 corresponding mutants is briefly described.

	HFKs immortalization	p53 degradation	hTERT up-regulation	In HPV16
Wild type	✓	✓	✓	
Mutant 1: E39R	×	×	×	impair p53 ternary complex assembly and p53 degradation
Mutant 2: Y42R	×	×	✓	defective for p53 degradation
Mutant 3: D44A	×	✓	✓	impair p53 ternary complex assembly and p53 degradation
Mutant 4: F45E	×	×	✓	decrease E6AP binding and p53 degradation

5.6 β3 HPV AND HPV16 E6/E7 HFKs SHOW SOME SIMILARITIES IN THE ALTERATION OF CELLULAR GENE EXPRESSION

To gain more insight into the biological properties of E6 and E7 from the β3 types, the impact of β3 HPV E6 and E7 proteins on cellular gene expression was determined. Total RNA from HFKs (donor 1) transduced with recombinant retroviruses expressing E6/E7 of HPV49, 75, 76 and 115 was extracted and converted to cDNA, and subsequently to biotin-labelled single-stranded cRNA. The same procedure was carried out on HFKs carrying E6/E7 of HR type 16 and β2 type 38 as well as HFKs from two different donors transduced with an empty retrovirus. The samples were hybridized on HumanHT-12 Expression BeadChips (Illumina) and the signals were read with the Illumina BeadArray Reader. Afterwards, the raw data were analyzed using BRB-ArrayTools software as described in material and methods by the "Genetic Cancer Susceptibility Group", IARC (France). The two pLXSNØ HFKs were used as control and probes with a p-value of < 0.001, with a minimum of 1.5-fold change compared to pLXSNØ HFKs and a False Discovery rate (FDR) of <0.01 were considered significantly differentially expressed.

5.6.1 HIERARCHICAL CLUSTERING REVEAL HIGHER SIMILARITY BETWEEN β3 TYPES AND HPV16 E6/E7 KERATINOCYTES

First, the heat map of figure 25 was generated with the genes that are specifically de-regulated by the expression of E6/E7 from the different β3 HPV types. This representation of the data is useful to have an overall overview of the de-regulated genes and it allows to visualize and compare the different conditions in a simple and effective method.

As expected, the hierarchical clustering analysis revealed that among the β3 HPV types, the non-immortalizing HKFs expressing E6 and E7 from HPV115 have the most divergent profile from the mRNA profile of HPV16 (fig. 25). Interestingly, HPV38 E6/E7 HKFs are more divergent from HPV16 than HPV115, despite the ability of HPV38 onco-proteins to immortalize primary keratinocytes (fig. 25). HFKs expressing

E6/E7 from HPV75 have a higher number of de-regulated genes compared to all other keratinocytes. This does not reflect in growth ability of these cells since E6/E7 of HPV75 in donor 1 has a slower rate of growth when compared to HPV16, 49 and 76 expressing keratinocytes (fig. 25).

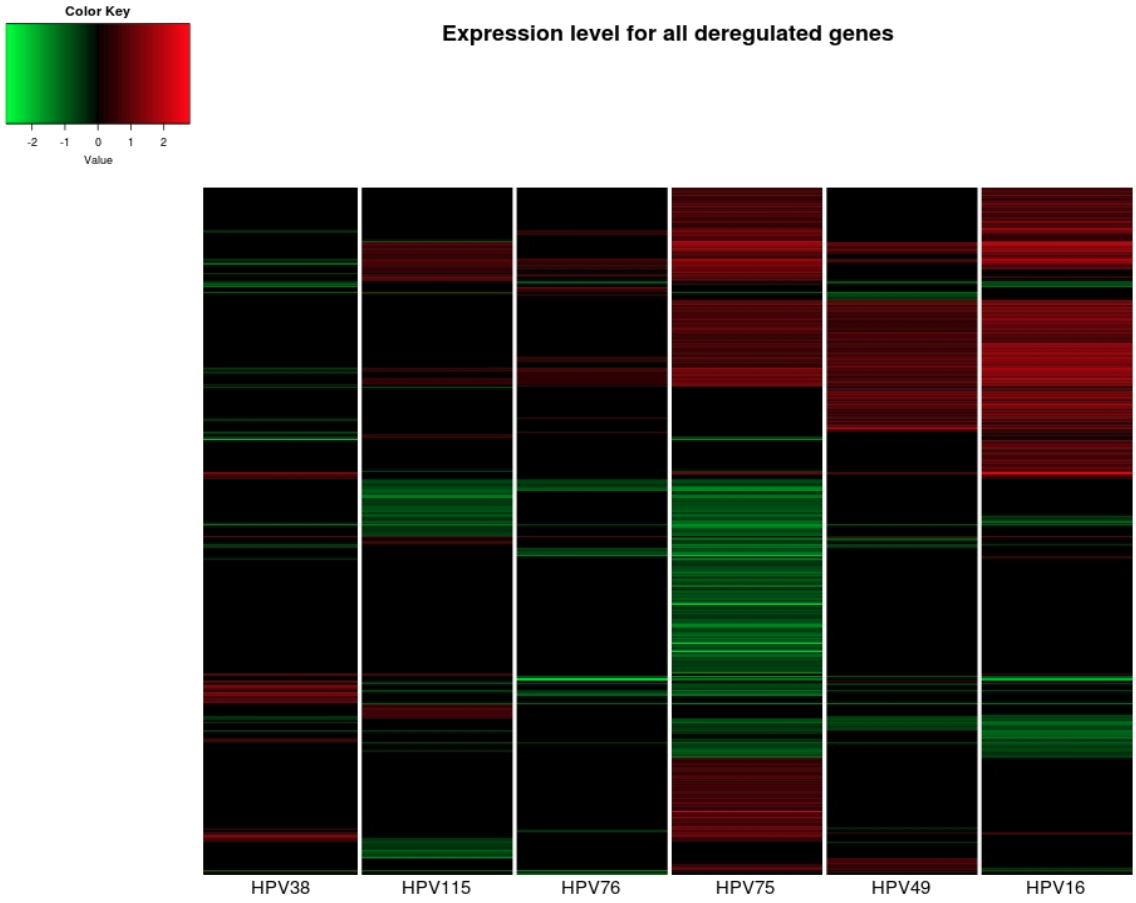

Figure 25: β3 E6/E7 HFKs have an expression profile similar to HR type 16. Heat map of the significantly de-regulated genes in the HFKs expressing E6/E7 from the indicated HPVs. The colour represents the expression level of the gene: red represents the higher expression, while green represents lower expression compared to gene expression in empty vector HFKs. mRNA was extracted prior immortalization.

5.6.2 PATHWAY ANALYSIS REVEALS AN OVERALL DE-REGULATION OF CELL CYCLE, p53 AND DNA REPLICATION PATHWAYS IN HFKs EXPRESSING E6/E7 FROM HPV49, 76 AND HR HPV16

Many studies have shown that viral onco-proteins have developed redundant mechanisms in deregulating cellular pathways. Thus, it is possible that viral proteins are able to deregulate the expression of genes encoding proteins involved in the same pathways. To evaluate this hypothesis an *in silico* pathway enrichment analysis was performed.

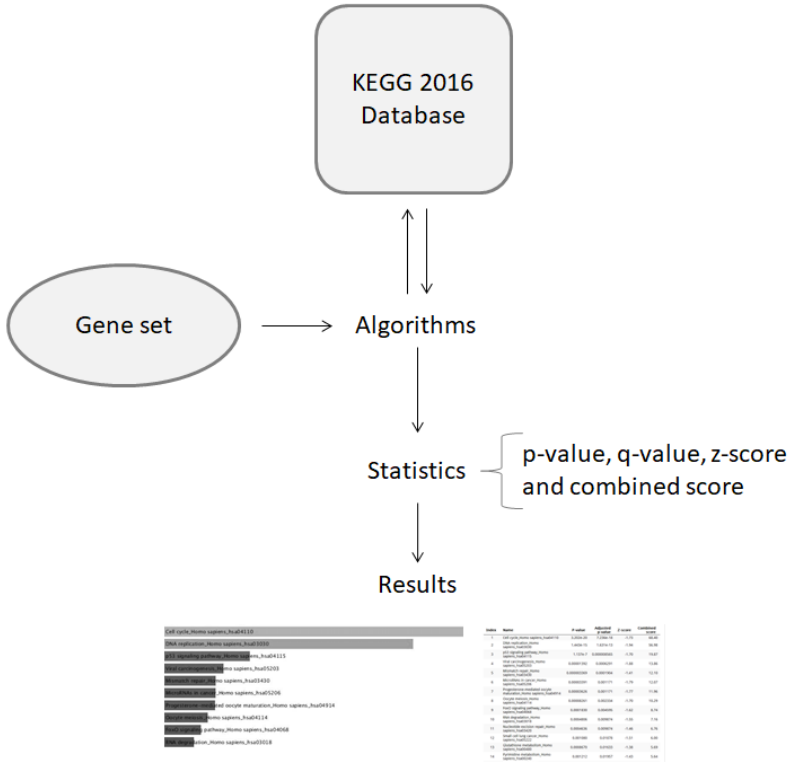

Figure 26: Schematic representation of the *in silico* pathway analysis. The genes de-regulated in E6/E7 from a specific HPV type ("gene set") are compared with the KEGG database, using Enirchr algorithms. Enirchr software applies then statistical analysis and returns the results in the form of a histogram and a table with the enriched pathway and their statistical significance.

The enrichment analysis is a computational method for inferring knowledge on an input gene set, using annotated gene sets representing prior biological knowledge. For this experiment, the input gene set is represented by the genes de-regulated in E6/E7 expressing keratinocytes while the annotated gene set is represented by the KEGG database, 2016 version (fig. 26). The enrichment analysis analyses whether there is an overlap between the input set and the annotated gene set, it then applies statistical analysis and calculates p-value, q-value, z-score and combined score in order to determine if the overlap is significant (fig. 26). The output obtained from the Enrichr software is a bar graph where the length of the bar represents the significance of that specific term. The brighter the color, the more significant that term is (fig. 26). For this experiment, the terms are ranked based on the combined score, from the more significant to the less significant. Moreover, a table with the statistical values can be obtained.

Figure 27 shows the results of the pathway enrichment performed on the genes de-regulated in HFKs expressing E6/E7 from HPV16, 38, 49, 75, 76 and 115 in comparison to mock HFKs. Of note, the size of the gene sets is different, with HPV75 E6/E7 HFKs having the biggest gene set (1085 de-regulated genes) and HPV76 E6/E7 HFKs having the smallest gene set (172 de-regulated genes) (fig. 27). Interestingly, the pathway analysis of HFKs expressing E6/E7 of HPV38 did not show a significant enrichment in any of the pathways in the KEGG database, with a combined score ranging from 1.27 to 1.76 for the pathway showed in the bar graph of figure 27.

The pathway analysis revealed that the genes de-regulated in the β3 HPV E6/E7 HFKs were enriched in cell cycle related genes, an enrichment shared also by HPV16 E6/E7 HFKs but not by β2 type 38 E6/E7 HFKs (fig. 27 and table 14). Moreover, the analysis showed that only the β3 types E6/E7 that are able to prolong the HFKs lifespan have de-regulated genes enriched in the p53 pathway and DNA repair, an enrichment obtained also for E6/E7 HPV16 HFKs but not for E6/E7 HPV38 HFKs (fig. 27 and table 14). Finally, only the immortalizing type 16, 49 and 76 share an enrichment in de-regulated genes involved in DNA replication (fig. 27 and table 14).

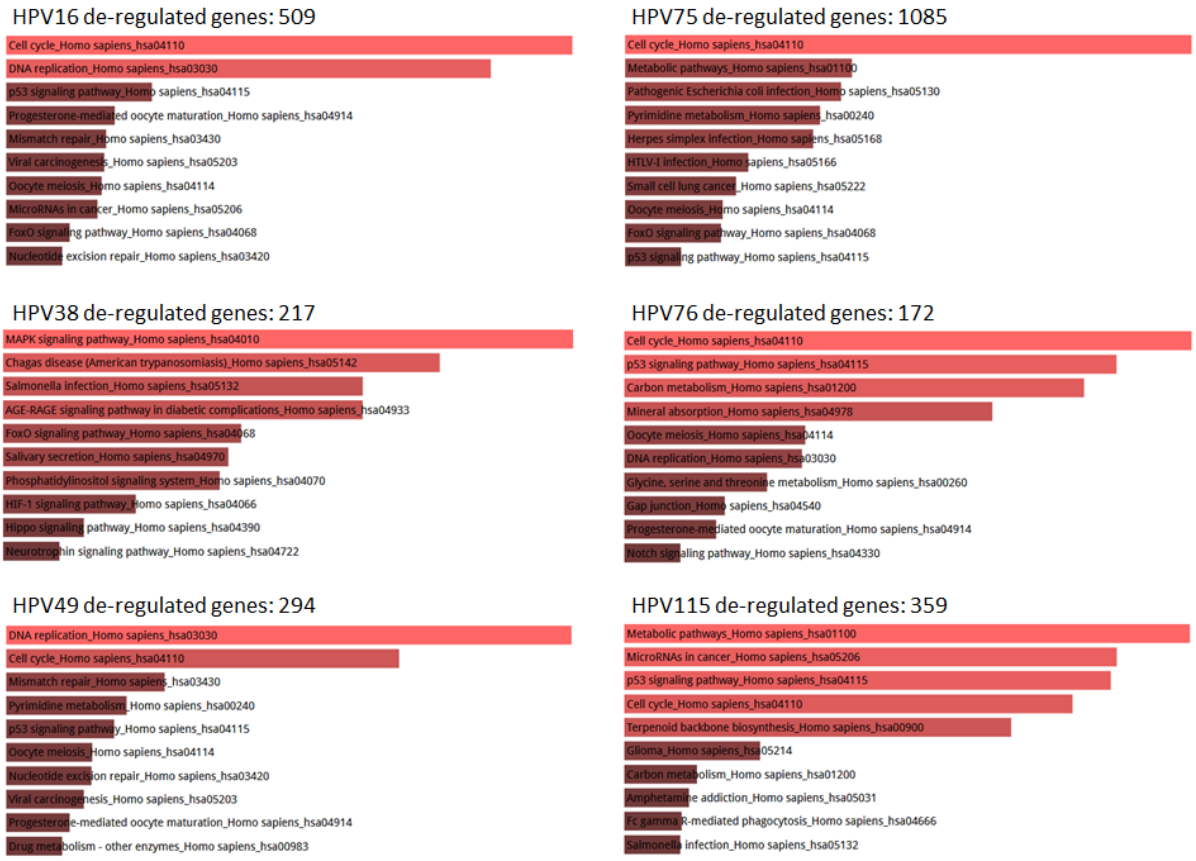

Figure 27: β3 E6/E7 HFKs share pathway enrichment with HPV16 E6/E7 HFKs. Pathway analysis (Enrichr) of the significantly de-regulated genes in cells expressing E6/E7 of the indicated HPVs. The length of the bar and the brightness of the colour represent the significance of the specific pathway (combined score range: HPV16 8.25-72.34; HPV38 1.27-1.76; HPV49 6.88-72.91; HPV75 5.06-14.60; HPV76 2.57-6.99; HPV115 3.27-5.94). Gene set sizes are indicated by the number on top of each histogram.

Table 14: Summary of the enrichment pathway analysis. The HFKs expressing E6/E7 of all the β 3 types are enriched in the cell cycle pathway, while only the HFKs with prolonged lifespan (HPV49, 75 and 76) share enrichment in the p53/DNA repair pathway. Only the immortalizing β 3 types share enrichment in the DNA replication pathway. The symbol ✓ indicates that the pathway is found enriched in the HFKs expressing E6/E7 of that particular HPV type. The symbol × indicates that the genes de-regulated in HFKs expressing E6/E7 of that particular HPV type are not enriched in the indicated pathway.

	Cell cycle (gene set size: 1706)	**DNA replication (gene set size: 296)**	**p53 and DNA repair (gene set size: 594)**
HPV16	✓	✓	✓
HPV49	✓	✓	✓
HPV75	✓	×	✓
HPV76	✓	✓	✓
HPV115	✓	×	×
HPV38	×	×	×

5.6.3 β3 E6/E7 EXPRESSING KERATINOCYTES SHARE MORE DE-REGULATED GENES WITH HR HPV16 THAN WITH β2 HPV38

The above experiments on E6/E7 properties from β3 types showed that E6 and E7 from HPV49, 75 and 76 shares some similarities with E6 and E7 of the HR type 16 (paragraphs 5.2.2, 5.3 and 5.4). Moreover, the pathway analysis showed common enrichment of genes involved in cell cycle, DNA replication and DNA repair (paragraph 5.6.2). Therefore, the similarity between the expression profiles of β3 HPV types and HPV16 E6/E7 HFKs was examined. For this, a comparative analysis between each of the β3 HPV types, HPV16 and HPV38 expressing keratinocytes was performed. The Venn

diagram in figure 28A shows the type of analysis performed using HPV76 as an example and the results of all the comparative analysis are summarized in the histogram of figure 28B. The genes de-regulated in HPV76 E6/E7 HFKs were compared to the genes de-regulated in HPV16 E6/E7 HFKs and to the genes de-regulated in HPV38 E6/E7 HFKs. The Venn diagram shows the number of genes similarly de-regulated in HPV16 and HPV76, the genes similarly de-regulated in HPV38 and HPV76, the genes similarly de-regulated in HPV16, HPV38 and HPV76, and the genes exclusively de-regulated in HPV76 (fig. 28A). Of particular interest is the number of genes that HPV76 share exclusively with HPV16 or with HPV38. As shown by the percentages in the histogram of figure 28B, all the HFKs expressing E6/E7 from the β3 HPV types share more de-regulated genes with HFKs expressing E6/E7 of the α type 16 than with HFKs expressing β2 HPV38 E6/E7.

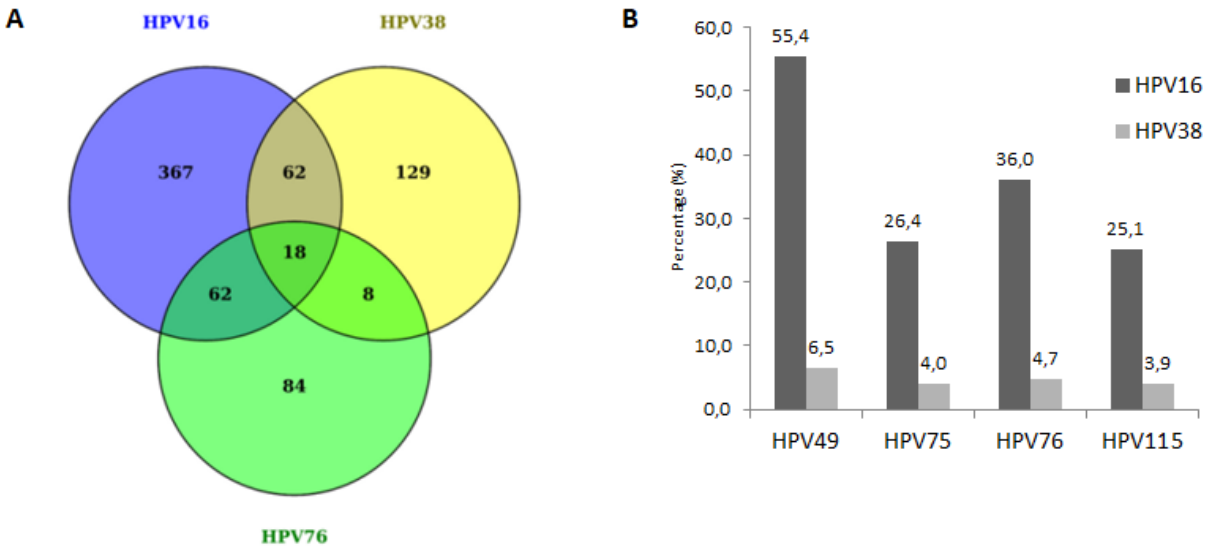

Figure 28: β3 HFKs shares more de-regulated genes with HPV16 than with HPV38 HFKs. (A) Venn diagram of the genes de-regulated in the cells expressing E6/E7 from HPV16, HPV38 and HPV76. (B) Percentage of genes of the indicated β3 type that are also deregulated in HPV16 or HPV38. Common genes with opposite deregulation trends have been excluded from the analysis.

5.6.4 ARRAY VALIDATION

As a final step, the gene expression data detected with Illumina platform was validated by RT RT-PCR. Both mRNA for the microarray and for RT RT PCR validation were extracted at the same cell passages, in the pre-immortalization status.

Four genes were selected for the validation, based on their pattern of de-regulation in the different HPV types as well as their possible role in the immortalization process.

The gene cdk2, which is involved in the regulation of the cell cycle, was found up-regulated in cells expressing E6/E7 from HPV16, HPV49, HPV75 and HPV76 but not in HPV115 when compared to HFKs. The RT RT-PCR analysis confirmed the data obtained from the array (fig. 16B).

SERPINE1 encodes for the plasminogen activator inhibitor 1 (PAI1), a serine protease inhibitor that functions as the principal inhibitor of tissue plasminogen activator (tPA) and urokinase (uPA). Interestingly, elevated levels of PAI1 in oral squamous carcinoma (OSC) are a prognostic marker of poor outcome while a low level of PAI1 is detected in HPV-positive OSC [149]. Confirming the data of the array, down-regulation of SERPINE1 was found in HFKs expressing E6/E7 from HPV16, 49 and 76 while up-regulation was found in HFKs expressing E6/E7 from HPV75 and 115 when compared to mock HFKs (fig. 29A).

GADD45a is a gene that is highly transcribed following cellular stress-dependent growth arrest or treatment with the DNA-damaging agent, and its transcription is mediated by both p53-dependent and p53-independent mechanisms. Interestingly, GADD45a is up-regulated in the HFKs expressing E6/E7 of HPV75 and HPV115 but not in the other β3 HPV types or in HPV16 E6/E7 expressing keratinocytes (fig. 29B).

The last gene tested for the array validation is MT1X, a Metallothionein whose function is still not fully understood. However, a recent study showed that a significant loss of MT1X expression is observed in Oral Squamous Cell Carcinoma [150]. The RT RT-PCR on this gene showed a significant loss of MT1X in in HFKs expressing E6/E7 from HPV16, 49 and 76 but not in HPV75 and HPV115 E6/E7 expressing keratinocytes (fig. 29C).

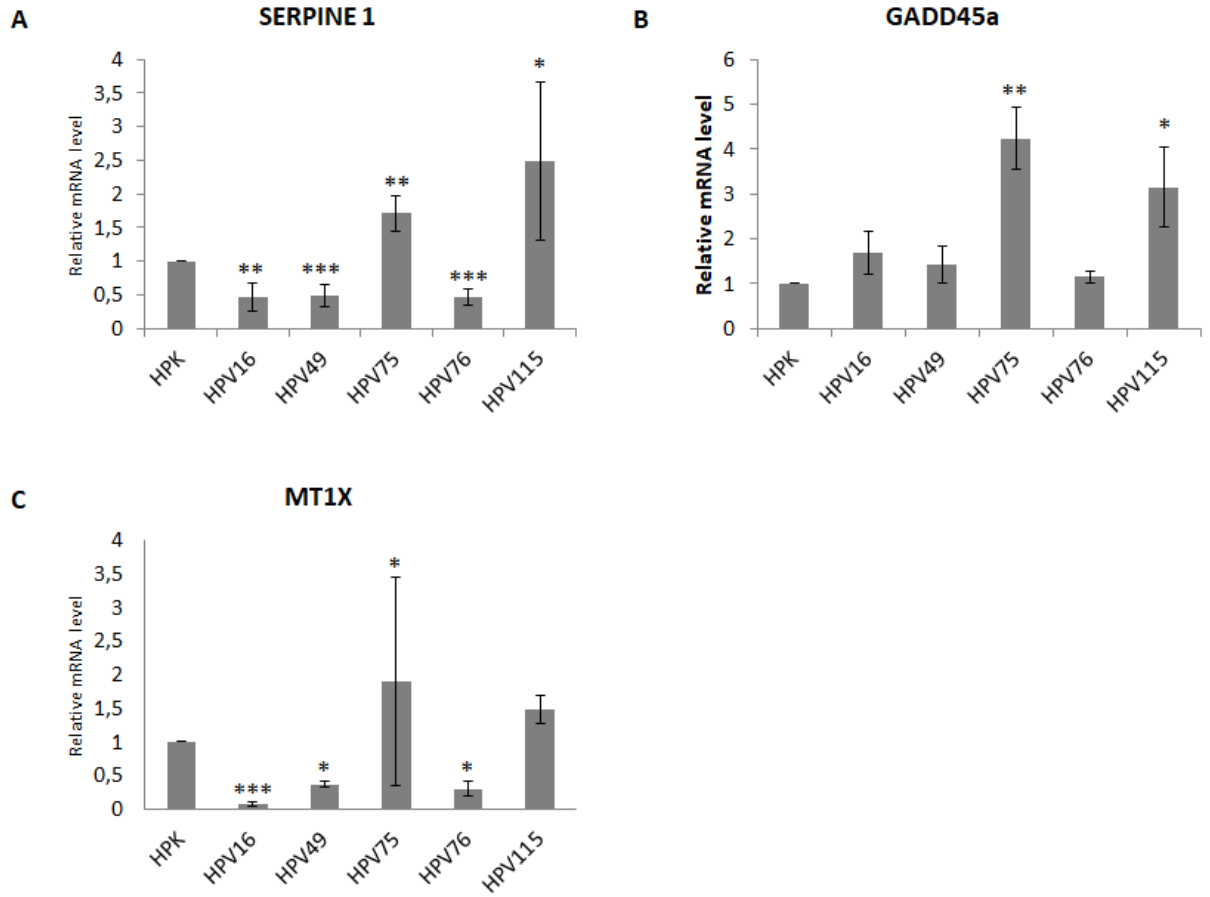

Figure 29: total RNA extracted from the indicated E6/E7 expressing HFKs (donor 1) was retro-transcribed and used as a template for were RT-Real-Time PCR analysis of SERPINE1, GADD45a and MT1X gene expression, normalized to GAPDH. The result shown in the histogram is the mean of three independent experiments.

5.7 METABOLISM AND TRANSFORMATION

In cancer development, the rewiring of the cellular metabolism is a key process for the cancer cells to support the new biosynthetic needs, in particular, cellular metabolism must adapt to support the increased cell proliferation seen in cancer cells. The first evidence showed that different to normal non-cancerous cells, the metabolism of cancer cells relies mostly on glycolysis, even in the presence of sufficient oxygen [151]. More recent studies have shown that the glucose metabolism is not the only altered metabolic pathway, but also nucleotides and protein synthesis are altered to support the transformation of the cells [152].

Additionally, the presence of HPV16 onco-proteins favors metabolic changes that might be important for the cellular transformation. As an example, a study showed that the expression of E7 from HPV16 causes a significant increase in the glycolytic rate and a significant increase in the conversion of glucose to lactate [153]. This study showed that E7 is also able to physically interact with M2-pyruvate kinase, an enzyme that plays a crucial role in metabolism reprogramming and cell cycle progression [154], stabilizing the dimeric form in presence of metabolites that favor the tetrameric form [153, 75].

The alteration of metabolism in HPKs expressing E6/E7 from different HPV type can be detected not only inside the cells but also in the alteration of the intake or secretion of metabolites. Of particular interest could be the secretion of new metabolites or an increase in a metabolite secretion as a marker of infection. Therefore, in collaboration with the Nutrition and Metabolism - Biomarkers Group of IARC, metabolites produced by the HFKs expressing E6/E7 from the β3 HPV types and from HPV16 were analyzed by liquid chromatography coupled with the mass spectrometry (LC/MS). The LC/MS and the subsequent processing of the data were performed by William Cheung.

To better understand the results obtained on the metabolites produced by the HFKs expressing E6 and E7, a brief overview of the experimental model is given below and it's schematically represented in figure 30.

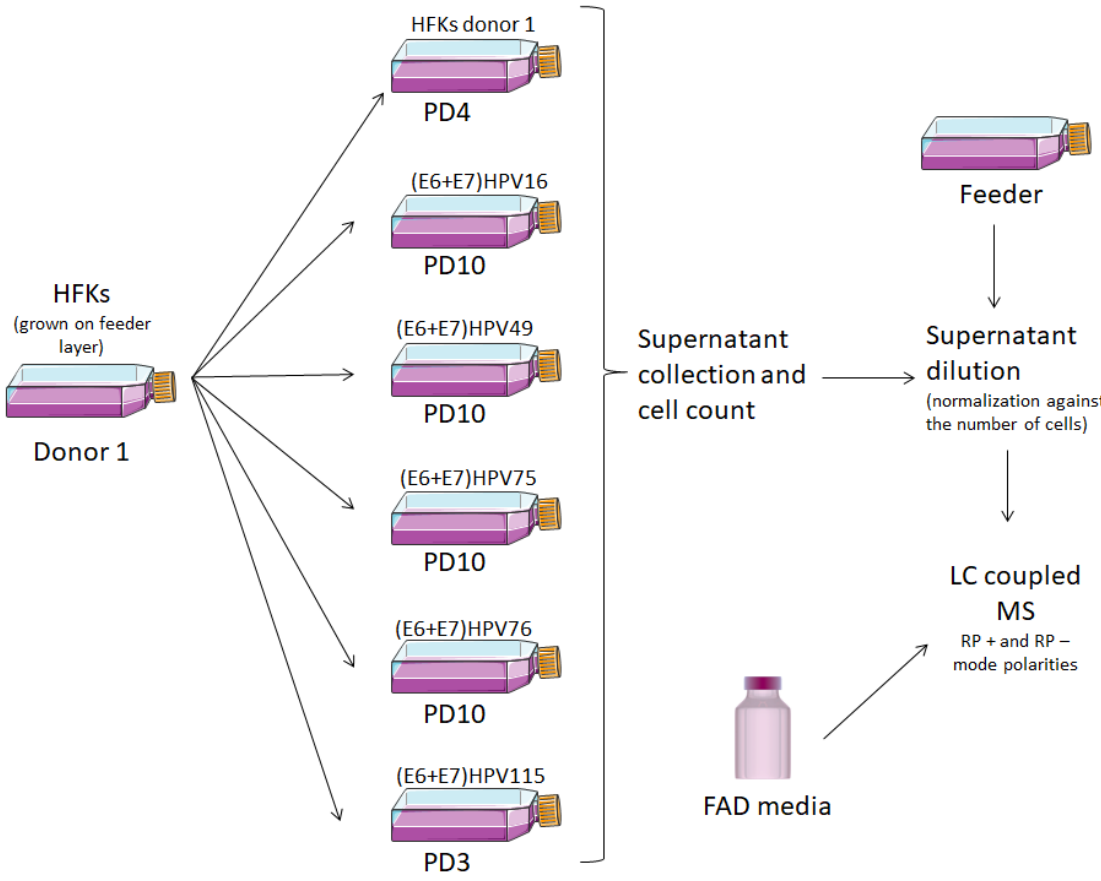

Figure 30: Schematic representation of the metabolites analysis experimental design. Human primary keratinocytes were stably transduced with E6 and E7 of β3 HPV types or E6 and E7 from HPV16 and kept in culture on a feeder layer. At passage 10 the supernatant was collected, divided into 5 aliquots and the cells counted; the supernatant was collected, and the cells counted at PD3 for HPV115 E6/E7 expressing keratinocytes and at PD4 for HFKs. The supernatant was also collected from 3 cultures of a feeder layer. The supernatants were diluted in order to normalize against the number of cells and analyzed via liquid chromatography coupled with mass spectrometry. Three aliquots of FAD media were also analyzed via LC coupled MS.

After the stable expression of E6 and E7 from the different HPV types, the cells have been kept in culture and at PD10 the supernatants were collected, and the cells were counted. For the HFKs expressing E6/E7 of HPV115, the supernatant was collected at PD3, given their short lifespan. Also for the donor HFKs, the supernatant was collected at earlier PD (PD4), a passage in which the cells are still actively proliferating and do not show any sign of senescence. As a control, NIH/3T3 fibroblasts inactivated with mitomycin C (only feeders) were cultured with FAD media and after 2 days the supernatant was collected and the cells were counted. Afterwards, the supernatant

samples were cell-count normalized by dilution in the FAD media and analyzed with liquid chromatography (LC) in tandem with mass spectrometry (MS). Additionally, a sample of FAD media was analyzed via LC coupled with MS (fig. 30).

The MS features obtained from the LC/MS were processed as schematically represented in figure 31: the features found in the FAD media or in the feeder cells were not retained for further analysis as they are not the product of the HFKs metabolism. All the features that were not present in all the 5 replicates of each HPV type were discarded as considered unreliable data. Ultimately, only MS features that could be matched to metabolites in either the Human Metabolome Database or the METLIN database based on their accurate mass were retained. All the MS features that were retained were tested with Kruskal-Wallis ANOVA and manually checked and corrected for integration error (fig. 31).

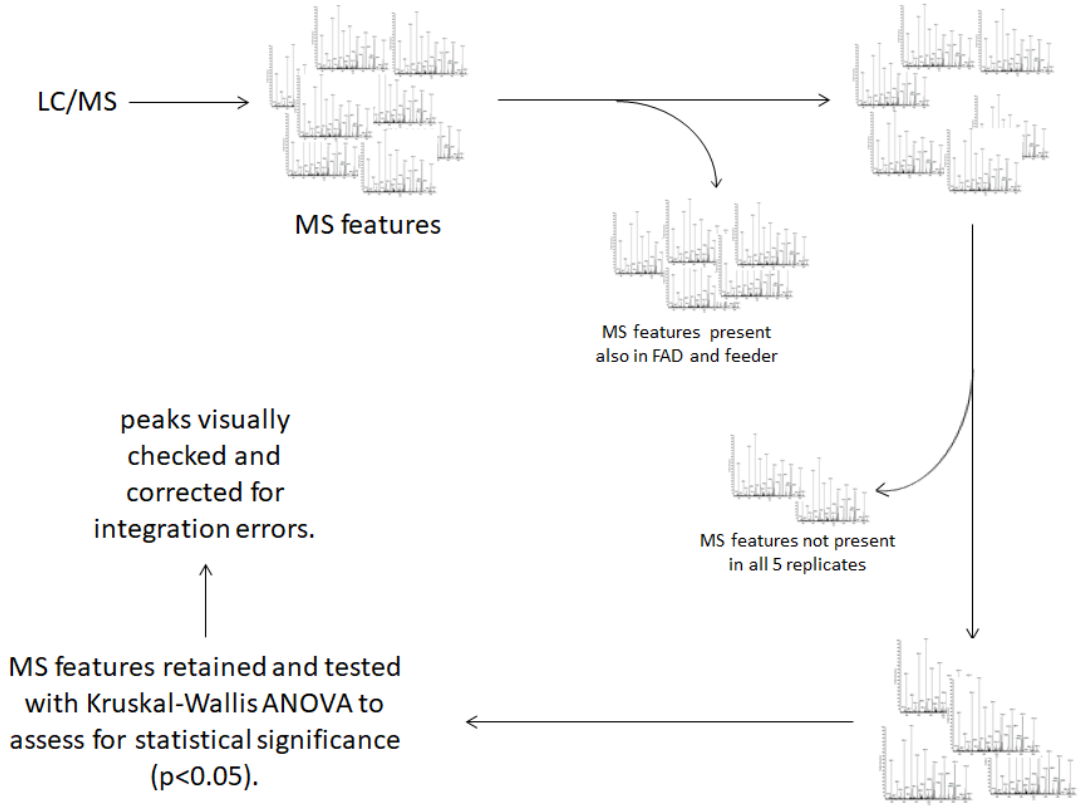

Figure 31: Schematic representation of the raw data preprocessing and filtration. The MS features obtained from the LC/MS were filtered and features present also in FAD media and in the feeder at were discarded. A quality control filter was applied, and all the features not present in the 5 replicates of the same sample were discarded. The remaining features were tested with Kruskal-Wallis ANOVA and manually checked.

The ion abundance of each feature in E6/E7 HFKs was compared to the corresponding ion abundance in primary keratinocytes and only the features with a significant difference were used for the heat map and the hierarchical clustering map generation.

After processing, 54 significant MS features were found in the positive mode and 16 features were found in the negative mode. Heat map and hierarchical cluster analysis (HCA) were generated using the online graphic user interface platform "Metaboanalyst" on the retained features and the results are shown in figures 32 and 33, respectively for the positive and negative mode. In the heat map, the red represents metabolites that are more concentrated in the E6/E7 keratinocytes than in the mock HFKs, therefore, they are metabolites that are produced by the E6/E7 HFKs. By contrast, the blue represents metabolites that are less concentrated in the E6/E7 keratinocytes than in the mock HFKs, therefore, they are metabolites that are not produced or produced less by the E6/E7 HFKs.

The heat map on the positive mode MS feature (fig. 32, left panel) shows that HPV76 and HPV49 E6/E7 expressing HFKs have a very similar pattern of metabolite de-regulation, correlating with the similarities observed in the growth abilities and in the interference with the major cellular pathways. HPV16 and HPV115 E6/E7 expressing HFKs have very different metabolites de-regulation patterns, results expected given the opposite ability of E6 and E7 of these types to immortalize the keratinocytes (fig. 32, left panel). The hierarchical cluster analysis (fig. 32, right panel) revealed that the 5 replicates of each HPV type in the positive mode cluster together, indicating that the results obtained are reliable. Moreover, as shown also in the heat map, HPV115 (in red) is clustering alone and it is the more distant from both HPV16 and the other β3 E6/E7 expressing HFKs (fig. 32, right panel). As observed in the heat map, the HCA showed that HPV49 and HPV76 E6/E7 expressing HFKs cluster together while HPV75 E6/E7 expressing HFKs cluster with HFKs expressing E6/E7 from HPV16 (fig. 32 right panel).

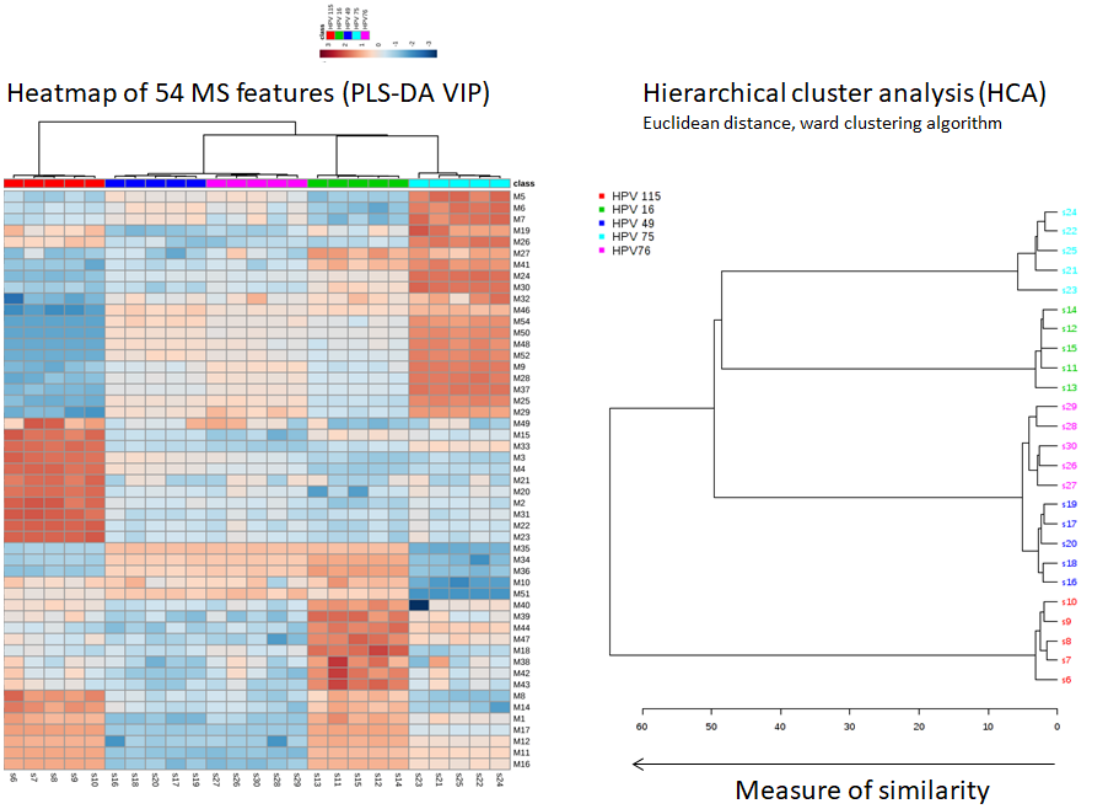

Figure 32: Immortalizing β3 E6/E7 HFKs cluster together with HPV16 E6/E7 HFKs in positive mode metabolism LC/MS analysis. The heat map of the positive mode was generated using the 54 retained MS features obtained after the processing. In blue the molecules that are less present in the samples than in the HFKs and in red the molecules more present in the samples than in the HFKs (left panel). The 54 retained MS features were used to generate a hierarchical clustering dendrogram, using Euclidean distance and ward clustering algorithm (right panel). The length of the arms is a measure of similarity between the sample.

The heat map on the negative mode MS feature (fig. 33, left panel) shows that HPV76 and HPV49 E6/E7 expressing HFKs have a very similar pattern of metabolite de-regulation, similar to what was shown on the positive mode. For the negative mode, HPV16 and HPV115 E6/E7 expressing HFKs have almost opposite metabolite de-regulation (fig. 33, left panel). The hierarchical cluster analysis (fig. 33, right panel) revealed that the 5 replicates of HFKs expressing E6 and E7 from HPV49 and 76 do not perfectly cluster within the types, indicating a less accurate analysis compared to the positive mode. Moreover, as shown also in the heat map, HPV75 and HPV16 E6/E7 expressing HFKs cluster together and the remaining β3 E6/E7 expressing HFKs cluster together (fig. 33, right panel). The negative mode pole results are not in concordance with

the positive mode results and they are overall less accurate when compared to the positive mode. It is important to note that the number of feature of negative mode before the processing is significantly lower compared to the positive mode.

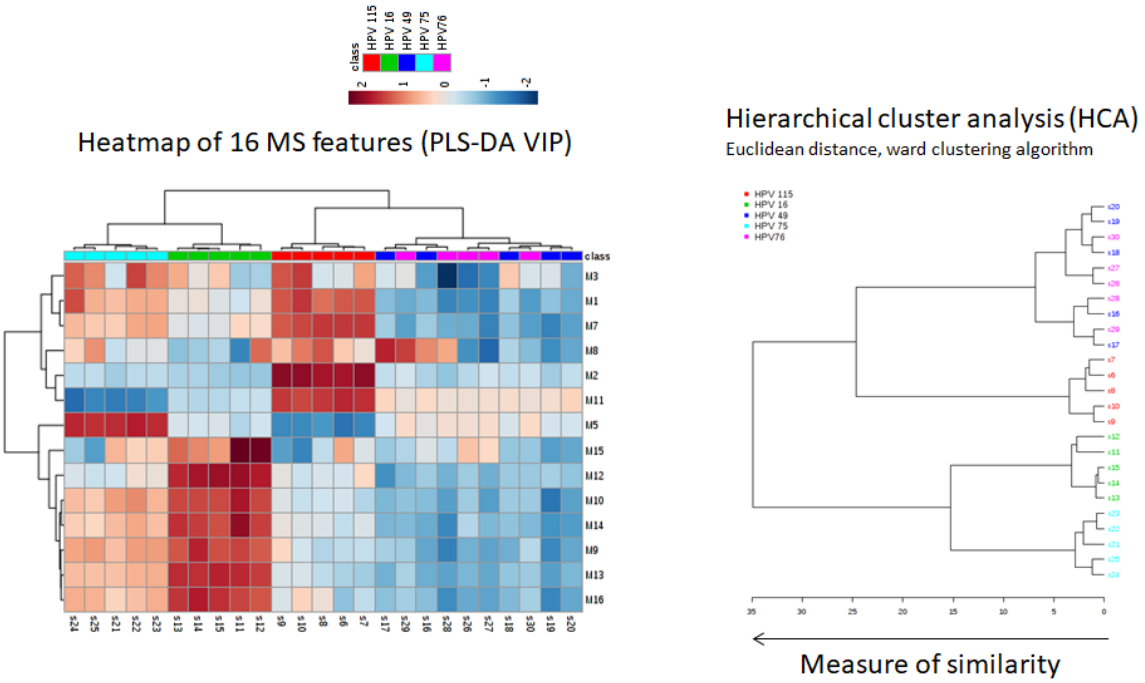

Figure 33: HPV16 and HPV75 E6/E7 HFKs cluster together in negative mode metabolism LC/MS analysis. The heat map of the positive mode was generated using the 16 retained MS features obtained after the processing. In blue the molecules that are less present in the samples than in the HFKs and in red the molecules more present in the samples than in the HFKs (left panel). The 16 retained MS features were used to generate a hierarchical clustering dendrogram, using Euclidean distance and ward clustering algorithm (right panel). The length of the arms is a measure of similarity

6 DISCUSSION AND CONCLUSIONS

The first beta HPV types (HPV5 and 8) were isolated from the skin of patients suffering from the genetic disease *epidermodysplasia verruciformis* (EV). β HPV genomes have been detected in 90% of the squamous cell carcinoma in patients with EV [103, 104]. Moreover, β HPV genomes have been detected in skin warts and in SCC of organ transplant recipient patients, supporting the hypothesis that β HPVs are the etiologic agent of NMSC in immunosuppressed individuals [112, 113, 114]. However, β HPV genomes are also detected in the skin of healthy immune-competent individuals [115, 116]. As a consequence, all the beta HPV types belonging to the 5 species (beta-1-5) are classified, by assumption, as cutaneous types.

Epidemiological studies on the association between β HPVs and cutaneous SCC have shown that β1 and β2 genomes are often found on the skin of immune-competent individuals [155, 156, 157]. In particular, the findings of a recent meta-analysis suggested an association between the β1 and β2 HPV types 5, 8, 15, 17, 20, 24, 36, and 38 and development of SCC [155]. Epidemiological serological studies have also suggested an association between SCC and β HPV types, in particular with the β1 HPVs [156]. On the contrary, in all the studies mentioned above, β3 HPV types were rarely found on the skin of healthy individuals and they were never associated with an increased risk of SCC development [157].

Interestingly, recent epidemiological studies have shown that β3 HPV types are found, with different prevalence, in mucosal epithelia [137, 135]. *Hampras et al.* showed that the β3 HPV types are differently distributed at different anatomical sites. HPV49 appears to be more abundant in the mucosal tissues (anal and oral mucosa) than in the keratinized tissues (genital and forearm skin, eyebrow hairs). Instead, HPV76 is equally distributed in eyebrow hair and anal mucosa but is present with low prevalence in the oral mucosa. HPV75 has been detected in the anal mucosa, with low prevalence in eyebrow hair and forearm skin [135]. Another recent epidemiological study showed that HPV115 is rarely found in the mucosal anatomical sites (genital, anal canal and oral cavity), an expected

result given the non-transforming abilities of E6 and E7 of this type [158]. In the same study, HPV76 is the β3 type with the highest prevalence in genital and anal canal tissue, 13.1% and 6% respectively, followed by HPV49 with 7.9% prevalence in genital tissue and 3.5% in the anal canal. HPV75, paralleling the lower transforming abilities of its E6/E7, is found in the genital tissue and in the anal canal with only 3.3% and 1.1% prevalence [158].

The data contained in this thesis demonstrates that the β3 types are a sub-group of HPVs that share some biological similarities with both β2 HPV types (e.g. HPV38) and HR α HPV types (e.g.HPV16). The mechanism of interaction of β3 E6 and E7 with the pRb pathway is similar to what is known for the β2 type 38 [120]. The expression of β HPV types E6 and E7 in *in vitro* models leads to an accumulation of the phosphorylated form of pRb, which loses its ability to bind E2F, while mucosal HR HPV types induce the degradation of hypo-phosphorylated pRb with the consequent release of E2F transcription factors [65]. Contrarily, β3 HPV E6 and E7 can induce an accumulation of $p16^{INK4a}$ in a manner similar to E7 derived from the HR α types [81]. Moreover, β3 types shares with HR α type 16 the ability to degrade p53 via the proteasome pathway, mediated by the interaction with the ubiquitin ligase E6AP, while β2 HPV38 E7 promotes the accumulation of p53 and p73 antagonist ΔNp73α [86, 85, 84, 58, 121]. The expression profile analysis showed that β3 immortalizing types share with HR HPV16 an enrichment of de-regulated genes involved in p53, DNA repair pathway and DNA replication. Interestingly, both α type 16 and β2 type 38 induce the up-regulation of hTERT expression, a property also shared by β3 immortalizing types.

The phylogenetic classification of papillomaviruses is based on the gene sequence of the major capsid protein L1, and the DNA sequence of the L1 ORF must differ by more than 10% from the closest known PV type to be considered a new type [1]. To date, only four β3 HPVs have been isolated, but the existence of additional types cannot be ruled out. It is likely that with the introduction of next-generation sequencing technology new PV types will be found. The presence of the known β3 HPVs in mucosal tissue and their biological properties suggest that the research of new β3 should be carried out in an

anatomical region other than skin. Moreover, the phylogenetic assembly does not necessary reflect the biological properties or the tissue tropism of the viruses. Corroborating this statement, the alpha genus includes mucosal as well as cutaneous types. Among the mucosal types, there are low-risk and high-risk HPV types that are associated, respectively, with benign and malignant genital lesions [159]. Hence, it is plausible to hypothesize that not all the β HPVs share similar tissue tropism and biological properties.

The biological similarities between HPV49 and HPV16 onco-proteins are further corroborated by *in vivo* studies on mouse models. Massimo Tommasino's group have developed two different transgenic mice (Tg) models that express β2 HPV38 or β3 HPV49 E6 and E7 proteins in epithelial cells under the control of the keratin 14 promoter. These animal models have highlighted the ability of the β HPV types to synergize with different environmental risk factors in promoting cancer development. *Viarisio et al.* showed that Tg mice expressing E6/E7 of HPV16 and HPV49 in the basal layer of the epithelia are highly susceptible to the development of upper digestive tract cancer upon treatment with the tobacco-equivalent chemical 4-nitroquinoline 1-oxide (4NQO) [139]. Whole exome sequencing of DNA extracted form upper-digestive tract cancers revealed that 4NQO treatment promoted accumulation of DNA mutation signature of tobacco use (unpublished data). By contrast, wild type mice and Tg mice expressing E6/E7 from HPV38 treated with 4NQO developed a significantly lower number of lesions, mostly histologically benign in origin [139]. Vice versa, β2 HPV38 E6 and E7 Tg mice are highly susceptible to UV-driven skin carcinogenesis [131, 130]. Exposure to chronic UV irradiation resulted in the development of AK-like lesions and subsequently of SCC [130]. Whole exome sequencing showed that chronic UV irradiation of β2 HPV38 E6/E7 transgenic mice resulted in the accumulation of a large number of UV-induced DNA mutations, which resembles the mutation pattern detected in human NMSC [131]. Using the same model of UV-exposure, the wild type and the Tg mice expressing E6/E7 HPV49 did not develop skin cancer and did not accumulate UV-induced mutations [139, 130].

It is not yet clear whether β3 HPV types are involved in specific human pathological conditions, such as cancer. To date, there are no available studies on the presence of β3 HPVs in tumour tissue. A well-recognized hypothesis is that β1 and β2 HPVs act with a "hit and run" mechanism, favoring the initial stage of tumour development and the accumulation of UV-induced mutations. Supporting this hypothesis, a recent *in vivo* study on Tg expressing β2 HPV38 E6/E7 in the basal layer of the epithelia showed that the knock down of E6/E7 expression after the development of the cancerous lesions do not cause a regression of the tumour [131]. Moreover, β2 HPV genomes are usually found in high copy number/cell (>50 copies/cell) in the pre-cancerous AK tissue while the genomes are almost completely lost with the development of SCC (less than 1 copy/cell), indicating a loss of HPV genome during the cancer development [118].

It is plausible to hypothesize that also the β3 HPV types act with a "hit and run" mechanism, with E6 and E7 favoring the accumulation of mutations caused by additional environmental factors. β3 HPVs might play an important role in the early stage of the tumour development and in the establishment of a transformed phenotype of the cells.

To better understand the role of β3 HPVs in the development of cancer, it would be interesting to characterize the changes in the methylome induced by the expression of β3 E6/E7 and compare it with the signature of fully characterized human cancers. Changes in the DNA methylation are an irreversible epigenetic signature driven by environmental factors. Several studies have reported that HPVs are able to interfere with the DNA methylation machinery, creating methylome signatures [160]. Supporting this notion is evidence that the progression from normal tissue to HPV-driven cervical cancer is associated with a progressive cellular genome hypomethylation [161]. However, certain genomic DNA regions become hypermethylated, causing the silencing of the tumour suppressor genes (reviewed in [162]).

6.1 FUTURE PROSPECTIVES

The data presented in this thesis characterized some of the β3 E6/E7 functions, however, some questions require further clarification.

The data presented here show that E6 is able to interact with E6AP, however, it has been previously shown that HPV E6 proteins preferentially interact with MAML1 over E6AP, with the exception of the α HPV types [123]. Moreover, *White et al.* showed that HPV76 is able to degrade p53 but preferentially binds MAML1 over E6AP [122]. Both MAML1 and E6AP contain the same LXXLL motif that is recognized by the different E6 proteins and, given the similarities between β3 and the α HPV types, it is plausible to hypothesize that β3 E6s are able to physically interact with both MAML1 and E6AP. The analysis of mutation on the HPV76 E6 region responsible for the interaction with p53 and E6AP showed that D44A mutant retain both the ability to degrade p53 and up-regulate hTERT, however it is unable to collaborate with E7 in the immortalization assay. A possible explanation could be that this particular mutant is still able to interact with p53 and E6AP but the interaction with MAML1 is impaired, causing the inability to immortalize the HFKs. Further molecular analysis is required to understand the interaction of β3 E6s with both MAML1 and E6AP.

Another interesting question is the biological significance of $p16^{INK4a}$ overexpression. In fact, it has been previously shown that in HPV16 E6/E7 expressing HFKs, $p16^{INK4a}$ favors proliferation and survival through more than one molecular mechanism =[82]=[82]. It remains unclear if β3 E6/E7 HFKs are also "addicted" to the up-regulation of $p16^{INK4a}$ and how this protein, which is normally classified as a tumour suppressor, plays a role in the transformation process of β3 HFKs.

Finally, the association between β3 HPVs and human diseases could be facilitated by the identification of markers of infection. For this purpose, the analysis of the metabolome was performed. The initial data highlighted differences in metabolite secretion between the immortalizing and non-immortalizing types. Additional studies are required to characterize these differences with the view to find potential disease or pre-malignant lesion biomarkers to aid disease identification.

ACRONYMS AND ABBREVIATIONS

^{0} C: Degree Celsius

4NQO: 4-nitroquinoline 1-oxide

AK: actinic keratosis

Amp: Ampicillin

APS: Ammonium persulfate

bp: base pairs

CDK: cyclin dependent kinase

Chl: Chloramphenicol

CIN: Cervical intraepithelial neoplasia

DMEM: Dulbecco´s modified Eagles medium

DMSO: Dimethyl sulfoxide

Ds: Double stranded

E.coli: Escherichia coli

E6: Human papillomavirus early protein 6

E6AP: E6 Associated protein

E7: Human papillomavirus early protein 7

EDTA: Ethylen-di-amino-tetra-acetate

EV: epidermodysplasia verruciformis

Fw: primer forward

H: Hours

HAT: histone acetyl transferase

HFK: human foreskin keratinocyte

HPV: Human Papillomavirus

HR: High risk

hTERT: human telomerase

K14: keratin 14

Kan: Kanamycin

kb: Kilo base pair

kDa: kilo Dalton

l: Liter

L1: Human papillomavirus major capsid protein

L2: Human papillomavirus minor capsid protein

LB: Luria Broth

LR: low risk

M: Molar

mA: milli Ampère

MAML1: mastermind-like 1

MBP: maltose binding protein

min: minutes

ml: Milliliter

mM: Millimolar

mRNA: Messenger RNA

MS: Mass-spectrometry

nM: Nanomolar

NMSC: Non melanoma skin cancer

ORF: open reading frame

Ori: Origin of replication

OTR: organ transplant recipients

PBS: Phosphate buffered saline

PBS-Tween: Phosphate buffered saline-tween

PCR: Polymerase chain reaction

PDGF: Plated derived growth factor

PV: Papillomaviruses

Rb: Retinoblastoma protein

Rev: primer reverse

RNA: Ribonucleic acid

rpm: Revolutions per minute

RT: Room temperature

SCC: Squamous cell carcinoma

SDS: Sodium dodecyl sulfate

siRNA: Short interference RNA

TEMED: N,N,N´,N´-tetra-methylethylendiamin

Tg: Transgenic

URR: Upstream regulatory region

UV: ultra-violet

wt: Wild type

μg: Microgram

μl: Microliter

μM: Micromolar

AMINO ACIDS

One letter symbol	Amino-acid
A	Alanine
C	Cysteine
D	Aspartate
E	Glutamate
F	Phenylalanine
G	Glycine
H	Histidine
I	Isoleucine
K	Lysine
L	Leucine
M	Methionine
N	Asparagine
P	Proline
Q	Glutamine
R	Arginine
S	Serine
T	Threonine
V	Valine
W	Tryptophan
Y	Tyrosine

REFERENCES

[1] Ethel-Michele de Villiers, Claude Fauquet, Thomas R Broker, Hans-Ulrich Bernard, and Harald zur Hausen. Classification of papillomaviruses. *Virology*, 324(1):17 – 27, 2004.

[2] Nagayasu Egawa, Kiyofumi Egawa, Heather Griffin, and John Doorbar. Human papillomaviruses; epithelial tropisms, and the development of neoplasia. *Viruses*, 7(7):3863–3890, 2015.

[3] Margaret A. Stanley. Epithelial cell responses to infection with human papillomavirus. *Clinical Microbiology Reviews*, 25(2):215–222, April 2012.

[4] Stenlund A. Sedman, J. Co-operative interaction between the initiator e1 and the transcriptional activator e2 is required for replicator specific dna replication of bovine papillomavirus in vivo and in vitro. *The EMBO Journal*, 14(24):6218â€“6228, 1995.

[5] Van G. Wilson, Michael West, Kelly Woytek, and Dandapani Rangasamy. Papillomavirus e1 proteins: Form, function, and features. *Virus Genes*, 24(3):275–290, 2002.

[6] Pauline B. McIntosh, Peter Laskey, Kate Sullivan, Clare Davy, Qian Wang, Deborah J. Jackson, Heather M. Griffin, and John Doorbar. E1^e4-mediated keratin phosphorylation and ubiquitylation: a mechanism for keratin depletion in hpv16-infected epithelium. *Journal of Cell Science*, 123:2810–22, Aug 2010.

[7] Pauline B. McIntosh, Stephen R. Martin, Deborah J. Jackson, Jameela Khan, Erin R. Isaacson, Lesley Calder, Kenneth Raj, Heather M. Griffin, Qian Wang, Peter Laskey, John F. Eccleston, and John Doorbar. Structural analysis reveals an amyloid form of the human papillomavirus type 16 e1(∧) e4 protein and provides a molecular basis for its accumulation. *Journal of Virology*, 82:8196–203, Aug 2008.

[8] Banks L. Pim D, Collins M. Human papillomavirus type 16 e5 gene stimulates the transforming activity of the epidermal growth factor receptor. *Oncogene*, 7(1)::27–32, 1992.

[9] Daniel DiMaio and Lisa M. Petti. The {E5} proteins. *Virology*, 445(1â€“2):99 – 114, 2013. Special Issue: The Papillomavirus Episteme.

[10] Marcel Dreer, Saskia van de Poel, and Frank Stubenrauch. Control of viral replication and transcription by the papillomavirus e8^e2 protein. *Virus Research*, pages –, 2016.

[11] John Doorbar, Wim Quint, Lawrence Banks, Ignacio G. Bravo, Mark Stoler, Tom R. Broker, and Margaret A. Stanley. The biology and life-cycle of human papillomaviruses. *Vaccine*, 30, Supplement 5:F55 – F70, 2012. Comprehensive Control of HPV Infections and Related Diseases.

[12] Massimo Tommasino. The biology of beta human papillomaviruses. *Virus Research*, pages –, 2016.

[13] Patricia M. Day and Mario Schelhaas. Concepts of papillomavirus entry into host cells. *Current Opinion in Virology*, 4:24 – 31, 2014. Virus entry / Environmental virology.

[14] B M Steinberg, K J Auborn, J L Brandsma, and L B Taichman. Tissue site-specific enhancer function of the upstream regulatory region of human papillomavirus type 11 in cultured keratinocytes. *Journal of Virology*, 63(2):957–960, 1989.

[15] Matthias Ottinger, Jennifer A. Smith, Michal-Ruth Schweiger, Dana Robbins, Maria L.C. Powell, Jianxin You, and Peter M. Howley. Cell-type specific transcriptional activities among different papillomavirus long control regions and their regulation by E2. *Virology*, 395(2):161 – 171, 2009.

[16] John Doorbar. The E4 protein; structure, function and patterns of expression. *Virology*, 445(1-2):80 – 98, 2013. Special Issue: The Papillomavirus Episteme.

[17] Catherine de Martel, Jacques Ferlay, Silvia Franceschi, Jerome Vignat, Freddie Bray, David Forman, and Martyn Plummer. Global burden of cancers attributable to infections in 2008: a review and synthetic analysis. *The Lancet. Oncology*, 13:607–15, Jun 2012.

[18] Iarc monographs volume 90.

[19] Vincent Cogliano, Robert Baan, Kurt Straif, Yann Grosse, Beatrice Secretan, and Fatiha El Ghissassi. Carcinogenicity of human papillomaviruses. *The Lancet Oncology*, 6(4):204.

[20] Harald zur Hausen. Papillomaviruses and cancer: from basic studies to clinical application. *Nature reviews. Cancer*, 2:342–50, May 2002.

[21] A. G. Ostor. Natural history of cervical intraepithelial neoplasia: a critical review. *International journal of gynecological pathology : official journal of the International Society of Gynecological Pathologists*, 12:186–92, Apr 1993.

[22] R. W. Jones, J. S. Park, M. R. McLean, and K. V. Shah. Human papillomavirus in women with vulvar intraepithelial neoplasia iii. *The Journal of reproductive medicine*, 35:1124–6, Dec 1990.

[23] P. K. Magnusson, P. Sparen, and U. B. Gyllensten. Genetic link to cervical tumours., Jul 1999.

[24] V. Moreno, N. Munoz, F. X. Bosch, S. de Sanjose, L. C. Gonzalez, L. Tafur, M. Gili, I. Izarzugaza, C. Navarro, and A. Vergara. Risk factors for progression of cervical intraepithelial neoplasm grade iii to invasive cervical cancer. *Cancer epidemiology, biomarkers & prevention : a publication of the American Association for Cancer Research, cosponsored by the American Society of Preventive Oncology*, 4:459–67, Jul-Aug 1995.

[25] Victor Moreno, F. Xavier Bosch, Nubia Munoz, Chris J. L. M. Meijer, Keerti V. Shah, Jan M. M. Walboomers, Rolando Herrero, and Silvia Franceschi. Effect of oral contraceptives on risk of cervical cancer in women with human papillomavirus infection: the iarc multicentric case-control study. *Lancet (London, England)*, 359:1085–92, Mar 2002.

[26] M. H. Schiffman, N. J. Haley, J. S. Felton, A. W. Andrews, R. A. Kaslow, W. D. Lancaster, R. J. Kurman, L. A. Brinton, L. B. Lannom, and D. Hoffmann. Biochemical epidemiology of cervical neoplasia: measuring cigarette smoke constituents in the cervix. *Cancer research*, 47:3886–8, Jul 1987.

[27] Maura L. Gillison, Anil K. Chaturvedi, and Douglas R. Lowy. Hpv prophylactic vaccines and the potential prevention of noncervical cancers in both men and women. *Cancer*, 113:3036–46, Nov 2008.

[28] Anil K. Chaturvedi, Eric A. Engels, Ruth M. Pfeiffer, Brenda Y. Hernandez, Weihong Xiao, Esther Kim, Bo Jiang, Marc T. Goodman, Maria Sibug-Saber, Wendy Cozen, Lihua Liu, Charles F. Lynch, Nicolas Wentzensen, Richard C. Jordan, Sean Altekruse, William F. Anderson, Philip S. Rosenberg, and Maura L. Gillison. Human papillomavirus and rising oropharyngeal cancer incidence in the united states. *Journal of clinical oncology : official journal of the American Society of Clinical Oncology*, 29:4294–301, Nov 2011.

[29] M. L. Gillison, W. M. Koch, R. B. Capone, M. Spafford, W. H. Westra, L. Wu, M. L. Zahurak, R. W. Daniel, M. Viglione, D. E. Symer, K. V. Shah, and D. Sidransky. Evidence for a causal association between human papillomavirus and a subset of head and neck cancers. *Journal of the National Cancer Institute*, 92:709–20, May 2000.

[30] Ciaran B. J. Woodman, Stuart I. Collins, and Lawrence S. Young. The natural history of cervical hpv infection: unresolved issues. *Nature Reviews Cancer*, 7:11, January 2007.

[31] V. Bouvard, G. Matlashewski, Z. M. Gu, A. Storey, and L. Banks. The human papillomavirus type 16 e5 gene cooperates with the e7 gene to stimulate proliferation of primary cells and increases viral gene expression. *Virology*, 203:73–80, Aug 1994.

[32] Sybil M. Genther Williams, Gary L. Disbrow, Richard Schlegel, Daekee Lee, David W. Threadgill, and Paul F. Lambert. Requirement of epidermal growth factor receptor for hyperplasia induced by e5, a high-risk human papillomavirus oncogene. *Cancer research*, 65:6534–42, Aug 2005.

[33] J. M. Arbeit, K. Munger, P. M. Howley, and D. Hanahan. Progressive squamous epithelial neoplasia in k14-human papillomavirus type 16 transgenic mice. *Journal of virology*, 68:4358–68, Jul 1994.

[34] C. C. Baker, W. C. Phelps, V. Lindgren, M. J. Braun, M. A. Gonda, and P. M. Howley. Structural and transcriptional analysis of human papillomavirus type 16 sequences in cervical carcinoma cell lines. *Journal of virology*, 61:962–71, Apr 1987.

[35] Stuart I. Collins, Christothea Constandinou-Williams, Kaisheng Wen, Lawrence S. Young, Sally Roberts, Paul G. Murray, and Ciaran B. J. Woodman. Disruption of the e2 gene is a common and early event in the natural history of cervical human papillomavirus infection: a longitudinal cohort study. *Cancer research*, 69:3828–32, May 2009.

[36] S. A. Corden, L. J. Sant-Cassia, A. J. Easton, and A. G. Morris. The integration of hpv-18 dna in cervical carcinoma. *Molecular pathology : MP*, 52:275–82, Oct 1999.

[37] H. Shirasawa, Y. Tomita, S. Sekiya, H. Takamizawa, and B. Simizu. Integration and transcription of human papillomavirus type 16 and 18 sequences in cell lines derived from cervical carcinomas. *The Journal of general virology*, 68 (Pt 2):583–91, Feb 1987.

[38] L. Pirami, V. Giache, and A. Becciolini. Analysis of hpv16, 18, 31, and 35 dna in pre-invasive and invasive lesions of the uterine cervix. *Journal of clinical pathology*, 50:600–4, Jul 1997.

[39] A. P. Cullen, R. Reid, M. Campion, and A. T. Lorincz. Analysis of the physical state of different human papillomavirus dnas in intraepithelial and invasive cervical neoplasm. *Journal of virology*, 65:606–12, Feb 1991.

[40] E. Schwarz, U. K. Freese, L. Gissmann, W. Mayer, B. Roggenbuck, A. Stremlau, and H. zur Hausen. Structure and transcription of human papillomavirus sequences in cervical carcinoma cells. *Nature*, 314:111–4, Mar 1985.

[41] Luis M. Alvarez-Salas and Joseph A. DiPaolo. Molecular approaches to cervical cancer therapy. *Current drug discovery technologies*, 4:208–19, Oct 2007.

[42] S. Yasumoto, A. L. Burkhardt, J. Doniger, and J. A. DiPaolo. Human papillomavirus type 16 dna-induced malignant transformation of nih 3t3 cells. *Journal of virology*, 57:572–7, Feb 1986.

[43] M. Durst, R. T. Dzarlieva-Petrusevska, P. Boukamp, N. E. Fusenig, and L. Gissmann. Molecular and cytogenetic analysis of immortalized human primary keratinocytes obtained after transfection with human papillomavirus type 16 dna. *Oncogene*, 1:251–6, 1987.

[44] L. Pirisi, S. Yasumoto, M. Feller, J. Doniger, and J. A. DiPaolo. Transformation of human fibroblasts and keratinocytes with human papillomavirus type 16 dna. *Journal of virology*, 61:1061–6, Apr 1987.

[45] A. Storey, D. Pim, A. Murray, K. Osborn, L. Banks, and L. Crawford. Comparison of the in vitro transforming activities of human papillomavirus types. *The EMBO journal*, 7:1815–20, Jun 1988.

[46] M. A. Bedell, K. H. Jones, S. R. Grossman, and L. A. Laimins. Identification of human papillomavirus type 18 transforming genes in immortalized and primary cells. *Journal of virology*, 63:1247–55, Mar 1989.

[47] S. A. Sedman, M. S. Barbosa, W. C. Vass, N. L. Hubbert, J. A. Haas, D. R. Lowy, and J. T. Schiller. The full-length e6 protein of human papillomavirus type 16 has transforming and trans-activating activities and cooperates with e7 to immortalize keratinocytes in culture. *Journal of virology*, 65:4860–6, Sep 1991.

[48] Anthony J. Schaeffer, Marie Nguyen, Amy Liem, Denis Lee, Cristina Montagna, Paul F. Lambert, Thomas Ried, and Michael J. Difilippantonio. E6 and e7 oncoproteins induce distinct patterns of chromosomal aneuploidy in skin tumors from transgenic mice. *Cancer research*, 64:538–46, Jan 2004.

[49] Rebeccah R. Riley, Stefan Duensing, Tiffany Brake, Karl Munger, Paul F. Lambert, and Jeffrey M. Arbeit. Dissection of human papillomavirus e6 and e7 function in transgenic mouse models of cervical carcinogenesis. *Cancer research*, 63:4862–71, Aug 2003.

[50] C. Meyers, M. G. Frattini, J. B. Hudson, and L. A. Laimins. Biosynthesis of human papillomavirus from a continuous cell line upon epithelial differentiation. *Science (New York, N.Y.)*, 257:971–3, Aug 1992.

[51] S. C. Dollard, J. L. Wilson, L. M. Demeter, W. Bonnez, R. C. Reichman, T. R. Broker, and L. T. Chow. Production of human papillomavirus and modulation of the infectious program in epithelial raft cultures. off. *Genes & development*, 6:1131–42, Jul 1992.

[52] C. Meyers and L. A. Laimins. In vitro systems for the study and propagation of human papillomaviruses. *Current topics in microbiology and immunology*, 186:199–215, 1994.

[53] Levana Sherman, Anna Jackman, Hagar Itzhaki, Melissa Conrad Stöppler, Debbie Koval, and Richard Schlegel. Inhibition of serum- and calcium-induced differentiation of human keratinocytes by hpv16 e6 oncoprotein: Role of p53 inactivation. *Virology*, 237(2):296 – 306, 1997.

[54] F. Stubenrauch and L. A. Laimins. Human papillomavirus life cycle: active and latent phases. *Seminars in cancer biology*, 9:379–86, Dec 1999.

[55] N. Sanjib Banerjee, Hsu-Kun Wang, Thomas R. Broker, and Louise T. Chow. Human papillomavirus (hpv) e7 induces prolonged g2 following s phase reentry in differentiated human keratinocytes. *Journal of Biological Chemistry*, 286(17):15473–15482, 2011.

[56] Xiaobo Zhou and Karl Munger. Expression of the human papillomavirus type 16 e7 oncoprotein induces an autophagy-related process and sensitizes normal human keratinocytes to cell death in response to growth factor deprivation. *Virology*, 385:192–7, Mar 2009.

[57] G. I. Evan and K. H. Vousden. Proliferation, cell cycle and apoptosis in cancer. *Nature*, 411:342–8, May 2001.

[58] M. Scheffner, B. A. Werness, J. M. Huibregtse, A. J. Levine, and P. M. Howley. The e6 oncoprotein encoded by human papillomavirus types 16 and 18 promotes the degradation of p53. *Cell*, 63:1129–36, Dec 1990.

[59] T. Kiyono, S. A. Foster, J. I. Koop, J. K. McDougall, D. A. Galloway, and A. J. Klingelhutz. Both rb/p16ink4a inactivation and telomerase activity are required to immortalize human epithelial cells. *Nature*, 396:84–8, Nov 1998.

[60] A. J. Klingelhutz, S. A. Foster, and J. K. McDougall. Telomerase activation by the e6 gene product of human papillomavirus type 16. *Nature*, 380:79–82, Mar 1996.

[61] H. Sato, S. Watanabe, A. Furuno, and K. Yoshiike. Human papillomavirus type 16 e7 protein expressed in escherichia coli and monkey cos-1 cells: immunofluorescence detection of the nuclear e7 protein. *Virology*, 170:311–5, May 1989.

[62] Michael Angeline, Eric Merle, and Junona Moroianu. The e7 oncoprotein of high-risk human papillomavirus type 16 enters the nucleus via a nonclassical ran-dependent pathway. *Virology*, 317:13–23, Dec 2003.

[63] N. Dyson, P. M. Howley, K. Munger, and E. Harlow. The human papilloma virus-16 e7 oncoprotein is able to bind to the retinoblastoma gene product. *Science (New York, N.Y.)*, 243:934–7, Feb 1989.

[64] Hugh Cam and Brian David Dynlacht. Emerging roles for e2f: beyond the g1/s transition and dna replication. *Cancer cell*, 3:311–6, Apr 2003.

[65] E. Berezutskaya, B. Yu, A. Morozov, P. Raychaudhuri, and S. Bagchi. Differential regulation of the pocket domains of the retinoblastoma family proteins by the hpv16 e7 oncoprotein. *Cell growth & differentiation : the molecular biology journal of the American Association for Cancer Research*, 8:1277–86, Dec 1997.

[66] S. N. Boyer, D. E. Wazer, and V. Band. E7 protein of human papilloma virus-16 induces degradation of retinoblastoma protein through the ubiquitin-proteasome pathway. *Cancer research*, 56:4620–4, Oct 1996.

[67] J. O. Funk, S. Waga, J. B. Harry, E. Espling, B. Stillman, and D. A. Galloway. Inhibition of cdk activity and pcna-dependent dna replication by p21 is blocked by interaction with the hpv-16 e7 oncoprotein. *Genes & development*, 11:2090–100, Aug 1997.

[68] D. L. Jones, R. M. Alani, and K. Munger. The human papillomavirus e7 oncoprotein can uncouple cellular differentiation and proliferation in human keratinocytes by abrogating p21cip1-mediated inhibition of cdk2. *Genes & development*, 11:2101–11, Aug 1997.

[69] R. M. Alani, J. Hasskarl, and K. Munger. Alterations in cyclin-dependent kinase 2 function during differentiation of primary human keratinocytes. *Molecular carcinogenesis*, 23:226–33, Dec 1998.

[70] F. Noya, W. M. Chien, T. R. Broker, and L. T. Chow. p21cip1 degradation in differentiated keratinocytes is abrogated by costabilization with cyclin e induced by human papillomavirus e7. *Journal of virology*, 75:6121–34, Jul 2001.

[71] R. Honda, H. Tanaka, and H. Yasuda. Oncoprotein mdm2 is a ubiquitin ligase e3 for tumor suppressor p53. *FEBS letters*, 420:25–7, Dec 1997.

[72] D. L. Jones and K. Munger. Analysis of the p53-mediated g1 growth arrest pathway in cells expressing the human papillomavirus type 16 e7 oncoprotein. *Journal of virology*, 71:2905–12, Apr 1997.

[73] G. W. Demers, C. L. Halbert, and D. A. Galloway. Elevated wild-type p53 protein levels in human epithelial cell lines immortalized by the human papillomavirus type 16 e7 gene. *Virology*, 198:169–74, Jan 1994.

[74] S. E. Seavey, M. Holubar, L. J. Saucedo, and M. E. Perry. The e7 oncoprotein of human papillomavirus type 16 stabilizes p53 through a mechanism independent of p19(arf). *Journal of virology*, 73:7590–8, Sep 1999.

[75] S. Mazurek, W. Zwerschke, P. Jansen-Durr, and E. Eigenbrodt. Effects of the human papilloma virus hpv-16 e7 oncoprotein on glycolysis and glutaminolysis: role of pyruvate kinase type m2 and the glycolytic-enzyme complex. *The Biochemical journal*, 356:247–56, May 2001.

[76] S. Duensing and K. Munger. Centrosome abnormalities, genomic instability and carcinogenic progression. *Biochimica et biophysica acta*, 1471:M81–8, 2001.

[77] A. Brehm, S. J. Nielsen, E. A. Miska, D. J. McCance, J. L. Reid, A. J. Bannister, and T. Kouzarides. The e7 oncoprotein associates with mi2 and histone deacetylase activity to promote cell growth. *The EMBO journal*, 18:2449–58, May 1999.

[78] Agnieszka K. Witkiewicz, Karen E. Knudsen, Adam P. Dicker, and Erik S. Knudsen. The meaning of p16(ink4a) expression in tumors: Functional significance, clinical associations and future developments, Aug 2011.

[79] S. N. Khleif, J. DeGregori, C. L. Yee, G. A. Otterson, F. J. Kaye, J. R. Nevins, and P. M. Howley. Inhibition of cyclin d-cdk4/cdk6 activity is associated with an e2f-mediated induction of cyclin kinase inhibitor activity. *Proceedings of the National Academy of Sciences of the United States of America*, 93:4350–4, Apr 1996.

[80] R H Medema, R E Herrera, F Lam, and R A Weinberg. Growth suppression by p16ink4 requires functional retinoblastoma protein. *Proceedings of the National Academy of Sciences*, 92(14):6289–6293, 1995.

[81] Margaret E. McLaughlin-Drubin, Donglim Park, and Karl Munger. Tumor suppressor p16ink4a is necessary for survival of cervical carcinoma cell lines. *Proceedings of the National Academy of Sciences of the United States of America*, 110:16175–80, Oct 2013.

[82] Alexander Pauck, Barbara Lener, Monika Hoell, Andreas Kaiser, Andreas M. Kaufmann, Werner Zwerschke, and Pidder Jansen-Durr. Depletion of the cdk inhibitor p16ink4a differentially affects proliferation of established cervical carcinoma cells. *Journal of virology*, 88:5256–62, May 2014.

[83] M. S. Barbosa, D. R. Lowy, and J. T. Schiller. Papillomavirus polypeptides e6 and e7 are zinc-binding proteins. *Journal of virology*, 63:1404–7, Mar 1989.

[84] D. L. Jones, D. A. Thompson, and K. Munger. Destabilization of the rb tumor suppressor protein and stabilization of p53 contribute to hpv type 16 e7-induced apoptosis. *Virology*, 239:97–107, Dec 1997.

[85] M. Scheffner, J. M. Huibregtse, R. D. Vierstra, and P. M. Howley. The hpv-16 e6 and e6-ap complex functions as a ubiquitin-protein ligase in the ubiquitination of p53. *Cell*, 75:495–505, Nov 1993.

[86] P. Beer-Romero, S. Glass, and M. Rolfe. Antisense targeting of e6ap elevates p53 in hpv-infected cells but not in normal cells. *Oncogene*, 14:595–602, Feb 1997.

[87] U. Nuber, S. E. Schwarz, and M. Scheffner. The ubiquitin-protein ligase e6-associated protein (e6-ap) serves as its own substrate. *European journal of biochemistry*, 254:643–9, Jun 1998.

[88] Denise Martinez-Zapien, Francesc Xavier Ruiz, Juline Poirson, Andre Mitschler, Juan Ramirez, Anne Forster, Alexandra Cousido-Siah, Murielle Masson, Scott Vande Pol, Alberto Podjarny, Gilles Trave, and Katia Zanier. Structure of the e6/e6ap/p53 complex required for hpv-mediated degradation of p53. *Nature*, 529:541–5, Jan 2016.

[89] Sara M. Reed and Dawn E. Quelle. p53 acetylation: Regulation and consequences, Mar 2015.

[90] Mary C. Thomas and Cheng-Ming Chiang. E6 oncoprotein represses p53-dependent gene activation via inhibition of protein acetylation independently of inducing p53 degradation. *Molecular cell*, 17:251–64, Jan 2005.

[91] A. E. Griep, R. Herber, S. Jeon, J. K. Lohse, R. R. Dubielzig, and P. F. Lambert. Tumorigenicity by human papillomavirus type 16 e6 and e7 in transgenic mice correlates with alterations in epithelial cell growth and differentiation. *Journal of virology*, 67:1373–84, Mar 1993.

[92] H. Pan and A. E. Griep. Temporally distinct patterns of p53-dependent and p53-independent apoptosis during mouse lens development. *Genes & development*, 9:2157–69, Sep 1995.

[93] Marco van Ham and Wiljan Hendriks. Pdz domains-glue and guide. *Molecular biology reports*, 30:69–82, Jun 2003.

[94] Marie L. Nguyen, Minh M. Nguyen, Denis Lee, Anne E. Griep, and Paul F. Lambert. The pdz ligand domain of the human papillomavirus type 16 e6 protein is required for e6's induction of epithelial hyperplasia in vivo. *Journal of virology*, 77:6957–64, Jun 2003.

[95] L. Gewin and D. A. Galloway. E box-dependent activation of telomerase by human papillomavirus type 16 e6 does not require induction of c-myc. *Journal of virology*, 75:7198–201, Aug 2001.

[96] S. T. Oh, S. Kyo, and L. A. Laimins. Telomerase activation by human papillomavirus type 16 e6 protein: induction of human telomerase reverse transcriptase expression through myc and gc-rich sp1 binding sites. *Journal of virology*, 75:5559–66, Jun 2001.

[97] T. Veldman, I. Horikawa, J. C. Barrett, and R. Schlegel. Transcriptional activation of the telomerase htert gene by human papillomavirus type 16 e6 oncoprotein. *Journal of virology*, 75:4467–72, May 2001.

[98] Lindy Gewin, Hadley Myers, Tohru Kiyono, and Denise A. Galloway. Identification of a novel telomerase repressor that interacts with the human papillomavirus type-16 e6/e6-ap complex. *Genes & development*, 18:2269–82, Sep 2004.

[99] Rachel A. Katzenellenbogen, Portia Vliet-Gregg, Mei Xu, and Denise A. Galloway. Nfx1-123 increases htert expression and telomerase activity posttranscriptionally in human papillomavirus type 16 e6 keratinocytes. *Journal of virology*, 83:6446–56, Jul 2009.

[100] Xuefeng Liu, Jeffrey Roberts, Aleksandra Dakic, Yiyu Zhang, and Richard Schlegel. Hpv e7 contributes to the telomerase activity of immortalized and tumorigenic cells and augments e6-induced htert promoter function. *Virology*, 375:611–23, Jun 2008.

[101] S. Jablonska, J. Dabrowski, and K. Jakubowicz. Epidermodysplasia verruciformis as a model in studies on the role of papovaviruses in oncogenesis. *Cancer research*, 32:583–9, Mar 1972.

[102] G. Orth, S. Jablonska, M. Favre, O. Croissant, M. Jarzabek-Chorzelska, and G. Rzesa. Characterization of two types of human papillomaviruses in lesions of epidermodysplasia verruciformis. *Proceedings of the National Academy of Sciences of the United States of America*, 75:1537–41, Mar 1978.

[103] S. Majewski and S. Jablonska. Human papillomavirus-associated tumors of the skin and mucosa. *Journal of the American Academy of Dermatology*, 36:659–85; quiz 686–8, May 1997.

[104] Veronique Bouvard, Robert Baan, Kurt Straif, Yann Grosse, Beatrice Secretan, Fatiha El Ghissassi, Lamia Benbrahim-Tallaa, Neela Guha, Crystal Freeman, Laurent Galichet, and Vincent Cogliano. A review of human carcinogens–part b: biological agents., Apr 2009.

[105] Aron Gewirtzman, Brenda Bartlett, and Stephen Tyring. Epidermodysplasia verruciformis and human papilloma virus. *Current opinion in infectious diseases*, 21:141–6, Apr 2008.

[106] S. Jablonska and G. Orth. Epidermodysplasia verruciformis. *Clinics in dermatology*, 3:83–96, Oct-Dec 1985.

[107] Nicolas Ramoz, Luis-Alfredo Rueda, Bakar Bouadjar, Luz-Stella Montoya, Gerard Orth, and Michel Favre. Mutations in two adjacent novel genes are associated with epidermodysplasia verruciformis. *Nature genetics*, 32:579–81, Dec 2002.

[108] Maciej Lazarczyk, Christian Pons, Jose-Andres Mendoza, Patricia Cassonnet, Yves Jacob, and Michel Favre. Regulation of cellular zinc balance as a potential mechanism of ever-mediated protection against pathogenesis by cutaneous oncogenic human papillomaviruses. *The Journal of experimental medicine*, 205:35–42, Jan 2008.

[109] Agnieszka Kalinska-Bienias, Cezary Kowalewski, and Slawomir Majewski. The ever genes - the genetic etiology of carcinogenesis in epidermodysplasia verruciformis and a possible role in non-epidermodysplasia verruciformis patients. *Postepy dermatologii i alergologii*, 33:75–80, Apr 2016.

[110] J. N. Bouwes Bavinck, B. J. Vermeer, F. J. van der Woude, J. P. Vandenbroucke, G. M. Schreuder, J. Thorogood, G. G. Persijn, and F. H. Claas. Relation between skin cancer and hla antigens in renal-transplant recipients. *The New England journal of medicine*, 325:843–8, Sep 1991.

[111] Sylvie Euvrard, Jean Kanitakis, and Alain Claudy. Skin cancers after organ transplantation. *The New England journal of medicine*, 348:1681–91, Apr 2003.

[112] S. Euvrard, Y. Chardonnet, C. Pouteil-Noble, J. Kanitakis, M. C. Chignol, J. Thivolet, and J. L. Touraine. Association of skin malignancies with various and multiple carcinogenic and noncarcinogenic human papillomaviruses in renal transplant recipients. *Cancer*, 72:2198–206, Oct 1993.

[113] V. Shamanin, M. Glover, C. Rausch, C. Proby, I. M. Leigh, H. zur Hausen, and E. M. de Villiers. Specific types of human papillomavirus found in benign proliferations and carcinomas of the skin in immunosuppressed patients. *Cancer research*, 54:4610–3, Sep 1994.

[114] V. Shamanin, H. zur Hausen, D. Lavergne, C. M. Proby, I. M. Leigh, C. Neumann, H. Hamm, M. Goos, U. F. Haustein, E. G. Jung, G. Plewig, H. Wolff, and E. M. de Villiers. Human papillomavirus infections in nonmelanoma skin cancers from renal transplant recipients and nonimmunosuppressed patients. *Journal of the National Cancer Institute*, 88:802–11, Jun 1996.

[115] G. Astori, D. Lavergne, C. Benton, B. Hockmayr, K. Egawa, C. Garbe, and E. M. de Villiers. Human papillomaviruses are commonly found in normal skin of immunocompetent hosts. *The Journal of investigative dermatology*, 110:752–5, May 1998.

[116] Bishr Aldabagh, Jorge Gil C. Angeles, Adela R. Cardones, and Sarah T. Arron. Cutaneous squamous cell carcinoma and human papillomavirus: is there an association? *Dermatologic surgery : official publication for American Society for Dermatologic Surgery [et al.]*, 39:1–23, Jan 2013.

[117] Jad Chahoud, Adele Semaan, Yong Chen, Ming Cao, Alyssa G. Rieber, Peter Rady, and Stephen K. Tyring. Association between beta-genus human papillomavirus and cutaneous squamous cell carcinoma in immunocompetent individuals-a meta-analysis. *JAMA dermatology*, 152:1354–1364, Dec 2016.

[118] Soenke Jan Weissenborn, Ingo Nindl, Karin Purdie, Catherine Harwood, Charlotte Proby, Judy Breuer, Slawomir Majewski, Herbert Pfister, and Ulrike Wieland. Human papillomavirus-dna loads in actinic keratoses exceed those in non-melanoma skin cancers. *The Journal of investigative dermatology*, 125:93–7, Jul 2005.

[119] D. S. Preston and R. S. Stern. Nonmelanoma cancers of the skin. *The New England journal of medicine*, 327:1649–62, Dec 1992.

[120] Sandra Caldeira, Ingeborg Zehbe, Rosita Accardi, Ilaria Malanchi, Wen Dong, Marianna Giarre, Ethel-Michele de Villiers, Raffaele Filotico, Petra Boukamp, and Massimo Tommasino. The e6 and e7 proteins of the cutaneous human papillomavirus type 38 display transforming properties. *Journal of virology*, 77:2195–206, Feb 2003.

[121] Rosita Accardi, Wen Dong, Anouk Smet, Rutao Cui, Agnes Hautefeuille, Anne-Sophie Gabet, Bakary S. Sylla, Lutz Gissmann, Pierre Hainaut, and Massimo Tommasino. Skin human papillomavirus type 38 alters p53 functions by accumulation of Î”np73, Mar 2006.

[122] Elizabeth A. White, Rebecca E. Kramer, Min Jie Alvin Tan, Sebastian D. Hayes, J. Wade Harper, and Peter M. Howley. Comprehensive analysis of host cellular interactions with human papillomavirus e6 proteins identifies new e6 binding partners and reflects viral diversity, Dec 2012.

[123] N. Brimer, C. Lyons, A. E. Wallberg, and S. B. Vande Pol. Cutaneous papillomavirus e6 oncoproteins associate with maml1 to repress transactivation and notch signaling. *Oncogene*, 31:4639–46, Oct 2012.

[124] Jordan M. Meyers, Jennifer M. Spangle, and Karl Munger. The human papillomavirus type 8 e6 protein interferes with notch activation during keratinocyte differentiation. *Journal of virology*, 87:4762–7, Apr 2013.

[125] Min Jie Alvin Tan, Elizabeth A. White, Mathew E. Sowa, J. Wade Harper, Jon C. Aster, and Peter M. Howley. Cutaneous beta-human papillomavirus e6 proteins bind mastermind-like coactivators and repress notch signaling. *Proceedings of the National Academy of Sciences of the United States of America*, 109:E1473–80, Jun 2012.

[126] L. Wu, J. C. Aster, S. C. Blacklow, R. Lake, S. Artavanis-Tsakonas, and J. D. Griffin. Maml1, a human homologue of drosophila mastermind, is a transcriptional co-activator for notch receptors. *Nature genetics*, 26:484–9, Dec 2000.

[127] A. Rangarajan, C. Talora, R. Okuyama, M. Nicolas, C. Mammucari, H. Oh, J. C. Aster, S. Krishna, D. Metzger, P. Chambon, L. Miele, M. Aguet, F. Radtke, and G. P. Dotto. Notch signaling is a direct determinant of keratinocyte growth arrest and entry into differentiation. *The EMBO journal*, 20:3427–36, Jul 2001.

[128] Kristin M. Bedard, Michael P. Underbrink, Heather L. Howie, and Denise A. Galloway. The e6 oncoproteins from human betapapillomaviruses differentially activate telomerase through an e6ap-dependent mechanism and prolong the lifespan of primary keratinocytes. *Journal of virology*, 82:3894–902, Apr 2008.

[129] Anne-Sophie Gabet, Rosita Accardi, Angelica Bellopede, Susanne Popp, Petra Boukamp, Bakary S. Sylla, J. Arturo Londono-Vallejo, and Massimo Tommasino. Impairment of the telomere/telomerase system and genomic instability are associated with keratinocyte immortalization induced by the skin human papillomavirus type 38. *FASEB journal : official publication of the Federation of American Societies for Experimental Biology*, 22:622–32, Feb 2008.

[130] Daniele Viarisio, Karin Mueller-Decker, Ulrich Kloz, Birgit Aengeneyndt, Annette Kopp-Schneider, Hermann-Josef Grone, Tarik Gheit, Christa Flechtenmacher, Lutz Gissmann, and Massimo Tommasino. E6 and e7 from beta hpv38 cooperate with ultraviolet light in the development of actinic keratosis-like lesions and squamous cell carcinoma in mice. *PLoS pathogens*, 7:e1002125, Jul 2011.

[131] Daniele Viarisio, Karin MÃ¼ller-Decker, Rosita Accardi, Alexis Robitaille, Matthias DÃ¼rst, Katrin Beer, Lars Jansen, Christa Flechtenmacher, Matthias Bozza, Richard Harbottle, Catherine Voegele, Maude Ardin, Jiri Zavadil, Sandra Caldeira, Lutz Gissmann, and Massimo Tommasino. Beta hpv38 oncoproteins act with a hit-and-run mechanism in ultraviolet radiation-induced skin carcinogenesis in mice. *PLOS Pathogens*, 14(1):e1006783, January 2018.

[132] Danielle Bottalico, Zigui Chen, Anne Dunne, Janae Ostoloza, Sharod McKinney, Chang Sun, Nicolas F. Schlecht, Mahnaz Fatahzadeh, Rolando Herrero, Mark Schiffman, and Robert D. Burk. The oral cavity contains abundant known and novel human papillomaviruses from the betapapillomavirus and gammapapillomavirus genera. *The Journal of infectious diseases*, 204:787–92, Sep 2011.

[133] Christine M. Pierce Campbell, Jane L. Messina, Mark H. Stoler, Drazen M. Jukic, Massimo Tommasino, Tarik Gheit, Dana E. Rollison, Laura Sichero, Bradley A. Sirak, Donna J. Ingles, Martha Abrahamsen, Beibei Lu, Luisa L. Villa, Eduardo Lazcano-Ponce, and Anna R. Giuliano. Cutaneous human papillomavirus types detected on the surface of male external genital lesions: a case series within the hpv infection in men study. *Journal of clinical virology : the official publication of the Pan American Society for Clinical Virology*, 58:652–9, Dec 2013.

[134] Maria Gabriella Dona, Tarik Gheit, Maria Fenicia Vescio, Alessandra Latini, Domenico Moretto, Maria Benevolo, Antonio Cristaudo, Massimo Tommasino, and Massimo Giuliani. Incidence, clearance and duration of cutaneous beta and gamma human papillomavirus anal infection., Oct 2016.

[135] Shalaka S. Hampras, Dana E. Rollison, Anna R. Giuliano, Sandrine McKay-Chopin, Lucia Minoni, Karen Sereday, Tarik Gheit, and Massimo Tommasino. Prevalence and concordance of cutaneous beta human papillomavirus infection at mucosal and cutaneous sites. *The Journal of infectious diseases*, 216:92–96, Jul 2017.

[136] Ilir Agalliu, Susan Gapstur, Zigui Chen, Tao Wang, Rebecca L. Anderson, Lauren Teras, Aimee R. Kreimer, Richard B. Hayes, Neal D. Freedman, and Robert D. Burk. Associations of oral alpha-, beta-, and gamma-human papillomavirus types with risk of incident head and neck cancer. *JAMA oncology*, Jan 2016.

[137] Ola Forslund, Hanna Johansson, Klaus Gregaard Madsen, and Kristian Kofoed. The nasal mucosa contains a large spectrum of human papillomavirus types from the betapapillomavirus and gammapapillomavirus genera. *The Journal of infectious diseases*, 208:1335–41, Oct 2013.

[138] Iris Cornet, Veronique Bouvard, Maria Saveria Campo, Miranda Thomas, Lawrence Banks, Lutz Gissmann, Jerome Lamartine, Bakary S. Sylla, Rosita Accardi, and Massimo Tommasino. Comparative analysis of transforming properties of e6 and e7 from different beta human papillomavirus types. *Journal of virology*, 86:2366–70, Feb 2012.

[139] Daniele Viarisio, Karin Muller-Decker, Paola Zanna, Ulrich Kloz, Birgit Aengeneyndt, Rosita Accardi, Christa Flechtenmacher, Lutz Gissmann, and Massimo Tommasino. Novel ss-hpv49 transgenic mouse model of upper digestive tract cancer. *Cancer research*, 76:4216–25, Jul 2016.

[140] B. Lynn Allen-Hoffmann, Sandra J. Schlosser, Cathy A. R. Ivarie, Lorraine F. Meisner, Sean L. Oâ€™Connor, and Carol A. Sattler. Normal growth and differentiation in a spontaneously immortalized near-diploid human keratinocyte cell line, niks. *Journal of Investigative Dermatology*, 114(3):444–455, March 2000.

[141] J. G. Rheinwald and H. Green. Serial cultivation of strains of human epidermal keratinocytes: the formation of keratinizing colonies from single cells. *Cell*, 6:331–43, Nov 1975.

[142] K. Alitalo, E. Kuismanen, R. Myllyla, U. Kiistala, S. Asko-Seljavaara, and A. Vaheri. Extracellular matrix proteins of human epidermal keratinocytes and feeder 3t3 cells. *The Journal of cell biology*, 94:497–505, Sep 1982.

[143] Karo Gosselin, Emeric Deruy, SÃ©bastien Martien, Chantal Vercamer, Fatima Bouali, Thibault Dujardin, Christian Slomianny, Ludivine Houel-Renault, Fazia Chelli, Yvan De Launoit, and Corinne Abbadie. Senescent keratinocytes die by autophagic programmed cell death, Feb 2009.

[144] Noboru Mizushima. Autophagy: process and function. *Genes & development*, 21:2861–73, Nov 2007.

[145] Terence Kin-Wah Lee, Tracy Ching-Man Lau, and Irene Oi-Lin Ng. Doxorubicin-induced apoptosis and chemosensitivity in hepatoma cell lines. *Cancer chemotherapy and pharmacology*, 49:78–86, Jan 2002.

[146] Hikisz Paweł and Kiliańska Zofia. Puma, a critical mediator of cell death – one decade on from its discovery, 2012.

[147] Wafik S. El-Deiry. p21(waf1) mediates cell-cycle inhibition, relevant to cancer suppression and therapy. *Cancer research*, 76:5189–91, Sep 2016.

[148] Katia Zanier, Sebastian Charbonnier, Abdellahi Ould M'hamed Ould Sidi, Alastair G. McEwen, Maria Giovanna Ferrario, Pierre Poussin-Courmontagne, Vincent Cura, Nicole Brimer, Khaled Ould Babah, Tina Ansari, Isabelle Muller, Roland H. Stote, Jean Cavarelli, Scott Vande Pol, and Gilles Trave. Structural basis for hijacking of cellular lxxll motifs by papillomavirus e6 oncoproteins. *Science (New York, N.Y.)*, 339:694–8, Feb 2013.

[149] Marzena Wyganowska-Swiatkowska and Jerzy Jankun. Plasminogen activation system in oral cancer: Relevance in prognosis and therapy (review). *International journal of oncology*, 47:16–24, Jul 2015.

[150] Marco T. Brazao-Silva, Maria Fernandes S. Rodrigues, Ana Lucia A. Eisenberg, Fernando L. Dias, Luciana M. de Castro, Fabio D. Nunes, Paulo R. Faria, Sergio V. Cardoso, Adriano M. Loyola, and Suzana C. O. M. de Sousa. Metallothionein gene expression is altered in oral cancer and may predict metastasis and patient outcomes. *Histopathology*, 67:358–67, Sep 2015.

[151] Warburg O. Uber den stoffwechsel der carcinomzelle. *Naturwissenschaften 12, 1131-1137*, 1924.

[152] Jie Hu, Jason W. Locasale, Jason H. Bielas, Jacintha O'Sullivan, Kieran Sheahan, Lewis C. Cantley, Matthew G. Vander Heiden, and Dennis Vitkup. Heterogeneity of tumor-induced gene expression changes in the human metabolic network. *Nature biotechnology*, 31:522–9, Jun 2013.

[153] W. Zwerschke, S. Mazurek, P. Massimi, L. Banks, E. Eigenbrodt, and P. Jansen-Durr. Modulation of type m2 pyruvate kinase activity by the human papillomavirus type 16 e7 oncoprotein. *Proceedings of the National Academy of Sciences of the United States of America*, 96:1291–6, Feb 1999.

[154] Weiwei Yang and Zhimin Lu. Pyruvate kinase m2 at a glance. *Journal of Cell Science*, 128(9):1655–1660, May 2015.

[155] Chahoud J, Semaan A, Chen Y, and et al. Association between Î²-genus human papillomavirus and cutaneous squamous cell carcinoma in immunocompetent individuals: a meta-analysis. *JAMA Dermatology*, 152(12):1354–1364, 2016.

[156] Michelle R. Iannacone, Tarik Gheit, Tim Waterboer, Anna R. Giuliano, Jane L. Messina, Neil A. Fenske, Basil S. Cherpelis, Vernon K. Sondak, Richard G. Roetzheim, Kristina M. Michael, Massimo Tommasino, Michael Pawlita, and Dana E. Rollison. Case-control study of cutaneous human papillomaviruses in squamous cell carcinoma of the skin. *Cancer epidemiology, biomarkers & prevention : a publication of the American Association for Cancer Research, cosponsored by the American Society of Preventive Oncology*, 21:1303–13, Aug 2012.

[157] Ola Forslund, Thomas Iftner, Kristin Andersson, Bernt Lindelof, Eva Hradil, Peter Nordin, Bo Stenquist, Reinhard Kirnbauer, Joakim Dillner, and Ethel-Michele de Villiers. Cutaneous human papillomaviruses found in sun-exposed skin: Beta-papillomavirus species 2 predominates in squamous cell carcinoma. *The Journal of infectious diseases*, 196:876–83, Sep 2007.

[158] Emily Montosa Nunes, Staci L. Sudenga, Tarik Gheit, Massimo Tommasino, Maria Luiza Baggio, Silvaneide Ferreira, Lenice Galan, Roberto C. Silva, Christine M. Pierce Campbell, Eduardo Lazcano-Ponce, Anna R. Giuliano, Luisa L. Villa, and Laura Sichero. Diversity of beta-papillomavirus at anogenital and oral anatomic sites of men: The him study. *Virology*, 495:33–41, Aug 2016.

[159] Davit Bzhalava, Peng Guan, Silvia Franceschi, Joakim Dillner, and Gary Clifford. A systematic review of the prevalence of mucosal and cutaneous human papillomavirus types. *Special Issue: The Papillomavirus Episteme*, 445(1):224–231, October 2013.

[160] Prakriti Sen, Pooja Ganguly, and Niladri Ganguly. Modulation of dna methylation by human papillomavirus e6 and e7 oncoproteins in cervical cancer. *Oncology letters*, 15:11–22, Jan 2018.

[161] Fu-Fen Yin, Ning Wang, Xiao-Ning Bi, Xiao Yu, Xiao-Hui Xu, You-Lin Wang, Cheng-Quan Zhao, Bing Luo, and Yan-Kui Wang. Serine/threonine kinases 31(stk31) may be a novel cellular target gene for the hpv16 oncogene e7 with potential as a dna hypomethylation biomarker in cervical cancer. *Virology journal*, 13:60, Apr 2016.

[162] Alfonso DueÃ±as-GonzÃ¡lez, Marcela Lizano, Myrna Candelaria, Lucely Cetina, Claudia Arce, and Eduardo Cervera. Epigenetics of cervical cancer. an overview and therapeutic perspectives. *Molecular Cancer*, 4:38–38, October 2005.

ACKNOWLEDGMENTS

I want to express my gratitude to all the people who have been fundamental in the successful completion of my PhD.

I had the opportunity to complete my PhD under the supervision of three great scientists: Dr. Massimo Tommasino, Dr. Martin Müller and Dr. Michael Pawlita. I am grateful to each of them for giving me the opportunity to learn something new every day. I would like to thank Dr. Tommasino for the opportunity he gave me and for the constant interaction we had in the past three years. A necessary thank you also goes to Dr. Pawlita for "adopting" me in his lab for the year I have spent at DKFZ. I'm also grateful to Dr. Müller for the help he and his lab gave me during the year at DKFZ.

I express my gratitude also to Dr. Rosita Accardi-Gheit, who gave me a constant support during the PhD, and to Dr. Tarik Gheit.

The shared PhD between DKFZ and IARC allowed me to meet people from all over the world and I want to thank all of them for enriching me in the past three years. A special thanks goes to my friends Almira, Cecilia, Daniele, Maria, Xin, Fan, Robin, Xueer, Caro, Nicole, Alicia, Dwain, Matthias, Alberto, Roberta and the rest of the Italian crew.

I would like to thank Antonin for his unconditional love and for his patience, especially in last few months.

Last but not least, a special thanks to my family. Words cannot express how grateful I am. My parents and my brother gave me constant support, standing by my side in the good and in the bad moments. They help me reaching this important milestone and they always believed in me, even when I wasn't. This thesis is also yours.